

VOLUME 1
ISSUE 1 | 2020

ADVANCES IN AGRICULTURAL & FOOD RESEARCH JOURNAL



MALAYSIAN SOCIETY OF
AGRICULTURAL AND FOOD ENGINEERS
Est. 1982



HH PUBLISHER



Editorial Board

Editor-in-Chief

Assoc. Prof. Dr. Rosnah Shamsudin (Malaysia)

Advisory Board Member

Prof. Azmi Yahya (Malaysia)

Prof. Keshavan Niranjana (United Kingdom)

Prof. Paul Heinemann (United States of America)

Prof. Ta-Te Lin (Taiwan)

Senior Editor

Dr. Norulhuda Mohamed Ramli (Malaysia)

Dr. Nur Hamizah Abd Ghani @ Hashim (Malaysia)

Editorial Board Member

Indonesia

Prof. Dr. Ir. Lilik Sutiarso

Malaysia

Assoc. Prof. Dr. Mohd Shamsul Anuar

Dr. Aimrun Wayayok

Dr. Jumardi Roslan

Dr. Mohd Zuhair Mohd Nor

Dr. Muhammad Hazwan Hamzah

Dr. Wan Nor Zanariah Zainol @ Abdullah

Ir. Dr. Mohammad Effendy Ya'acob

Ir. Mohd Fazly Mail

Thailand

Assoc. Prof. Dr. Jaturapatr Varith



Table of Contents

EDITORIAL NOTE

STEM Enculturation in Agricultural Engineering: The Needs for Government, Academia, Industry and Community Collaborations

Muhammad Hazwan Hamzah, Nurulhuda Khairudin, Anas Mohd Mustafah, Mahirah Jahari, Diyana Jamaludin

Agricultural and Food Industries in Malaysia

Rosnah Shamsudin, Christine Jamie Vincent

ORIGINAL RESEARCH ARTICLE

Mechanical Static Structural Analysis of CANTAS Sickle Blade

Ahmad Syazwan Ramli, Abd Rahim Shuib, Mohd Azwan Mohd Bakri, Mohd Ikmal Hafizi Mohd Azaman, Mohd Khairul Fadzly Md Radzi, Mohd Rizal Ahmad, Mohd Ramdhan Mohd Khalid, Salmah Jahis

Isolation of Nanocellulose from Saba' (*Musa acuminata x balbisiana*) Banana Peel by One-Pot Oxidation-Hydrolysis System

Suryani Saallah, Jumardi Roslan, Nurul Nadjwa Zakaria, Wolyna Pindi, Shafiquzzaman Siddiquee, Mailin Misson, Clarence M. Ongkudon, Nur Hidayah Azmirah Mohd Jamil, Wuled Lenggoro

A Study on Hybrid Power Vehicle for Electric Spraying Application

Mohd Azwan Mohd Bakri, Salmah J, Abd Rahim S, Syazwan R, M. Ikmal H.

Nutritional Properties of Orange-Fleshed Sweet Potato Juice

Nurul Ainina Zulkifli, Nurhanisah Mohammed Salleh, Mohd Zuhair Mohd Nor, Farah Nadia Omar, Alifdalino Sulaiman, Mohd Noriznan Mokhtar

Optimisation of Parameters Laser Cutting of Oil Palm Fronds Using Fibre Pulsed Laser of 1064 Nm Wavelength System

Mohd Ikmal Hafizi Azaman, Mohd Adzir Mahdi, Mohd Rizal Ahmad, Abd Rahim Shuib, Mohd Ramdhan Khalid, Mohd Azwan Bakri, Mohd Khairul Fadzly Md Radzi, Ahmad Syazwan Ramli

Anaerobic Co-digestion of Pineapple Wastes with Cow Dung: Effect of Different Total Solid Content on Bio-methane Yield

Adila Fazliyana Aili Hamzah, Muhammad Hazwan Hamzah, Fauzan Najmi Ahmad Mazlan, Hasfalina Che Man, Nur Syakina Jamali, Shamsul Izhar Siajam



Table of Contents

Effect of Different Jackfruit Puree Concentrations on the Mechanical Properties of Jackfruit Frozen Confection

Amiruddin Mat Johari, Nur Aliaa Abd Rahman, Roseliza Kadir Basha, Azhari Samsu Baharudin, Mohd Afandi P. Mohammed, Ahmad Tarmeze Talib, Minato Wakisata

Pemantauan Tanaman Padi Menggunakan Sistem Maklumat Geografi dan Imej Multispektral

Halip Rowena, Nik Norasma, Siva K Balasundram, Wan Fazilah Ilahi Fadzli, Rhushalshafira Roslee, Nor Athirah Roslin, Zulkarami Berahim, Mohamad Husni Omar

Editorial Note

STEM Enculturation in Agricultural Engineering: The Needs for Government, Academia, Industry and Community Collaborations

Muhammad Hazwan Hamzah^{1,2*}, Khairudin Nurulhuda^{1,2}, Anas Mohd Mustafah^{1,2}, Mahirah Jahari^{1,2}, Diyana Jamaludin^{1,2}

¹Department of Biological and Agricultural Engineering, Faculty of Engineering, Universiti Putra Malaysia, 43400 UPM Serdang, Selangor, Malaysia, hazwanhamzah@upm.edu.my, k_nurulhuda@upm.edu.my, anas_mustafah@upm.edu.my, jmahirah@upm.edu.my, diyana_upm@upm.edu.my

²Smart Farming Technology Research Centre, Faculty of Engineering, Universiti Putra Malaysia, 43400 UPM Serdang, Selangor, Malaysia

*Corresponding author: Muhammad Hazwan Hamzah, Department of Biological and Agricultural Engineering, Faculty of Engineering, Universiti Putra Malaysia, 43400 UPM Serdang, Selangor, Malaysia; hazwanhamzah@upm.edu.my

Received: 25th April 2020

Accepted: 4th May 2020

Published: 8th May 2020

Citation: Hamzah MH, Khairudin N, Mohd Mustafah A, *et al.* STEM Enculturation in Agricultural Engineering: The Needs for Government, Academia, Industry and Community Collaborations. *Adv Agri Food Res J* 2020; 1(1): a0000081. <https://doi.org/10.36877/aafrij.a0000081>

Main Text

Science, Technology, Engineering, Mathematics and Education (STEM) is life-long learning which integrates knowledge of STEM either in formal or informal teaching and learning paradigm. The Ministry of Education Malaysia has developed the STEM education initiative in Malaysia Blueprint 2013–2025 which aims to strengthen the quality of STEM education through an improved curriculum, training of teachers, and use of blended learning approaches (Ministry of Education Malaysia, 2013; Ng & Adnan, 2018). It is vital to increase interest and awareness in STEM to all students across all ages from early childhood, primary, secondary, and tertiary education levels, and at industrial or community linkages through campaigns and partnerships (Ministry of Education Malaysia, 2013, 2017). The challenge remains on creating interest and awareness in STEM across various stakeholders.

The STEM transformation in Malaysia aims to produce a STEM literate society and sufficient professionals and qualified STEM workforce that can contribute towards new innovations (Hafizan *et al.*, 2017). Active involvement of stakeholders such as academia, government, industry and community will ensure successful STEM enculturation. Empowering the next generation through STEM could be attained by human capital development, programme development, facilities, research, visibility, promotion and partnerships (Academy of Sciences Malaysia, 2018a). The statistics provided by the Ministry of Science, Technology and Innovation showed that only 44% of secondary and vocational school students studied STEM subjects in 2018; a decrease from 48% in 2012 (The Star,

2019). The current number of students engaged in STEM subjects (334, 742) is low compared to the government's target which is 60:40 ratio of students pursuing science and arts stream (570,858) (Ramli & Talib, 2017; Zulkifli, 2020). A major cause of this low ratio may be due to the slowing demand of STEM knowledge-based workforce in industries and perception of subject difficulties held by students discouraging them from undertaking STEM courses (Cuff, 2017; Lau, 2019).

Collaborative networking between the government and academia is essential to improve the quality of education training and delivery system. The collaboration may allow for better facilities and wealth of resources in learning experiences of science and mathematics. The Ministry of Education Malaysia has been organising STEM workshops and conferences for academicians to share the best practices in teaching and learning STEM, such as applying gamification and theory inventive problem-solving. Industrial Revolution 4.0 is the impetus of the transformation of education in Malaysia as new technology is made available for enhanced teaching and learning experiences. Much effort to review and develop the science and mathematics curriculum at school has been made to meet future needs (Academy of Sciences Malaysia, 2012). Research on the development of STEM education could strengthen the planning and execution of STEM enculturation. Facilities at STEM centres need to be maintained or upgraded in line with the current emerging technologies.

Synergies between industry and academia will promote demand-driven research and development (Academy of Sciences Malaysia, 2018b). The industry through the corporate social responsibility arrangement, together with the academia could organise events or programmes related to STEM. A joint programme between academia and industry to educate the community in regard to agricultural engineering subjects such as vertical farming, waste treatment, hydroponics, green wall and many more could be conducted (Islamic Relief Malaysia, 2019; Juferi, 2020; Mustafah, 2019). The industry could provide a platform for promising talents in the STEM fields to enhance their skills and contribute to the community. Ultimately, Malaysia could produce future-proof graduates who meet the needs of jobs with their cognitive, psychomotor and skills.

The Department of Biological and Agricultural Engineering (DBAE), Faculty of Engineering, Universiti Putra Malaysia (UPM) was established in 1996, and currently offers a 4-year course of Bachelor of Agricultural and Biosystems Engineering. Four specialised areas offered by the department are mechanisation and automation, agricultural informatics, soil and water resources, as well as postharvest and environment. As one of the leading research universities where agriculture is the research niche, UPM through the DBAE has actively organised STEM programmes for students, indigenous people and other communities with the aim to contribute towards wealth creation and nation-building. The aim was achieved through the exploration and dissemination of knowledge. Such a programme enhanced the visibility of UPM in pursuit of the 3rd university's goal which is to boost industry and community network services.

For instance, Urban Agrischool module which aims at educating students on agriculture focuses on the appealing side of urban agriculture through the greenhouse concept (Mustafah

et al., 2019). Collaboration between academia, industries and communities have led to the success of the programme. The module was developed by the DBAE, UPM. The module was successfully conducted by the DBAE, UPM in collaboration with Kulim (M) Berhad, Agri Space Tech Sdn. Bhd., Malaysian Society of Agricultural and Food Engineers — Student Chapters, SK Sedenak, Johor and Parent-Teacher Association, SK Sedenak, Johor. Kulim (M) Berhad and Faculty of Engineering, UPM provided the fund while Agri Space Tech Sdn. Bhd. provided a temporary mini greenhouse for the programme. The community at school was proactive in helping with the planning and execution of the programme. According to the pre and post survey conducted during the programme, Urban AgriSchool: Greenhouse module has increased the interest in agriculture of about 30% amongst the students. In future, this programme will be continued to reach as many young people as possible to introduce the concept of urban agriculture and transform the perception of agricultural sectors.

Success is the sum of small efforts, repeated day in and day out. More effort and time are needed in order to integrate STEM into the mind and habits of the community (Academy of Sciences Malaysia, 2018a). As demonstrated through the success story of Urban Agrischool programme at SK Sedenak, Johor, STEM enculturation requires support from the government, academia, industry and community. Planning and developing strategic directions and action plans of STEM programmes in terms of how to adapt, adopt and apply the STEM concepts are essential. Let us foster and strengthen the collaborations across the government, academia, industry and community to instil interests of the young generations in science, technology, engineering and mathematics so that they may become enablers of technological innovations and advancements in future.

Author Contributions: Conceptualization, M.H.H., A.M.M., K.N., M.J. and D.J.; Funding Acquisition, D.J. and M.H.H.; Project Administration, M.J. and K.N.; Writing – original draft, M.H.H.; Writing – review & editing, K.N. and A.M.M.

Funding: This work was funded by Faculty of Engineering, UPM, Kulim (M) Berhad and Agri Space Tech Sdn. Bhd.

Acknowledgments: The authors would like to thank DBAE, UPM, community and industries for their support and contribution throughout the programme.

Conflicts of Interest: The authors declare no conflict of interest.

References

- Academy of Sciences Malaysia. (2012). *Teaching and learning of Science and Mathematics in schools — Towards a more creative and innovative Malaysia: ASM advisory report 2/2011*. Kuala Lumpur.
- Academy of Sciences Malaysia. (2018a). *Science outlook 2017: Converging towards progressive Malaysia 2050*. Kuala Lumpur.
- Academy of Sciences Malaysia. (2018b). Thought leader. In *2018 Annual Report*. <https://doi.org/10.12681/sas.500>
- Cuff, B. M. P. (2017). *Perceptions of subject difficulty and subject choices: Are the two linked, and if so, how?* Retrieved from <https://www.gov.uk/government/publications/students-subject-choices-at-gcse-and-a-level>
- Hafizan, E., Shahali, M., Ismail, I., & Halim, L. (2017). STEM education in Malaysia: Policy, trajectories and initiatives. *Asian Research Policy*, 8(2), 122–133.

- Islamic Relief Malaysia. (2019). STEM cultivate interests in Science, Mathematics & Engineering for indigenous people. Retrieved April 23, 2020, from Islamic Relief Malaysia website: <https://islamic-relief.org.my/ms/stem-pupuk-minat-ilmu-sains-matematik-kejuruteraan-kepada-orang-asli/>
- Juferi, N. E. (2020). Orang asli student community outreach programme. *E-Putra Newsletter*, (53), 1–5.
- Lau, R. (2019, April 7). Tough love for STEM threatens labour market. *Borneo Post*.
- Ministry of Education Malaysia. (2013). Malaysia Education Blueprint 2013–2025 (Preschool to Post-Secondary Education). In *Ministry of Education Malaysia*. <https://doi.org/10.1016/j.tate.2010.08.007>
- Ministry of Education Malaysia. (2017). *Malaysia Education Blueprint 2013–2025: 2016 Annual Report*. Putrajaya.
- Mustafah, A. M. (2019). Reaching out urban agrischool: Urban agriculture education through greenhouse concept. *Synthesis*, (02), 1–28.
- Mustafah, A. M., Jamaludin, D., Jahari, M., Hamzah, M. H., & Khairudin, N. (2019). Urban AgriSchool: Urban Agriculture Education through the Greenhouse Module. In M. A. M. Jedi, M. H. Johari, Z. M. Nopiah, H. M. Affandi, N. Razali, H. Othman, ... M. H. Osman (Eds.), *National innovation and invention in engineering and built environment* (pp. 24–29). Bangi: Universiti Kebangsaan Malaysia.
- Ng, C. H., & Adnan, M. (2018). Integrating STEM education through Project-Based Inquiry Learning (PIL) in topic space among year one pupils. *IOP Conference Series: Materials Science and Engineering*, 296(1). <https://doi.org/10.1088/1757-899X/296/1/012020>
- Ramli, N. F., & Talib, O. (2017). Can education institution implement STEM? From Malaysian teachers' view. *International Journal of Academic Research in Business and Social Sciences*, 7(3), 2222–6990. <https://doi.org/10.6007/IJARBS/v7-i3/2772>
- The Star. (2019, September 28). Govt worried over dwindling number of STEM students. *The Star*, pp. 9–10.
- Zulkifli, N. (2020, February 10). Girls need to see women in science. *New Straits Times*.





Editorial Note

Agricultural and Food Industries in Malaysia

Rosnah Shamsudin¹ & Christine Jamie Vincent¹

¹ Department of Process & Food Engineering, Faculty of Engineering, Universiti Putra Malaysia, Serdang, 43400 Serdang Malaysia.

*Corresponding author: Rosnah Shamsudin, Department of Process & Food Engineering, Faculty of Engineering, Universiti Putra Malaysia, Serdang, 43400 Serdang Malaysia; rosnahs@upm.edu.my

Received: 25th July 2020

Accepted: 14th August 2020

Published: 24th August 2020

Citation: Shamsudin R & Vincent CJ. Agricultural and food industries in Malaysia. Adv Agri Food Res J 2020; 1(1): a0000107. <https://doi.org/10.36877/aafri.a0000107>

Main Text

Recent studies on the export of processed food in Malaysia have shown obvious increments in the acceptance of its food products in the overseas market. Malaysia consists of a very diverse population which contributes to the wide selection of unique food products produced locally. This opens a window for Malaysia to become a major exporter in the Association of Southeast Asian Nations (ASEAN) region where it is reported to have a population of over 600 million. Furthermore, with the country's major population being Muslims, it also provides the opportunity for the country to be positioned as an international-ready domestic market for halal food in the global market. Developments in the agricultural and agro-food processing sector in Malaysia have placed Malaysia among the leading ASEAN countries for the food and beverage industry, but to-date only big key players are able to benefit from these strong value propositions as currently, most business establishments in Malaysia are Small Medium Enterprises (SME) and there is still a huge lack in locally produced agricultural and agro-food processing machinery that could be of great help to the SMEs. To cater to the bulk production for the global market, there is a great need for new machines to be invented so that the cottage industries and SMEs could expand and sustain their business in the long run. Universities and research centres in Malaysia play important roles in the development of these machines that are able to complement the small-medium enterprises especially the cottage industries that are currently producing food and agricultural products in a smaller scale due to the lack of modernization involved. It is also crucial to sustain its position as one of the top countries for the exports of Halal food products. It is hoped that with these inventions, the small-medium enterprises involved in the cottage industry that are producing food products would not only benefit from the inventions but also increase the socio-economy of these business owners.

Malaysia is famous for its lush tropical lands and naturally grown resources that are utilised widely for cultivation, research and processing of foods, hence, agriculture is a sector

that contributes greatly to the nation's resources and wealth. The climate in Malaysia also allows for the sustainable supply of agricultural products throughout the whole year. The agriculture industry in Malaysia comprises of industrial commodities and agro-food. Palm oil, rubber and cocoa are planted on a large scale and therefore considered as industrial commodities. Agro-food which is mostly planted by smallholders and most of the time categorised under the Small Medium Enterprises (SMEs), include rice, fruits, vegetables, fisheries and livestock. These commodities are sent to small industries to be distributed to traders, hypermarkets and local sundry shop owners. Foodstuff is processed into food products such as chilli sauce, cereals and dairy products, while bakeries utilise eggs to produce cakes, pastries and cookies. There are many other commodities and trades in the Malaysian food and beverage industry. The increase in the production of agricultural productions is attributed to the development of the agricultural sector.

In Malaysia, the main economy generators are the Small and Medium Enterprises (SMEs) (Jamak *et al.*, 2011; Lo *et al.*, 2016; SME Corporation, 2015). According to the Department of Statistics Malaysia in July 2019, more than half of the total workforce in the country (~65%) consisted of business establishments in the Small Medium Enterprises (SMEs) category with the percentage of 98.5%, of which 21.2% were small businesses and 76.5% were micro-enterprises (Ramli & Taib, 2017). According to the definition of SMEs by the Central Bank of Malaysia (2015), SMEs are categorised into Micro, Small and Medium enterprises based on the number of employees and the total annual sales generated. The data provided by the SME Corp of Malaysia stated that SMEs contributed an average of about 36.6% of Gross Domestic Product (GDP) with an increment in total exports of 18.6% from 17.7% in 2016. It is of utmost importance to recognise the success formula of SMEs in these contributions to Malaysia's economic development and to try and maximise the growth further with necessary measures, be it in the advancement of the technology used or in the business performance itself.

According to the Malaysian Industrial Development Authority (MIDA) in its article entitled *Food Industry in Malaysia* (2019), processed food in Malaysia contributed about RM 21.1 billion and was exported to more than 200 countries, while import value of processed food amounted to RM 20.7 billion in 2017. It was deduced that Malaysia's Food Product recorded a growing acceptance in the global market due to the increasing number of processed food exports throughout the years. Malaysia consists of a very diverse population which contributes to the wide selection of unique food products produced locally. This opens a window for Malaysia to become a major exporter in the Association of Southeast Asian Nations (ASEAN) region of which it is reported to have a population of over 600 million. Furthermore, with the country's major population being Muslims, it also provides the opportunity for the country to be positioned as an international-ready domestic market for halal food in the global market. Developments in the agricultural and agro-food processing sector in Malaysia have placed Malaysia among the leading ASEAN countries for the food and beverage industry, but to-date the food-processing sector is only 10% of Malaysia's

manufacturing output. These 10% consist of mostly only big key players who are able to benefit from these strong value propositions as at present, most business establishments in Malaysia are Small Medium Enterprises (SME) and there is still a huge lack in locally produced agricultural and agro-food processing machinery that could be of great help to the SMEs.

On the other hand, the halal food industry conforms to the Syariah compliance and this promises the Muslims globally a sense of security for whatever they buy and use (Bohari *et al.*, 2013). Moreover, it is also crucial for societal development and national economic growth. The Malaysian government applied for the single Halal standard throughout the country and so was dubbed and cited by the United Nations as the world's best example of benchmarking of halal food in accordance with the Codex Alimentarius Commission adopting the Codex general guidelines for the use of the term halal in Geneva in 1997. Not only that but the Halal food market is also gaining attention amongst the non-Muslims as well for its symbol that indicates quality and safety (Talib, & Mohd Ali, 2009). As for the current halal industry in the global market, MIDA estimates the industry to be at US\$ 2.3 trillion and since Malaysia's major population is Muslims, it is well-positioned as an international-ready domestic market for halal food. These strong value propositions open up opportunities for the food processing industry.

In order to strengthen the advancement of agricultural and food industries, the Advances in Agricultural and Food Research Journal (AAFRJ) has been generated. This journal is aimed to spread the awareness of knowledge and new development of technologies in agriculture and food industries. AAFRJ is an open access international journal that publishes original research and review papers on any subject related to science and engineering in agriculture and food, particularly those of relevance to the industry. This can include applied agricultural, biological, environmental, natural resources, food and livestock farming to solve problems in complex living systems. In addition to science and engineering topics, we also welcome articles related to agriculture and food service extension, management and business either at the local or international level.

This journal is also an effort to continue in assisting farmers, entrepreneurs or industries related by enhancing the research and development in farming, harvesting, processing, manufacturing, quality, storage, sorting, product safety and services according to the good manufacturing process (GMP), enhancing coordination among the organisations involved in the development and promotion of agriculture and food, supply chain and many more. As the agricultural and food industries are growing rapidly, this journal might be one of the platforms for sharing, exchanging and transferring knowledge to the global industry.

Conflicts of Interest: The author declares no potential conflict of interest with respect to the research, authorship, and/or publication of this article.

References

Bohari, A.M., Hin, C.W., & Fuad, N. (2013). The competitiveness of halal food industry in Malaysia: A SWOT-

- ICT analysis. *Geografia Malaysia Journal of Society and Space*, 9(1), 1–9.
- Central Bank of Malaysia. (2015). Retrieved from http://www.bnm.gov.my/files/publication/ar/en/2015/ar2015_book.pdf
- Jamak, A., Salleh, A. B. S., Sivapalan, R. S., & Abdullah, A. (2011). Entrepreneurial challenges confronting micro-enterprise of Malaysian Malays. *World Academy of Science, Engineering and Technology*, 5(9), 862–867.
- Lo, M. C., Wang, Y. C., Wah, C. R. J., & Ramayah, T. (2016). The critical success factors for organizational performance of SMEs in Malaysia: A partial least squares approach. *Review of Business Management*, 18(61), 370–391.
- MIDA. (2019). *Food industry in Malaysia*. Retrieved from <https://www.mida.gov.my/home/33/pages/>
- Ramli, A. & Taib, M. (2017). Malaysian Malay micro businesses: Success factors in Langkawi Island. *Science International (Lahore)*, 29(6), 1191–1198.
- SME Corporation Malaysia. (2017). *Micro Enterprises*. Retrieved from <https://www.smecorp.gov.my/index.php/en/>
- SME Corporation Malaysia. (2015). *About SME Masterplan (2012–2020)*. Retrieved on June 19, 2020, from <http://www.smecorp.gov.my/index.php/en/policies/2015-12-21-09-16-12/about-sme-masterplan> (2015).
- Talib, H.A. & Mohd Ali, K.A. (2009). An overview of Malaysian food industry: The opportunity and quality aspects. *Pakistan Journal of Nutrition*, 8, 507–517.



Original Research Paper

Mechanical Static Structural Analysis of CANTAS Sickle Blade

Ahmad Syazwan Ramli^{1*}, Abd Rahim Shuib¹, Mohd Azwan Mohd Bakri¹, Mohd Ikmal Hafizi Mohd Azaman¹, Mohd Khairul Fadzly Md Radzi¹, Mohd Rizal Ahmad¹, Mohd Ramdhan Mohd Khalid¹, Salmah Jahis¹

¹Farm Mechanization Centre, Stesen Penyelidikan Usahasama MPOB/UKM, Jalan Sekolah, Pekan Bangi Lama, 43000 Kajang, Selangor, Malaysia

*Corresponding author: Ahmad Syazwan Ramli, Farm Mechanization Centre, Stesen Penyelidikan Usahasama MPOB/UKM, Jalan Sekolah, Pekan Bangi Lama, 43000 Kajang, Selangor, Malaysia; ahmad.syazwan@mpob.gov.my

Abstract: A CANTAS is a motorized palm tree cutter which is specially developed to ease the process of harvesting oil palm fresh fruit bunch (FFB). The most crucial part of this machine is the top sickle which is vibrated by the help of a motor to facilitate the cutting process. The current sickle design is made out of AISI 5160 high carbon spring steel. This paper investigates the static structural strength of the sickle by analyzing it using a Finite Element (FEM) simulation software. The mechanical structural properties of the sickle blade material are compared with A6061-T6 aluminum alloy and AISI 316 stainless steel in the software. The result of the analysis showed that spring steel has the least structural deformation when subjected under 300 N of cutting force which is only 6.42 mm compared to 6.98 mm by stainless steel and 18.94 mm by aluminum. The total stress experienced by the sickle made of spring steel, stainless steel and aluminum are 672 MPa, 671 MPa and 668 MPa respectively. Although spring steel sickle experiences the highest stress, the value does not exceed its ultimate tensile strength value which means that it will not break under such stress, unlike stainless steel and aluminum. In terms of weight, aluminum sickle is the lightest which is only 70.25 g when applied to the current design compared to 199.58 g for spring steel and 202.88 g for stainless steel. However, the disadvantage of spring steel compared to the other two materials is that the spring steel is prone to corrosion due to rust. In conclusion, the current material for the sickle design which is spring steel is the best choice of material for CANTAS when compared to aluminum and stainless steel based on the analysis done using FEM simulation.

Keywords: Oil palm fruit bunch; cutting machine; FEM analysis; material properties; metal strength

Received: 13th May 2020

Accepted: 11th June 2020

Published: 26th June 2020

Citation: Ramli AS, Shuib AR, Mohd Bakri MA, *et al.* Mechanical static structural analysis of CANTAS sickle blade. Adv Agri Food Res J 2020; 1(1): a0000095. <https://doi.org/10.36877/aafrij.a0000095>

1. Introduction

The oil palm industry is the biggest plantation commodity in Malaysia. It is also the second biggest palm oil producer in the world (Kushairi *et al.*, 2019). However, this industry still relies on traditional harvesting method which is using a sickle attached to a long pole. There is a need to develop an efficient harvesting method so that the harvesting cycle can be done within the required timeframe which is about 10 to 12 days intervals. Currently, the manual harvesting either using a sickle or the chisel is only able to produce 1 ton of fresh fruit bunch (FFB) of oil palm per man per day on average (Ismail *et al.*, 2015). Therefore, a better harvesting system is required to harvest the FFB in a more efficient way.

Malaysian Palm Oil Board (MPOB) has developed a new system of harvesting FFB by using a motorized oil palm cutter which vibrates the sickle in order to ease and make the cutting process faster and efficient. This technology is known as CANTAS and has been developed since 2007 as shown in Figure 1 (Jelani *et al.*, 2008).



Figure 1. A motorized oil palm cutter or CANTAS which was developed by MPOB.

Although CANTAS technology has been widely accepted by the oil palm industry, there is a lot of opportunities to further improve this technology so that it can be optimized and its performance can be further improved. This paper analyses the material of CANTAS's sickle part in terms of its suitability by comparing the material properties against other metals such as aluminum and stainless steel.

2. Materials and Methods

2.1. Material selection

The sickle part of CANTAS is made out of AISI 5160 high carbon steel or widely known as spring steel. This steel grade is the most common material used for a cutting tool such as sickle, short knife and machete in the agriculture sector. It consists of high carbon chromium alloy with maximum carbon content 0.61% and chromium content which is around 0.9%. It has excellent toughness, ductility and fatigue resistance. It is also used in industrial applications such as the automotive sector for various heavy-duty spring applications (The Material World, 2020). That is the reason why this steel grade is commonly known as spring steel.

The performance of spring steel material of CANTAS sickle is compared with AISI 316 stainless steel and A6061-T6 aluminum alloy. Stainless steel is chosen due to its hardness and non-corrosive characteristic which is the main reason why this material is often used to make kitchen utensils such as spoon, fork and knives. Aluminum, on the other hand, is not only chosen for its non-corrosive characteristic, but also for its lightweight characteristic. Weight of the sickle plays an important aspect because if the sickle is heavy, the stability of CANTAS is jeopardized during its operation. The extra load due to a heavy sickle will cause difficulty for the CANTAS operator to maneuver during the oil palm FFB harvesting process. Table 1 below summarizes the material properties of 3 chosen materials for this analysis.

Table 1. Material properties comparison for spring steel, stainless steel and aluminum.

Material	Density (g/cm ³)	Tensile ultimate strength (MPa)	Source
AISI 5160 Spring Steel	7.85	1025	(The Material World, 2020)
AISI Stainless Steel 316	8.03	515	(The World Material, 2020)
A6061-T6 Aluminum alloy	2.70	310	(MakeItFrom.com, 2020)

2.1. Analysis method

The comparison of the mechanical properties analysis between the 3 chosen materials is done by using a finite element method (FEM) simulation. In this analysis, FEM simulation predicts the structural mechanical behavior of the component based on the assigned physical phenomenon, loads and physical shape design via mathematical partial differential equations (Harish, 2019). Before running the simulation, a 3D computer-aided drawing (CAD) of CANTAS sickle needs to be prepared and uploaded into simulation software such as ANSYS. The sickle has a thickness of 1.2 mm and its dimension is shown in Figure 2.

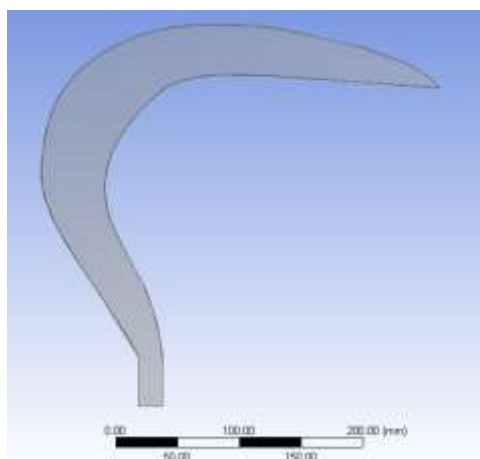


Figure 2. A 3D CAD design of CANTAS sickle.

In this software, the sickle is converted into small elements by using mesh generation tool. This enables the software to assign FEM algorithm to each and every element of the sickle design so that the computational tool in the software can perform engineering analysis to the sickle design. The mesh generation has divided the sickle CAD design into 63262 elements with 130159 nodes as shown in Figure 3.

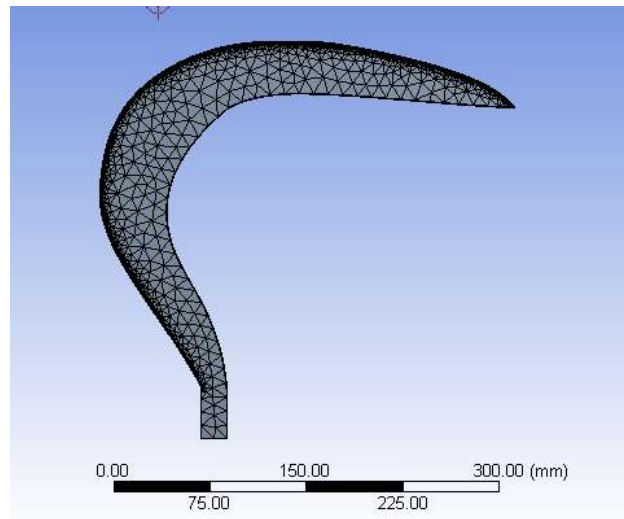


Figure 3. A CANTAS sickle after mesh generation.

Next, the specific material is assigned to the sickle design. In this simulation, material AISI 5160 high carbon steel or commonly known as spring steel is assigned to the material. This means that all of the mechanical and physical properties of the spring steel such as tensile yield and ultimate strength, density, shear and elasticity modulus and thermal expansion coefficient are pre-defined in the software. Then, the loads such as the cutting force and the fixed support are assigned to the sickle. In this case, 300 N of cutting force is applied to the upper sharp cutting edge of the sickle as shown in Figure 4 (Jelani *et al.*, 1998).

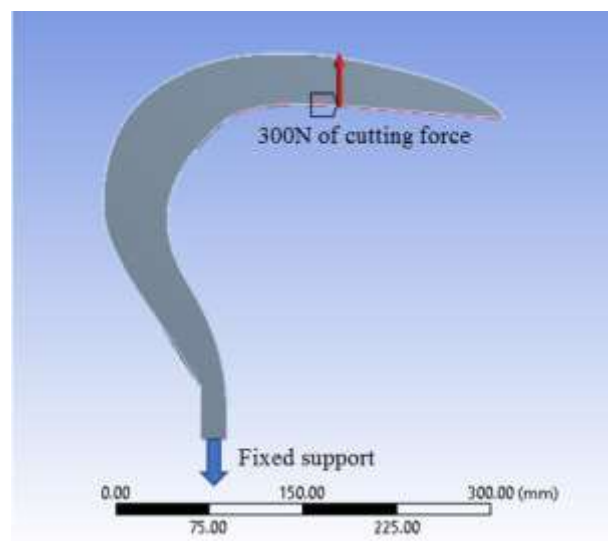


Figure 4. The loads which consist of cutting force and fixed support assigned to the sickle.

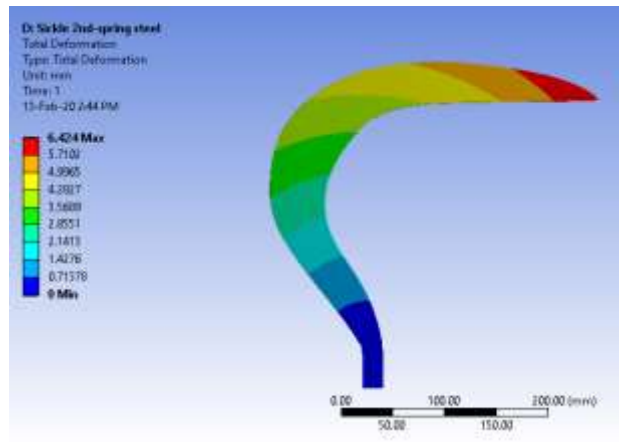
In addition, fixed support is assigned at the bottom part of the sickle which is connected to the CANTAS gearbox. After that, the software runs the computational calculation, and the simulation of how the sickle behaves under the pre-assigned loads is served as the result. The simulation is then repeated but this time, the assigned sickle material is changed to AISI 316 stainless steel and A6061-T6 aluminum alloy respectively. The obtained results such as the design weight, total deformation under loads, stress and strain experienced by the sickle design are then compared to determine which material is the most suitable for CANTAS.

3. Results and Discussion

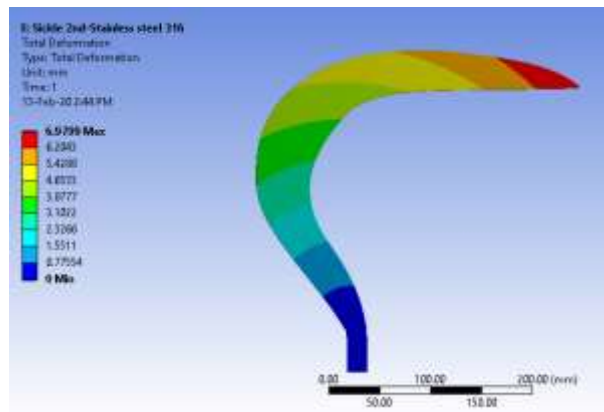
Table 2 summarizes the results obtained from the analysis. Based on the simulation done by the ANSYS software, the sickle has a total deformation of 6.42 mm at the end tip if spring steel is used as the sickle material. If the material is changed to stainless steel, the deformation of the sickle increases up to 6.98 mm which is about 8.7% increment. However, the sickle deformation has staggered much higher up to 18.94 mm which is more than double the increment of spring steel sickle if the material is aluminum alloy. Figure 5 shows the total deformations of each sickle based on the simulation result. In addition, Figure 6 compares the total deformation experienced by each metal under the cutting load graphically to determine the significance of the different deformation values.

Table 2. Summary of simulation results of spring steel, stainless steel and aluminum sickle when subjected under loads.

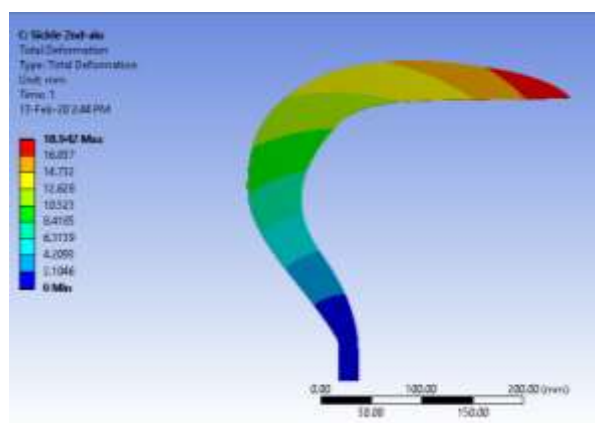
Material	Total Deformation (mm)	Stress (MPa)	Strain	Weight (g)	Corrosion Resistance
AISI 5160 Spring Steel	6.42	672	2.25×10^{-3}	199.58	No
AISI Stainless Steel 316	6.98	671	2.62×10^{-3}	202.88	Yes
A6061 Aluminum alloy	18.94	668	7.97×10^{-3}	70.25	Yes



(a)



(b)



(c)

Figure 5. The sickle's simulation result of total deformation of spring steel (a), stainless steel (b) and aluminum (c).

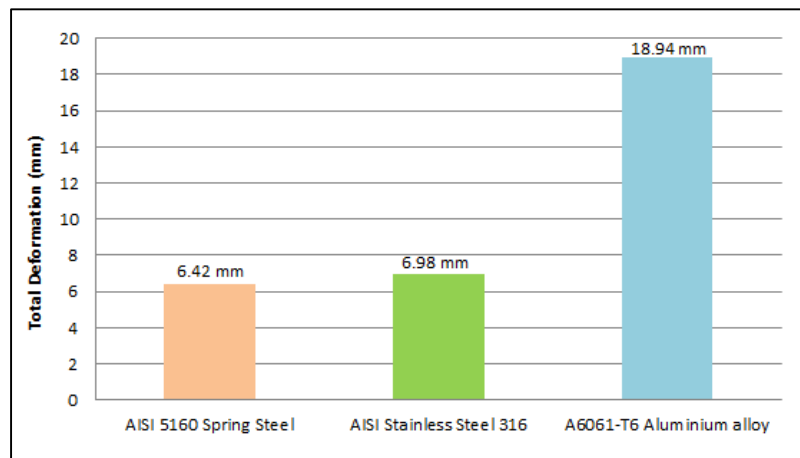
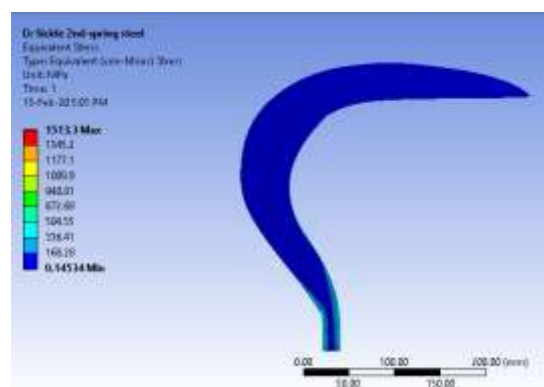


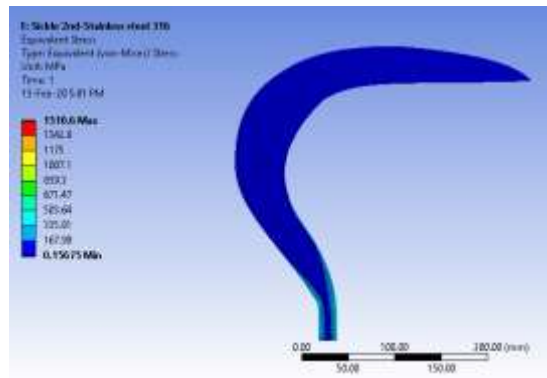
Figure 6. A graphical comparison of total deformation experienced by each metal under cutting load.

High deformation on the sickle is not favorable as it can decrease the efficiency of the cutting ability as well as cause mechanical failure to the sickle. This means that the sickle can break during its usage. As shown in Figure 6, the performance of the stainless-steel sickle in terms of material deformation only differs slightly which is 0.76 mm difference compared to spring steel sickle. However, the deformation of aluminum sickle differs up to 3 times the value of spring steel which makes the aluminum as unsuitable material for the sickle application.

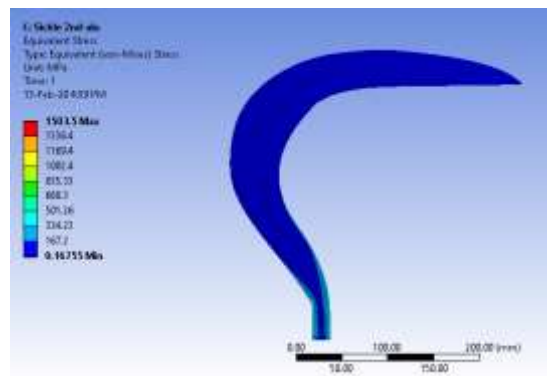
The results of stress and strain experienced by the sickle under the assigned loads are then compared among the different materials. The sickle using spring steel material experiences 672 MPa of stress. For the stainless-steel sickle, the stress is 671 MPa whereas, for aluminum alloy, the stress is 668 MPa. The results of the stress and strain experienced by the sickle with different materials are depicted in Figure 7. In addition, Figure 8 shows a comparison of the values for each metal against their respective ultimate tensile strength value to determine whether the sickle structure will fail or not when subjected under the cutting force.



(a)



(b)



(c)

Figure 7. The sickle’s simulation results of stress experienced by spring steel (a), stainless steel (b) and aluminum (c).

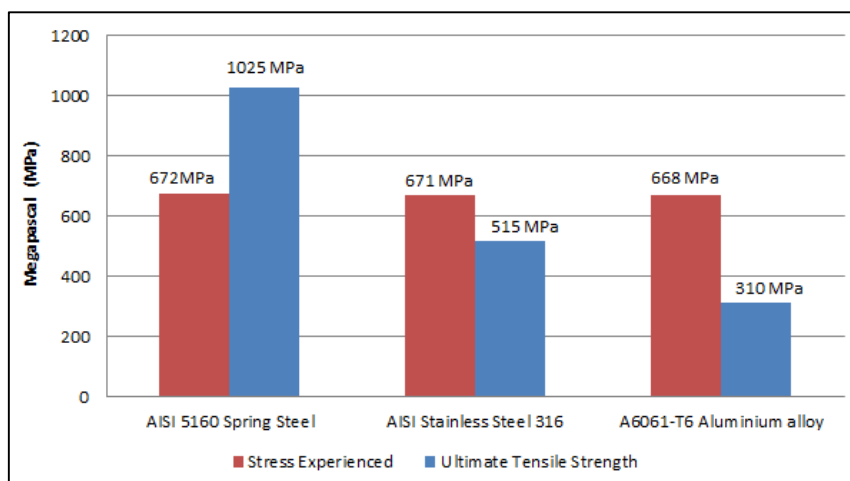


Figure 8. A graphical comparison of stresses experienced by each metal under cutting load versus the metal’s ultimate tensile strength value.

Based on the stress value, the spring steel sickle can withstand the stress because it does not exceed the material ultimate tensile strength which is 1025 MPa. As for stainless steel and aluminum sickles, the stress value experienced by each of the sickles already exceeds their ultimate tensile strength which means that the sickles will break when subjected under those cutting force and such stress. Other than that, the value of strain experienced by each of the metal is also simulated. The least strain value of the spring steel sickle means that it has the least deformation when subjected to the load of the cutting force. Figure 9 shows the simulation results for the strain experienced by each metal whereas Figure 10 compares the value of strains experienced by the metal graphically.

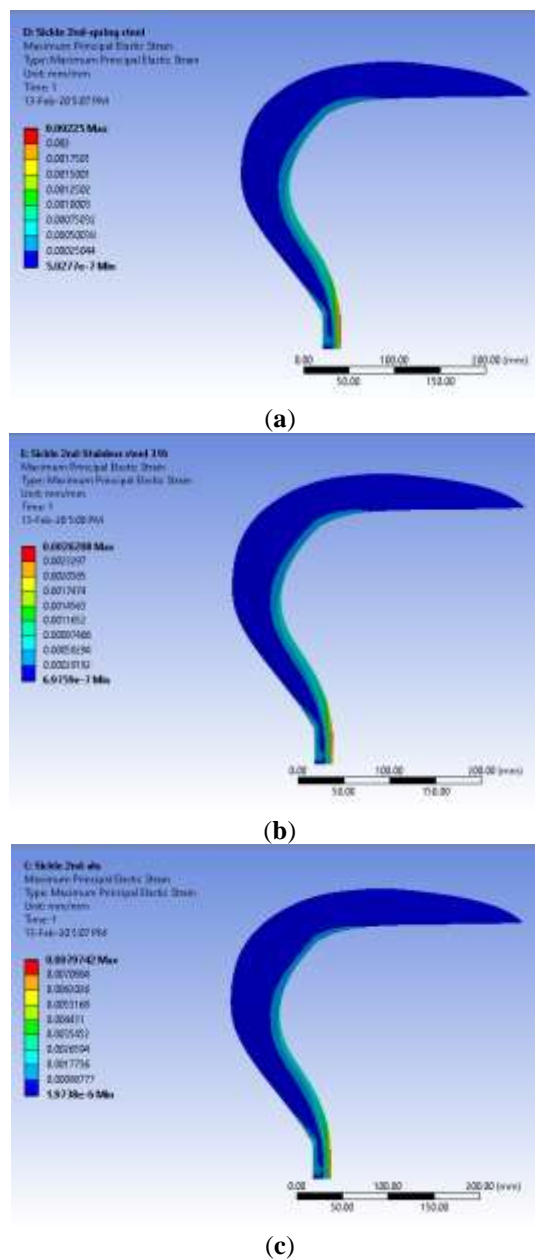


Figure 9. The sickle's simulation results of strain experienced by spring steel (a), stainless steel (b) and aluminum (c).

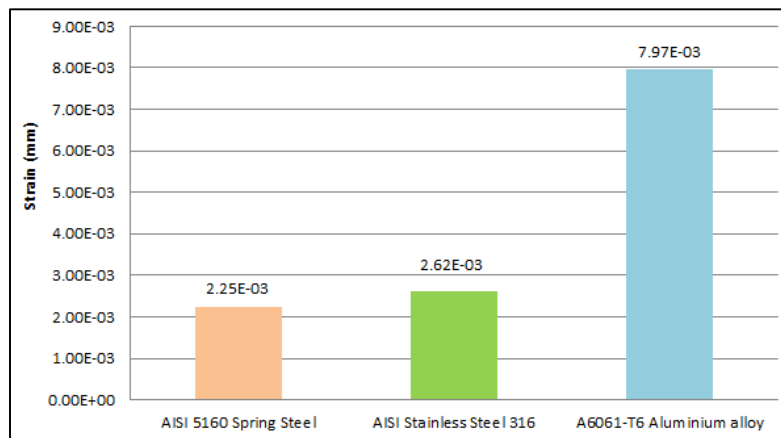


Figure 10. A graphical comparison of strain experienced by each metal under cutting load.

Based on the simulation result, the value of strain experienced by the spring steel sickle is 2.25×10^{-3} . The value of strain experienced by the stainless-steel sickle is slightly higher which is 2.62×10^{-3} whereas the aluminum sickle has the highest strain value which is 7.97×10^{-3} . As shown in Figure 10, the strain value of aluminum sickle is 3.5 times much higher than spring steel sickle. Thus, the performance of aluminum sickle in terms of strain experienced by the sickle is ranked as the worst compared to stainless steel and spring steel.

In addition, the weight of the sickle using different materials can be determined by the software since the density of each material is pre-defined and the software is able to determine the volume of the sickle based on its CAD shape design. Therefore, a comparison of weight can also be done to find the lightest sickle for CANTAS application. Lightweight is an important characteristic for a CANTAS sickle because its weight can produce an additional load or downward torque on the CANTAS pole. Figure 11 summarizes the weight comparison of a sickle if it is made out of these metals.



Figure 11. A graphical comparison of sickle weight with different metals.

Based on the software calculation, the weight of the sickle when using spring steel, stainless steel and aluminum are 199.58 g, 202.88 g and 70.25 g respectively. The weight of

the aluminum sickle is almost 3 times lighter compared to spring steel and stainless-steel sickles. This clearly shows that a sickle using aluminum has the advantage of being the lightest among the 3 chosen materials. Aluminum alloy also has a corrosion-resistant characteristic which means that it does not rust. It only oxidizes and produces an aluminum oxide layer that protects the surface from further corrosion. However, aluminum cannot be accepted as a suitable material for CANTAS sickle because the material has already failed to withstand the stress and the cutting load based on the simulation result. As for stainless steel, the material also cannot withstand the stress and failed when subjected under the assigned load. In addition, the extra weight due to its density also makes it less favorable in comparison with spring steel. Therefore, the only advantage it has as a material for a sickle is the corrosion resistance characteristic.

4. Conclusion

The results show that spring steel material is the most suitable material to be used for CANTAS sickle. This is because of its performance under the assigned loads which can withstand the cutting force of 300 N without experiencing any mechanical failure based on the simulation. This means that spring steel has a higher strength compared to the other 2 metals. The stress experienced by the spring steel sickle will not compromise its structural integrity as well as its ability to withstand deformation. Other materials which are stainless steel and aluminum alloy have proved to fail and break when subjected with such cutting force since the stress value experienced by the materials exceeds their respective ultimate tensile strength value. The strain value experienced by the spring steel is also the lowest compared to stainless steel and aluminum alloy. This means that spring steel experienced the least amount of deformation and thus is more favorable as a suitable material for a CANTAS sickle. Although the corrosion-resistant characteristic and weight of spring steel sickle cannot compete against the aluminum alloy sickle, these characteristics are not the main concern for a CANTAS sickle and only serve as an additional added value for it. Therefore, it can be concluded that spring steel is the best choice of material for a CANTAS sickle if it is compared with a sickle made out of stainless steel and aluminum alloy.

Author Contributions: Conceptualization, Ahmad Syazwan Ramli and Ikmal Hafizi Mohd Azaman; methodology, Mohd Rizal Ahmad; software, Ahmad Syazwan Ramli; validation, Mohd Khairul Fadzly Md Radzi, Mohd Azwan Mohd Bakri and Mohd Ramdhan Khalid; formal analysis, Ahmad Syazwan Ramli; investigation, Ahmad Syazwan Ramli; resources, Ahmad Syazwan Ramli; data curation, Ahmad Syazwan Ramli; writing — original draft preparation Ahmad Syazwan Ramli; writing — review and editing, Abd Rahim Shuib and Salmah Jahis.

Funding: No external funding was provided for this research.

Conflicts of Interest: The authors declare no conflict of interest.

References

- Harish, A. (2019, August 9). *Simscale*. Retrieved from: <https://www.simscale.com/blog/2016/10/what-is-finite-element-method/>
- Ismail, A., Ahmad, S. M., & Sharudin, Z. (2015). Labour productivity in the Malaysian oil palm plantation sector. *Oil Palm Industry Economic Journal*, 15(2), 1–10.

Jelani, A. R., Ahmad, D., Hitam, A., *et al.* (1998). For and energy requirements for cutting oil palm frond. *Journal of Oil Palm Research*, 10(2), 10–24.

Jelani, A. R., Hitam, A., & Jamak, J., *et al.* (2008). Cantas™ —A tool for the efficient harvesting of oil palm fresh fruit bunches. *Journal of Oil Palm Research*, 20, 548–558.

Kushairi, A., Ong-Abdullah, M., & Nambiappan, B., *et al.* (2019). Oil palm economic performance in Malaysia and r&d progress in 2018. *Journal of Oil Palm Research*, 31(2), 165–194.
doi:10.21894/jopr.2019.0026

MakeItFrom.com. (2020). 6061-T6 Aluminum. Retrieved February 3, 2020, from <https://www.makeitfrom.com/material-properties/6061-T6-Aluminum/>

The World Material. (2020). SAE AISI 5160 steel, high carbon 5160 spring steel properties, composition. Retrieved February 3, 2020, from <https://www.theworldmaterial.com/sae-aisi-5160-high-carbon-spring-steel/>

The World Material. (2020). Grade AISI 316 stainless steel, SS316 (UNS S31600) properties, density, composition, yield strength, thermal Conductivity. Retrieved February 3, 2020, from <https://www.theworldmaterial.com/aisi-316-ss316-stainless-steel-properties-composition/>



Copyright © 2020 by Ramli AS *et al.* and HH Publisher. This work is licensed under the Creative Commons Attribution-Noncommercial 4.0 International License (CC-BY-NC4.0)

Original Research Article

Isolation of nanocellulose from Saba' (*Musa acuminata x balbisiana*) banana peel by one-pot oxidation-hydrolysis system

Suryani Saallah^{1*}, Jumardi Roslan², Nurul Nadjwa Zakaria², Wolyna Pindi², Shafiquzzaman Siddiquee¹, Mailin Misson¹, Clarence M. Ongkudon¹, Nur Hidayah Azmirah Mohd Jamil¹, Wuled Lenggoro³

¹Bioetchnology Research Institute, Universiti Malaysia Sabah, Jalan UMS, 88400 Kota Kinabalu, Sabah.

²Faculty of Food Science and Nutrition, Universiti Malaysia Sabah, Jalan UMS, 88400 Kota Kinabalu, Sabah.

³Institute of Engineering, Tokyo University of Agriculture and Technology, 2-24-16 Nakacho, Koganei, Tokyo, 184-8588, Japan.

*Corresponding author: Suryani Saallah, Bioetchnology Research Institute, Universiti Malaysia Sabah, Jalan UMS, 88400 Kota Kinabalu, Sabah, suryani@ums.edu.my

Abstract: In the present study, a facile one-pot production of nanocellulose from ripe and unripe Saba' banana (*Musa acuminata x balbisiana*) peel was conducted by utilising hydrogen peroxide (H₂O₂) as an oxidising agent prior to hydrolysis with sulphuric acid (H₂SO₄) at different concentrations (8%, 24% and 40%). Proximate and chemical compositions of the ripe and unripe banana peel (BP) powder were analysed, followed by physicochemical characterisations of the resulting nanocellulose by using Scanning Electron Microscopy (SEM), Fourier Transform Infrared (FTIR) spectroscopy and Dynamic Light Scattering (DLS). FTIR analysis has confirmed the successful removal of non-cellulosic components from the BP through the distinguishable spectra of both the ripe and unripe BP powder with the H₂O₂/H₂SO₄- treated samples. SEM analysis revealed morphological changes of the BP powder from an irregular structure with the presence of starch granules to lamellar and fibrous structures after the H₂O₂/H₂SO₄ treatment and freeze-drying. The size of the nanocellulose is strongly influenced by the concentration of H₂SO₄ used. Nanocellulose from ripe BP produced by using the 40% H₂SO₄ has the smallest size with D₅₀ < 80 nm. These findings suggest the potential of banana peel, an abundant agricultural waste to be valorised into value-added materials with significant economic potentials.

Keywords: banana peel; nanocellulose; one-pot process; hydrogen peroxide pre-treatment; acid hydrolysis

Received: 18th May 2020

Accepted: 11th June 2020

Published: 26th June 2020

Citation: Saallah S, Roslan J, Zakaria NN, *et al.* Isolation of nanocellulose from Saba' (*Musa acuminata x balbisiana*) banana peel by one-pot oxidation-hydrolysis system. Adv Agri Food Res J 2020; 1(1): a0000096. <https://doi.org/10.36877/aafj.a0000096>

1. Introduction

The gradual depletion of petroleum sources has made it necessary for the investigation of renewable alternatives as a source of materials and energy. Therefore, research and development in nanocellulose production, a green, bio-based and renewable biopolymer is currently a subject of immense interest as a promising alternative to the conventional petroleum-based materials. A recent report by the Global Market Insights, Inc. (2019) forecasted that the global nanocellulose market will exceed USD 1 billion in 2024 with an impressive CAGR of 33.8%. Owing to its desirable attributes such as eco-friendly nature, good biocompatibility, exceptional mechanical strength, tailorable surface chemistry and unique rheological behaviour, nanocellulose is viewed as an important advanced biomaterial that opens a new horizon in material science and its application. This includes as a filler or reinforced agent for composites and polymer matrixes, stabilising and thickening agents in food and cosmeceutical products, drug delivery excipient, biodegradable packaging, environmental remediation, among others (Camacho *et al.*, 2017; Tibolla *et al.*, 2018).

In the last few years, agricultural wastes have been utilised as an attractive source for nanocellulose production because these wastes consist mainly of plant fibres that are rich in cellulose, the main component of plant cell walls. Isolation and characterisation of nanocellulose from agricultural wastes such as sugarcane and cassava bagasse, pineapple fibres, vegetable and fruit peels such as potato, carrot, tomato and banana have been reported in a number of research papers (Malladi *et al.*, 2018; Camacho *et al.*, 2017; Moreno *et al.*, 2018).

Banana is one of the world's most popular fruits and its cultivation is widespread in most tropical countries including Malaysia. Due to the high consumption and industrial processing of the edible parts of the banana, a huge quantity of by-products such as peel is generated. The peel which accounts for about 35% of the whole fruit weight is cellulose-rich residues. Orozco *et al.* (2014) reported that the cellulose content in banana peel (11.45%) was higher than mango peel (9.19%) and comparable to orange peel (11.93%). Thus, this is a potential material for further utilisation (Tibolla *et al.*, 2014; Harini *et al.*, 2018). In this sense, research for the utilisation of banana peel as a source of nanocellulose has become increasingly attractive.

In the existing method of isolation of nanocellulose, pre-treatment followed by acid hydrolysis are the typical procedures by which the non-cellulosic components such as lignin and hemicellulose are deconstructed into soluble ones, leaving behind the insoluble residue of nanocellulose (Tibolla *et al.*, 2017; Harini *et al.*, 2018). However, the conventional methods usually involve several pre-treatment steps such as alkalisation, bleaching and successive washing to prepare relatively pure cellulosic starting materials prior to hydrolysis. These tedious and time-consuming steps will impede large-scale production and applications of nanocellulose (Leung *et al.*, 2011). Moreover, the use of high acid concentration (typically in the range of 60 to 65%) during hydrolysis possesses several downsides such as corrosive, high tendency of cellulose over-degradation, low yield, requires a huge amount of water for neutralisation and generates a huge amount of waste which eventually causes environmental pollution (Chen, 2017; Harini *et al.*, 2018; Chen *et al.*, 2019).

In view of these drawbacks, the present study reported for the first time a facile one-pot production of nanocellulose from ripe and unripe Saba' banana (*Musa acuminata x balbisiana*) peel by utilising hydrogen peroxide as a bleaching agent prior to mild sulphuric acid hydrolysis with the concentration of 8%, 24% and 40%, much lower than the commonly used acid concentration. Hydrogen peroxide (H₂O₂) provides a safer alternative to the

chemicals commonly used for alkalisation and bleaching of banana peel such as potassium hydroxide (KOH), sodium hydroxide (NaOH) and sodium chlorite (NaClO₂) because the decomposition of H₂O₂ produces water and oxygen thus, creating no harmful by-product, eliminating the needs of successive washing procedures and ultimately enabling the application of the one-pot process in less severe conditions (Chen *et al.*, 2019). The findings of this study provide an insight into the improvement of the traditional nanocellulose isolation method from banana peel. Moreover, the utilisation of banana peel, an abundant agricultural waste would help to overcome environmental pollution issues and increase the economic value of the underutilised resources.

2. Materials and Methods

2.1. Materials

Unripe and ripe Saba' bananas (*Musa acuminata x balbisiana*) with maturity stage 1 (green) and stage 7 (yellow peel with little brown spot), respectively, were obtained from a local market in Kota Kinabalu, Sabah, Malaysia. All the chemicals used in this study such as hydrogen peroxide and sulphuric acid are of reagent grade and were purchased from Merck Malaysia. A cellulose standard (microcrystalline) was purchased from Sigma-Aldrich. Millipore deionised water was used throughout this work.

2.2. Preparation of Banana Peel (BP) Powder

The BPs were manually removed from the flesh and immediately soaked in 2% sodium metabisulfite solution for 24 h to prevent oxidation. Next, the peels were arranged in an aluminium tray followed by drying in an oven at 60°C for 48 h. The dried peels were then ground into fine powder and sieved through a 200-mesh sieve. The ripe and unripe BP powder was then stored in an airtight container at room temperature until further use. Procedures for the preparation of BP powder are as shown in Figure 1.



Figure 1. Procedures for the preparation of BP powder

2.3. Isolation of BP Nanocellulose by One-Pot Process

Fabrication of nanocellulose from the ripe and unripe BP powder was carried out by using a one-pot process following a method described by Chen *et al.* (2019) and Tibolla *et*

al. (2018) with modifications. Briefly, 10 g of the dried BP powder was soaked in deionised water under continuous stirring for 24 h and filtered to remove water from the sample. After that, bleaching was performed with the addition of 100 ml of 30 wt% hydrogen peroxide (H_2O_2) to the swollen banana peel in a conical flask. The process was conducted at $90^\circ C$ for 5 h with mechanical agitation in a shaking water bath (SW22, JULABO GmbH, Germany) to maintain the temperature. After completion of the bleaching process, the reaction mixture was cooled down to room temperature in an ice bath. Hydrolysis of the bleached suspension was performed by adding 8%, 24% and 40% of sulphuric acid (H_2SO_4) into the same pot containing the suspension and heated to $80^\circ C$ for 1 h. To stop the reaction, the mixture was cooled with ice cubes. Successive washing with deionised water and centrifugation at 12000 rpm ($25^\circ C$) were conducted until constant pH was obtained to remove the non-fibrillated cellulose components and excess reactants and concentrate the nanocellulose. The final insoluble residue was then ultrasonicated in a pulsing mode for 5 min to improve the dispersibility and reduce agglomeration. Finally, the resulting suspension was lyophilised and stored in a sealed container at $4^\circ C$ until further use. Figure 2 summarises the procedures for the isolation of nanocellulose from BP powder.

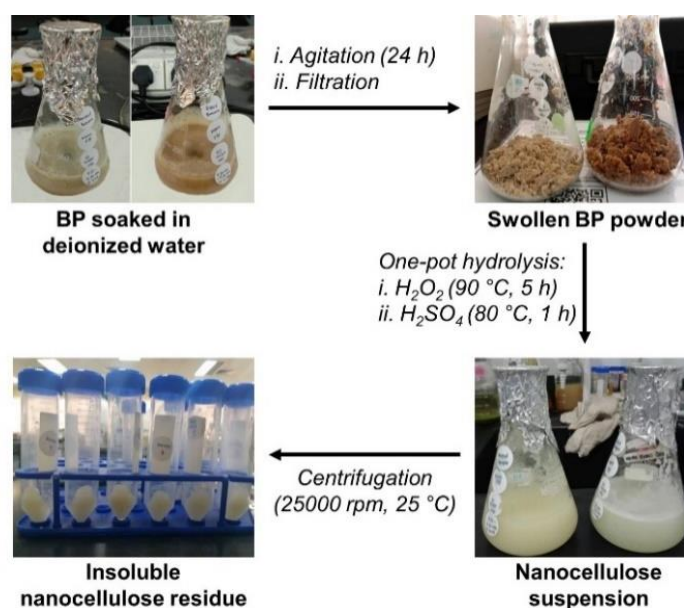


Figure 2. Steps involved in the isolation of nanocellulose from BP powder

2.4. Characterisations of the BP Powder and Nanocellulose

2.4.1 Proximate compositions analysis

Proximate compositions of the BP powder including moisture, crude protein, fat and ash contents were determined following the Association of Official Analytical Chemists (AOAC, 2005) procedure. Moisture content was determined by using the oven-dry method at $105^\circ C$

for 3 h until it reached a constant weight. The Kjeldahl method was used to determine the crude protein content using Tecator Kjeltex protein analyser (FOSS, Hillerod, Denmark). The fat content was analysed using the Soxhlet method, while the ash content was measured using a muffle furnace ashing method in which the samples were heated in a furnace at 550°C for 8–12 h. All the analyses were performed in triplicates and the results were reported as average.

2.4.2 Chemical compositions analysis

Lignocellulosic fractions of the BP powder including cellulose, hemicellulose and lignin were analysed according to the American Society for Testing and Materials (ASTM) standard methods, ASTM D1103-60, ASTM D 1104-56 and ASTM D1106-56, respectively. Each test was conducted in duplicates, and the average values were reported.

2.4.3 Fourier-Transform Infrared Spectroscopy (FTIR) Analysis

Fourier-Transform Infrared Spectroscopy (FTIR) was used to identify functional groups present in the samples and changes in chemical compositions of the BP powder after hydrolysis with 8%, 24% and 40% H₂SO₄. The absorbance spectra were collected using Agilent Cary 630 FTIR Spectrometer (Agilent Technologies Inc., USA) in the infrared region between 4000 and 600 cm⁻¹ with a spectral resolution of 4 cm⁻¹ and 32 scans at room temperature (Tibolla *et al.*, 2018). FTIR spectrum of standard cellulose was used as a reference.

2.4.4 Scanning Electron Microscope (SEM) Analysis

Morphology of the ripe and unripe BP powder and the lyophilised nanocellulose suspensions were viewed by using SEM. The samples were fixed on an aluminium stub and sputter-coated with gold prior to the SEM observation. The analysis was performed using an accelerating voltage of 10 kV. Morphology of the standard cellulose was also observed for comparison.

2.4.5 Dynamic Light Scattering (DLS) Analysis

Particle size distribution of the nanocellulose suspensions was measured using NanoPlus (Particulate Systems, USA) particle analyser. The nanocellulose suspensions were prepared by diluting the lyophilised samples in ethanol (0.1 wt%) followed by 5 min ultrasonication to improve sample dispersibility and reduce agglomeration. The DLS measurements were performed at room temperature (25°C). The result is presented as the average value of three measurements.

2.5. Statistical analysis

The SPSS 25.0 was used to perform the statistical analysis of ANOVA and Tukey test of multiple comparisons. A *p*-value of less than 0.05 was considered significant.

3. Results and Discussion

3.1. Proximate and Chemical Compositions of the BP Powder

Table 1 shows the proximate compositions of unripe and ripe BP powder. Both samples have relatively low moisture content ($7.13 \pm 0.12\%$ and $7.26 \pm 0.02\%$, respectively), indicating that the BP was less susceptible to microbial degradation and chemical changes, thus can be stored for a more extended period. As opposed to the unripe BP, the ripe BP has significantly higher ash, fat and protein contents ($p < 0.05$), which agrees with the findings reported by Ramli *et al.* (2010) and Emaga *et al.* (2007). The ash content of the sample gives information about the mineral element composition, associated with the absorption of mineral salts by the plant. The higher fat content of the ripe BP could be due to the continuous synthesis of fatty acids during fruit metabolism. The slightly higher crude protein content of the ripe BP ($7.48 \pm 0.36\%$) than that of the unripe BP ($6.56 \pm 0.06\%$) can be explained by the breakdown and synthesis of the protein that occurs during fruit ripening. An increase in the crude protein content of BP with increasing maturity has also been reported by Khawas and Deka (2016).

Table 1. Proximate compositions of unripe and ripe BP powder*

Component	Unripe BP powder	Ripe BP powder
Moisture (%)	7.13 ± 0.12	7.26 ± 0.02
Ash (%)	10.16 ± 0.03	15.62 ± 0.06
Fat (%)	9.78 ± 0.16	13.59 ± 0.11
Crude protein (%)	6.56 ± 0.06	7.48 ± 0.36

*Data are mean values of three replicates \pm standard deviation

Results of ASTM chemical compositions analysis of the ripe and unripe BP powder are shown in Table 2. Both samples have a considerable amount of cellulose that can be potentially exploited to produce nanocellulose. Based on the existing information on nanocellulose isolation from BP, most studies utilise the unripe BP as a source of cellulose instead of the ripe BP. But the present study found that the cellulose composition in the ripe BP powder is more than 50% higher than the unripe BP, associated with the increase in enzymatic activity of cellulose synthase during fruit ripening. This enzyme is responsible for the synthesis of cellulose in the primary and secondary walls of plant cells (Emaga *et al.*, 2008). This finding is supported by Khawas and Deka (2016) where the cellulose content of plantain banana peel (*Musa ABB*) is different at ripening stages.

As opposed to the cellulose content, the unripe BP shows significantly higher hemicellulose content than that of the ripe BP. Hemicellulose plays a vital role in maintaining the cell wall integrity together with lignin and cellulose. Cell biosynthesis, proliferation and prolongation at the early stages of fruit development are said to be the factors that contribute to the higher hemicellulose content of the unripe BP. Cell growth is modulated by enzymes that alter the structure of pectin and hemicellulose, thereby altering the interaction of these components. When growth is stopped, it is co-regulated by a reduction in the expression of the gene resulting in cell wall loosening and changes in the polysaccharide matrix leading to less cell extensible wall (Cosgrove, 2014). Lignification of the cell wall components during fruit ripening has resulted in higher lignin content in the ripe BP.

Table 2. Chemical compositions of unripe and ripe BP powder*

Component	Unripe BP powder	Ripe BP powder
Cellulose (%)	7.45 ± 1.92	11.89 ± 1.02
Hemicellulose (%)	21.56 ± 0.11	15.26 ± 0.67
Lignin (%)	7.31 ± 1.14	9.29 ± 1.30

*Data are mean values of three replicates ± standard deviation

3.3. FTIR analysis

FTIR spectroscopy analysis was used to identify changes in the chemical composition of the ripe and unripe BP in response to hydrolysis with different acid concentrations. As shown in Figure 3, the FTIR spectra of all samples have two major absorbance regions located in the high (3700-2800 cm⁻¹) and low (1800-800 cm⁻¹) wavenumbers. The broad -OH stretching vibration band in the 3700-3000 cm⁻¹ region reflected the hydrophilicity of the banana fibre and gave essential information regarding inter- and intra-molecular hydrogen bond vibrations. The similarity of the absorption peak between the raw materials (unripe and ripe BP powder) to that of the treated samples at this region is a clear indication that the crystalline cellulose in the raw materials was not disrupted during the nanocellulose isolation process. The peak located at ~2900 cm⁻¹ was due to the C-H stretching vibrations on polysaccharides (Chen *et al.*, 2017).

Overall, the spectra of ripe and unripe BP powder are almost similar except for the appearance of a peak at 1075 cm⁻¹ (pointed by the arrow in Figure 3(b)) for the unripe BP related to the presence of xylans associated with hemicellulose, which agrees well with the result of chemical composition analysis in Table 2 in which the unripe BP has higher hemicellulose content. The shoulder at 1730 cm⁻¹ in the ripe and unripe BP powder was attributed to vibrations of the acetyl and uronic ester groups of hemicelluloses or to the ester linkage of the carboxylic group of the ferulic and p-coumaric acids of lignin (Mukwaya *et al.*, 2017; Heloisa Tibolla *et al.*, 2017). The gradual disappearance of this peak for the

H₂O₂/H₂SO₄-treated samples indicated deacetylation of hemicellulose and delignification. An obvious peak at 1640 cm⁻¹ for the unripe BP powder is usually associated with adsorbed water and could also originate from carbonyl stretching conjugated with aromatic rings as observed by Tibolla *et al.* (2014) for nanocellulose isolated from *Musa paradisiaca* banana peel (Heloisa Tibolla *et al.*, 2014). For the ripe BP, the peak is located at lower wavenumber region (1603 cm⁻¹) associated with aromatic skeletal vibration (Han *et al.*, 2013). These peaks were gradually diminished as the ripe and unripe BP powder underwent one-pot hydrolysis with increasing acid concentration, indicating the removal of most of the lignin and hemicellulose fractions during the nanocellulose isolation process. The peak at 897 cm⁻¹ which referred to typical cellulose structure (Chen *et al.*, 2019) is not observed in the untreated samples but appears in the spectra of the standard and all the H₂O₂/H₂SO₄-treated samples confirming successful isolation of cellulose and nanocellulose from the BP powder.

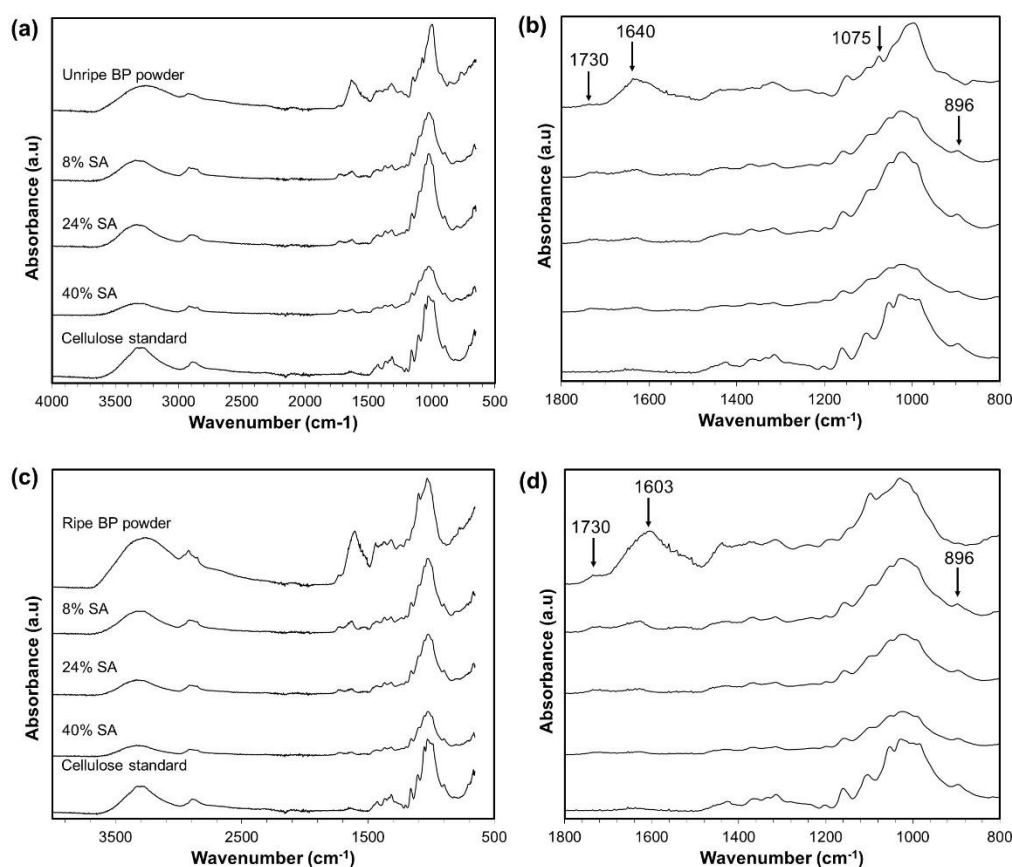


Figure 3. FTIR spectra of (a, b) unripe BP samples and (c, d) ripe BP samples after H₂O₂/H₂SO₄ treatment with different acid concentrations. Spectra of untreated ripe and BP powder and cellulose standard were also plotted for comparison.

3.4 Morphological characterisation

After the one-pot isolation process, the resulting nanocellulose suspensions were freeze-dried and their morphological structure was characterised by SEM as presented in Figure 4. The standard cellulose exhibited a compact structure (Figure 4a) which was attributed to the strong and tightly packed hydrogen bonding networks of cellulose fibrils which made them highly ordered and rigid. The unripe BP powder shows an irregular structure with rough surfaces (Figure 4b), while the ripe BP has a more consistent globular structure with the presence of starch granules (Figure 4c). Different morphology of the ripe and unripe BP powder could be due to the variation in proximate and chemical compositions.

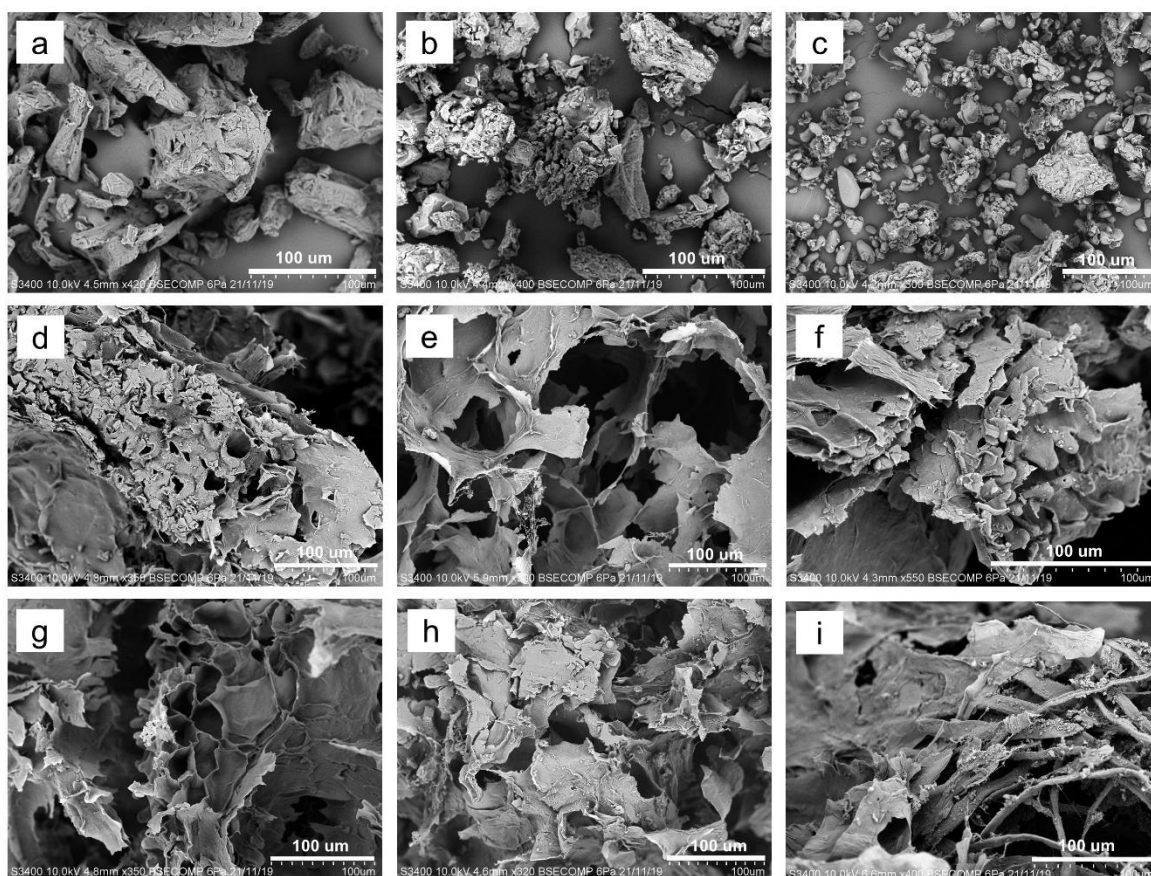


Figure 4. SEM images of (a) microcrystalline cellulose (standard), (b) unripe BP powder, (c) ripe BP powder, (d–f) $\text{H}_2\text{O}_2/\text{H}_2\text{SO}_4$ -treated unripe BP after $\text{H}_2\text{O}_2/\text{H}_2\text{SO}_4$ treatment with 8%, 24% and 40% sulphuric acid, respectively and (g–i) ripe BP after $\text{H}_2\text{O}_2/\text{H}_2\text{SO}_4$ treatment with 8%, 24% and 40% sulphuric acid, respectively.

Regardless of the BP source (ripe or unripe) and acid concentration, all the isolated nanocellulose samples appear as a porous network with a unique lamellar structure (Figure 4d to 4i). Closer observation revealed ultrafine fibres and particles adhere to the nanocellulose surface. Interestingly, a honeycomb structure can be clearly seen in Figure 4 (g). This structure is related to the good stability of the nanocellulose in colloidal suspension

(Lavoine & Bergström, 2017).

Possible mechanism of the formation of lamellar structure upon freeze-drying of nanocellulose could be inferred from the strong hydrogen bonding between the cellulose sub-units, promoting self-assembly of the nanocellulose (Han *et al.*, 2013). Before freezing, the nanocellulose was initially stable due to electrostatic repulsion between the negatively charged sulphate groups present on its surface. As the freeze-drying progresses, the development of ice crystals gradually forms a lamellar microstructure. This process causes the nanocellulose particles to concentrate and be trapped in the space between these ice crystals. As a result, the nanocellulose was reorganised in a longitudinal direction and induced self-assembly followed by the formation of larger cellulose clusters via hydrogen and van der Waals bonds.

Han *et al.* (2013) also postulated that the self-assembly mechanism of nanocellulose suspension is predominantly influenced by the concentration of nanocellulose in the suspension. Generally, at higher acid concentration, a higher concentration of nanocellulose suspension was produced. In this case, the gap between the self-assembled microfibre layers was very small, thus increasing the tendency of forming hydrogen bonding with the adjacent microfibrils. These microfibrils were aligned to form a dense, layered structure, as observed in Figure 4(f) and 4(i) for nanocellulose isolated with 40% acid concentration. In contrast, the nanocellulose that was isolated using lower acid concentration (8% and 24%) tended to form a loose structure with bigger space between the self-assembled microfibrils owing to the weakening hydrogen bonding and interfacial attraction.

3.5 Particle size distribution

A dynamic light scattering (DLS) analysis was used to analyse the size of the nanocellulose in the suspension and the results are presented in a cumulative frequency distribution. As shown in Figure 5, the average hydrodynamic size of the standard cellulose is 42918.6 ± 9658.2 nm, consistent with the size given by the manufacturer, indicating the reliability of the results obtained from the DLS measurements. The unripe BP powder subjected to the one-pot isolation process with sulphuric acid of 8%, 24% and 40% concentrations yielded nanocellulose with average sizes of 362.2 ± 191.5 nm, 328.1 ± 140.8 nm and 176.1 ± 48.6 nm, respectively (Figure 5a). For the ripe BP, the average sizes of the isolated nanocellulose are 701.6 ± 226.1 nm, 258.6 ± 111.2 nm and 78.6 ± 72.0 nm, respectively (Figure 5b). These results indicate that the source of raw material (ripe or unripe) and concentration of acid used for hydrolysis have a significant influence on the size of the isolated nanocellulose. The shown hydrodynamic size appears to decrease as the acid concentration increases because, during acid hydrolysis, the β -1,4 glycoside bond of cellulose is broken which causes the polymer chain to shorten and thus decreases the physical dimension (Camacho *et al.*, 2017).

Successful isolation of nanocellulose from BP powder can be confirmed as more than 95% of the volume fraction of the particles lies in the nanometric range, except for the ripe

BP powder treated with 8% sulphuric acid. This could be due to the higher lignin content of the raw material as presented earlier in the chemical composition and FTIR analyses. The ripe BP powder underwent about 10 folds reduction in size with increasing acid concentration from 8% to 40% while for the unripe BP, only two folds size reduction was observed, respectively. From all the samples investigated, the ripe BP powder treated with 40% sulphuric acid exhibited the smallest hydrodynamic size in which about 70% of the particles are having a size below 100 nm. However, the definite reason as to why the size reduction in ripe BP samples is more pronounced than the unripe BP with increasing acid concentration is unclear and rarely discussed. Moreover, to our knowledge, a comparison of nanocellulose isolation from ripe and unripe BP samples has never been reported. Therefore, future studies should focus on investigating the structural differences between the ripe and unripe BP powders that could elucidate these interesting findings.

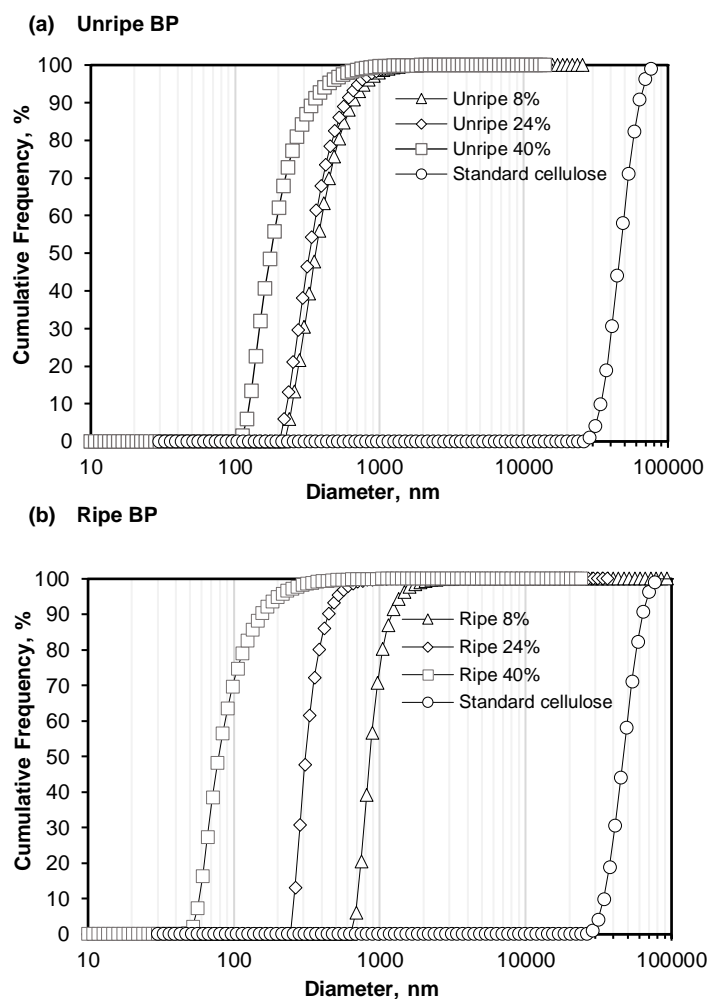


Figure 5. DLS analysis of ripe and unripe BP powder after one-pot $\text{H}_2\text{O}_2/\text{H}_2\text{SO}_4$ treatment with different acid concentration. Result of standard cellulose.

The use of 60–65% H₂SO₄ has been extensively reported for isolation of nanocellulose from various sources such as sugar beet (Leitner *et al.*, 2007), sugarcane bagasse (Mandal & Chakrabarty, 2011) and pomelo peel (Mat Zain *et al.*, 2014) with sizes of 30–100 nm, 18–220 nm and 100–150 nm, respectively. This is due to the premise that lower acid concentration would prevent the formation of nanocellulose (Camacho *et al.*, 2017; Maciel *et al.*, 2019; Shanmugarajah *et al.*, 2015). However, in this study, it is proven that nanocellulose can be isolated from banana peel under milder acid hydrolysis conditions with the aid of hydrogen peroxide as a green oxidising agent.

4. Conclusion

The present study has discovered the potential of unripe and ripe Saba' banana peel, underutilised lignocellulosic biomass to be valorised into nanocellulose. The unripe and ripe BP are having different proximate and chemical compositions, which influence the properties of the resultant nanocellulose. The application of one-pot oxidation-hydrolysis approach by utilising hydrogen peroxide as a green oxidising agent prior to hydrolysis with sulphuric acid at mild concentrations is proven effective for the isolation of nanocellulose. The nanocellulose exhibits a porous lamellar structure, typical behaviour of nanocellulose under freeze-drying condition while the chemical structure resembles those of the standard cellulose as verified by FTIR. Besides the source of the material (ripe or unripe), the concentration of sulphuric acid used has a strong impact on the size of the nanocellulose. This observation has been validated by the DLS results by which higher concentration of sulphuric acid favoured solubilisation of the non-cellulosic components including lignin and hemicellulose and facilitate isolation of nanocellulose with smaller size. The size reduction in ripe BP is more pronounced than the unripe BP with increasing acid concentration. However, the reason behind this finding remains unclear and calls for further investigation. Overall, the one-pot approach employed in this study provides a simpler alternative to the laborious and time-consuming conventional approach for isolation of nanocellulose from banana peel.

Author Contributions: Conceptualization, S.S*, J.R., W.P., and W.L.; funding acquisition, S.S*, J.R., M.M., S.S., and C.M.O.; investigation, N.N.Z. and N.H.A.M.J.; writing—original draft preparation, N.N.Z. and J.R.; writing—review and editing, S.S*, M.M., and W.L.

Funding: This research was funded by the Ministry of Education, Malaysia under FRGS-RACER scheme (RACER/1/2019/TK10/UMS//1) and Universiti Malaysia Sabah (PHD0020-2019).

Conflicts of Interest: The authors declare no conflict of interest.

References

- Camacho, M., Ureña, Y. R. C., Lopretti, M., *et al.* (2017). Synthesis and characterization of nanocrystalline cellulose derived from Pineapple peel residues. *Journal of Renewable Materials*, 5(3–4), 271–279. <https://doi.org/10.7569/JRM.2017.634117>
- Chen, Y. W. (2017). *Isolation and Characterization of Nanocrystalline Cellulose From Oil Palm Biomass Via Transition Metal Salt Catalyzed Hydrolysis Process*. Retrieved from

[http://studentsrepo.um.edu.my/7710/6/Thesis_\(Chen_You_Wei%2C_HGA_140012\).pdf](http://studentsrepo.um.edu.my/7710/6/Thesis_(Chen_You_Wei%2C_HGA_140012).pdf)

- Chen, Y. W., Hasanulbasori, M. A., Chiat, P. F., *et al.* (2019). Pyrus pyrifolia fruit peel as sustainable source for spherical and porous network based nanocellulose synthesis via one-pot hydrolysis system. *International Journal of Biological Macromolecules*, 123, 1305–1319. <https://doi.org/10.1016/j.ijbiomac.2018.10.013>
- Chen, Y. W., Tan, T. H., Lee, H. V., *et al.* (2017). Self-assembling behavior of cellulose nanoparticles during freeze-drying: Effect of suspension concentration, particle size, crystal structure, and surface charge. *Biomacromolecules*, 14(5), 1529–1540. <https://doi.org/10.1021/bm4001734>
- Emaga, H. T., Andrianaivo, R. H., Wathélet, B., *et al.* (2007). Effects of the stage of maturation and varieties on the chemical composition of banana and plantain peels. *Food Chemistry*, 103(2), 590–600.
- Emaga, H. T., Robert, C., Ronkart, S. N., *et al.* (2008). Dietary fibre components and pectin chemical features of peels during ripening in banana and plantain varieties. *Bioresource Technology*, 99(10), 4346–4354. <https://doi.org/10.1016/j.biortech.2007.08.030>
- Global Market Insights, Inc. (2019). Retrieved from <https://www.gminsights.com/pressrelease/nanocellulose-market>
- Han, J., Zhou, C., Wu, Y., *et al.* (2013). Self-assembling behavior of cellulose nanoparticles during freeze-drying: Effect of suspension concentration, particle size, crystal structure, and surface charge. *Biomacromolecules*, 14(5), 1529–1540. <https://doi.org/10.1021/bm4001734>
- Harini, K., Ramya, K., & Sukumar, M. (2018). Extraction of nano cellulose fibers from the banana peel and bract for production of acetyl and lauroyl cellulose. *Carbohydrate Polymers*, 201(June), 329–339. <https://doi.org/10.1016/j.carbpol.2018.08.081>
- Khawas, P., & Deka, S. C. (2016). Comparative Nutritional, Functional, Morphological, and Diffractogram Study on Culinary Banana (Musa ABB) Peel at Various Stages of Development. *International Journal of Food Properties*, 19(12), 2832–2853.
- Lavoine, N., & Bergström, L. (2017). Nanocellulose-based foams and aerogels: Processing, properties, and applications. *Journal of Materials Chemistry A*, 5(31), 16105–16117. <https://doi.org/10.1039/c7ta02807e>
- Leitner, J., Hinterstoisser, B., Wastyn, M., Keckes, J., & Gindl, W. (2007). Sugar beet cellulose nanofibril-reinforced composites. *Cellulose*, 14(5), 419–425. <https://doi.org/10.1007/s10570-007-9131-2>
- Leung, A. C. W., Hrapovic, S., Lam, E., Liu, Y., *et al.* (2011). Characteristics and properties of carboxylated cellulose nanocrystals prepared from a novel one-step procedure. *Small*, 7(3), 302–305. <https://doi.org/10.1002/sml.201001715>
- Maciel, M. M. Á. D., Benini, K. C. C. de C., Voorwald, H. J. C., *et al.* (2019). Obtainment and characterization of nanocellulose from an unwoven industrial textile cotton waste: Effect of acid hydrolysis conditions. *International Journal of Biological Macromolecules*, 126, 496–506. <https://doi.org/10.1016/j.ijbiomac.2018.12.202>
- Malladi, R., Nagalakshmaiah, M., Robert, M., *et al.* (2018). Importance of agriculture and industrial waste in the field of nano cellulose and its recent industrial developments: A review. *ACS Sustainable Chemistry & Engineering*, 6(3), 2807–2828. <https://doi.org/10.1021/acssuschemeng.7b03437>
- Mandal, A., & Chakrabarty, D. (2011). Isolation of nanocellulose from waste sugarcane bagasse (SCB) and its characterization. *Carbohydrate Polymers*, 86(3), 1291–1299. <https://doi.org/10.1016/j.carbpol.2011.06.030>
- Mat Zain, N. F. (2014). Preparation and Characterization of Cellulose and Nanocellulose From Pomelo (Citrus grandis) Albedo. *Journal of Nutrition & Food Sciences*, 05(01), 10–13. <https://doi.org/10.4172/2155-9600.1000334>
- Moreno, G., Ramirez, K., Esquivel, M., *et al.* (2018). Isolation and characterization of nanocellulose obtained from industrial

- crop waste resources by using mild acid hydrolysis. *Journal of Renewable Materials*, 6(4), 362–369. <https://doi.org/10.7569/JRM.2017.634167>
- Mukwaya, V., Yu, W., Asad, R. A. M., *et al.* (2017). An environmentally friendly method for the isolation of cellulose nano fibrils from banana rachis fibers. *Textile Research Journal*, 87(1), 81–90. <https://doi.org/10.1177/0040517515622155>
- Orozco, R. S., Hernández, P. B., Morales, G. R., *et al.* (2014). Characterization of lignocellulosic fruit waste as an alternative feedstock for bioethanol production. *BioResources*, 9(2), 1873–1885.
- Ramli, S., Ismail, N., Alkarkhi, A. F. M., *et al.* (2010). The use of principal component and cluster analysis to differentiate banana peel flours based on their starch and dietary fibre components. *Tropical Life Sciences Research*, 21(1), 91–100.
- Shanmugarajah, B., Kiew, P. L., Chew, I. M. L., *et al.* (2015). Isolation of Nanocrystalline Cellulose (NCC) from palm oil empty fruit bunch (EFB): Preliminary result on FTIR and DLS analysis. *Chemical Engineering Transactions*, 45(October), 1705–1710. <https://doi.org/10.3303/CET1545285>
- Tibolla, H., Pelissari, F. M., Martins, J. T., *et al.* (2018). Cellulose nanofibers produced from banana peel by chemical and mechanical treatments: Characterization and cytotoxicity assessment. *Food Hydrocolloids*, 75, 192–201.
- Tibolla, H., Pelissari, F. M., Martins, J. T., *et al.* (2018). Food Hydrocolloids Cellulose nano fibers produced from banana peel by chemical and mechanical treatments: Characterization and cytotoxicity assessment. *Food Hydrocolloids*, 75, 192–201. <https://doi.org/10.1016/j.foodhyd.2017.08.027>
- Tibolla, H., Pelissari, F. M., & Menegalli, F. C. (2014). Cellulose nanofibers produced from banana peel by chemical and enzymatic treatment. *LWT - Food Science and Technology*, 59(2P2), 1311–1318. <https://doi.org/10.1016/j.lwt.2014.04.011>
- Tibolla, H., Pelissari, F. M., Rodrigues, M. I., *et al.* (2017). Cellulose nanofibers produced from banana peel by enzymatic treatment: Study of process conditions. *Industrial Crops and Products*, 95, 664–674. <https://doi.org/10.1016/j.indcrop.2016.11.035>



Original Research Article

A Study on Hybrid Power Vehicle for Electric Spraying Application

Azwan M.B.^{1*}, Salmah J.¹, Abd Rahim S.¹, Syazwan R.¹, M. Ikmal H.¹

¹Mechanisation and Engineering Unit, Malaysia Palm Oil Board, Jln Sekolah, Pekan Bangi Lama, 43000 Kajang, Selangor, Malaysia.

*Corresponding author: Azwan M.B., Mechanisation and Engineering Unit, Malaysia Palm Oil Board, Jln Sekolah, Pekan Bangi Lama, 43000 Kajang, Selangor, Malaysia; azwan.bakri@mpob.gov.my

Abstract: Agriculture currently relies more on fossil fuel power for its mechanised operation. However, the electric power system embedded in agriculture machinery enables farm electrification that provides numerous advantages such as improve work efficiency, ease of equipment control, reduce energy requirement and more ergonomic. This study aims to analyse a hybrid power farm vehicle configuration to enable the electrification of farm operation such as herbicide spraying. Two methodologies are presented for this study, which are simulation analysis and in-field test validation. HOMER software indicates that fraction of energy for herbicide spraying operation and charging the battery pack is 70% from solar energy and 30% from the rectifier engine output. The 20Watt solar photovoltaic is selected due to installation area constraint on the farm utility vehicle, and simulation results indicate the capacity is adequate for the intended purpose. Besides that, the simulation results also show the setup incurs lower energy cost up to 30% as compared to direct utilisation of the fossil fuel generator for the herbicide spraying. The in-field test study has validated the simulation results. The analysis indicates that the battery performance is consistent throughout the trial for almost two months of operation at the area which covers nearly 150ha. The productivity of the machine obtained through the test is on average of 8ha per day for a single man operation. In conclusion, the study shows that incorporation of solar power as opportunity charging could stabilise battery condition and will prolong battery health. The results also indicate that electrification of the farm equipment and its application could bring the desired positive result in farm activity. Thus, a more sustainable development approach to agriculture practice could be met.

Keywords: Oil palm mechanisation; hybrid power vehicle; energy in agriculture production; sustainability; solar photovoltaic; herbicide spraying

Received: 18th May 2020

Accepted: 14th August 2020

Published: 2nd September 2020


Citation: Azwan MB, Salmah J, Abd Rahim S, *et al.* A study on hybrid power vehicle for electric spraying application. *Adv Agri Food Res J* 2020; 1(1): a0000103. <https://doi.org/10.36877/aafrij.a0000103>



1. Introduction

Electric farm tools and implements provide a lot of advantages in terms of controllability, higher efficiency distribution, easy installation and fuel saving. The advancement of a mechatronic technology enables the application of electric equipment in the agriculture sector that could lead to more advanced agriculture practice, such as automation and robotics use (Kushairi, Singh & Ong-Abdullah, 2017). Several studies had indicated better performance of the electrification of farm implements towards the agriculture practices (Abdelhamid *et al.*, 2018; Blackmore, Wang & Runov, 2005; Somà, 2017). The method of farm tool's electrification is realised by integrating the vehicle or tractor power system either alternating current (AC) or direct current (DC) architecture to electric power implements such as fertiliser spreader, chemical sprayer or other tools.

The farm electrification is much dependent on the requirement of the agriculture application and selection of the vehicle to provide the energy. The condition also depends on the voltage level of the energy system to be incorporated. Low energy agriculture application could apply a low voltage electrification system since the load requirement is small such as for herbicide spraying (Azwan *et al.*, 2016). Therefore, smaller footprint carrier or machinery, that is installed with the sufficient energy generation capacity could be deployed rather than to utilise bigger size tractor or vehicle. As comparative purposes, Table 1 indicates the advantages and disadvantages of the current technologies available for herbicide spraying in oil palm plantations.

Table 1. Available mechanised herbicide spraying technologies in oil palm plantation (Ludin *et al.*, 2014).

Available Technology	Description	Advantage	Disadvantage
 Knapsack sprayer	<ul style="list-style-type: none"> Hand-lever operated sprayer with 16 to 18 litres capacity tank. Coverage up to 1–2ha per day per operator. 	<ul style="list-style-type: none"> Very cheap Could be employed in various terrain condition. Able to utilise control droplet applicator. 	<ul style="list-style-type: none"> Low coverage and high operational cost per area. Intensive labour requirement. Hazardous handling of the chemical.

Spraying system on-board utility type vehicle		<ul style="list-style-type: none"> • Spraying system on-board the utility type vehicle that is using additional internal combustion engines for the operation with a capacity of 300–400L water. • Average coverage is about 7–10ha per day per machine. 	<ul style="list-style-type: none"> • Could be mobilised at a terrace or undulating topography. • A high-pressure pump powered by a petrol engine could extend the hose to about 20 metres from the vehicle. 	<ul style="list-style-type: none"> • Requires 2 to 3 workers for the operation. • Unable to utilise a low volume type nozzle. • Difficult to control water pressure for both flanks.
Tractor mounted spraying system		<ul style="list-style-type: none"> • Various spraying methods that usually employ spraying boom with low volume nozzle. More than 600L of water could be carried at a time. 	<ul style="list-style-type: none"> • Higher coverage of about 30–50ha per day. • Less labour requirement. • Able to utilise sensors and electronic measurement. 	<ul style="list-style-type: none"> • Very high capital cost. • Can only be utilised in a flat area topography only. • High maintenance cost for spraying system.

Electrification of the farm implements would also ensure less wastage to the farm input and provides significant productivity. A farm utility vehicle with sufficient power generation capability could embrace the advantages of the system. Thus, the sustainability of agriculture production, in general, is improving by balancing its input-output energy and decreasing its energy intensity (T. Li *et al.*, 2016). One of the systems that enables sufficient energy generation in a smaller footprint farm vehicle is the hybrid power system, where two or more sources of power are available.

Adopting hybrid power technology for a particular agriculture application provides advantages such as higher field coverage, improves the functionality of work, reduces fuel consumption and a few others (Llorens *et al.*, 2010). Besides, a hybrid power farm vehicle could also incorporate a renewable energy source to recharge the battery. The method allows the system to be more versatile and robust (Y. Li *et al.*, 2019).

Solar energy technology on-board a farm vehicle in Malaysia can provide at least 25% of the energy to power an agriculture electric vehicle (Azwan *et al.*, 2017) for an oil palm plantation operation. It is due to the fact that Malaysia receives about 4,000 to 5,000W/m² average solar irradiance and average sunshine duration between 4 to 8 hours a day (Daut *et al.*, 2012). However, solar is not suitable to be used as a primary energy source in agriculture machinery application since only 20% to 35% energy from the sun can penetrate the palm canopies or a broadleaf tree in Malaysia (Shahidan & Salleh 2007). Thus, making solar energy only as an opportunity source to charge the battery.

This study aims to analyse the performance of low-level electrification of agriculture implement on a lightweight and small footprint utility vehicle for herbicide spraying in oil palm plantation. The study comprises simulation assessment and a field trial. The simulation is conducted to assess energy generation and utilisation on the hybrid power system vehicle by using the HOMER software. The field assessment is carried out to validate the simulation result.

2. Materials and Methods

2.1. Hybrid power utility vehicle for herbicide spraying

A three-wheeled utility farm vehicle was fabricated to assemble the proposed system, as depicted in Figure 1. The prototype comprised a 7HP air-cooled diesel power engine, belted continuous variable transmission system, 20Watt solar photovoltaic and other auxiliaries. The diesel-powered machine with an electric starter and rectifier generator was selected since the power is adequate to cater for a proposed gross load of 400kg based on the free force analysis (Azwan *et al.*, 2017). The chassis of the three-wheeled utility vehicle was selected since the vehicle concept is widely used in Malaysian oil palm plantation operation (Awaludin *et al.*, 2015) and provides low cost of development. Another factor to consider in the development of the new farm utility vehicle chassis in this study was its weight consideration since the performance of the vehicle also depends on the engine capacity and its gross weight. Thus, a new chassis was developed and fabricated in consideration of those factors.



Figure 1. Three-wheel type machine with a solar charging and electric spraying system.

Another function to be incorporated in the prototype was the electrical spraying system. The system consists of a 12V electrical pump system, the water tank, the nozzles and also its auxiliaries. The diaphragm pump is activated by a handle switch together with electric solenoids for left or right nozzle selection. A pressure reduction system is also incorporated

at the spray boom to ensure the correct pressure enters the nozzles for higher spraying performance.

2.2. HOMER Software simulation

This study utilised the software developed by the United States National Renewable Energy Laboratory in simulating the energy generation and consumption based on input provided to the software. The software provides significant simulation results such as optimisation of the configuration, capacity of the energy generation for the intended application, and the techno-economic analysis of the system (Azwan *et al.*, 2017). The input data and design are discussed as follows:

2.2.1 System configuration and Solar energy resources

Figure 2 depicts the schematic diagram of the proposed design. A DC-bus provides 12V system configuration where solar and generator are the power sources and backed-up by a battery to provide a load for spraying application. However, both power sources are also required to recharge the cell by the excess power available. The battery is also needed to provide some energy for engine cranking. About 20amp current is required for cranking purposes, but the use is only on the instantaneous second and it was suggested to ignore for this simulation since the actual energy consumed for this particular application was hard to predict.

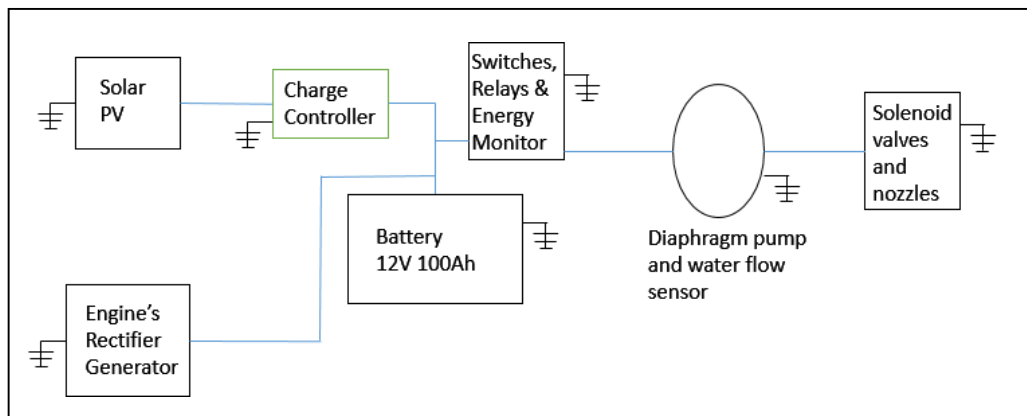


Figure 2. Schematic diagram of the proposed spraying system.

In HOMER, the energy was also investigated based on the baseline data. In this analysis, the solar power was referred from a previous study conducted on the integration of PV on-board EV in oil palm plantation operation (Azwan *et al.*, 2017). Figure 3 depicts the solar energy resource availability based on sky clearness index and daily radiation.

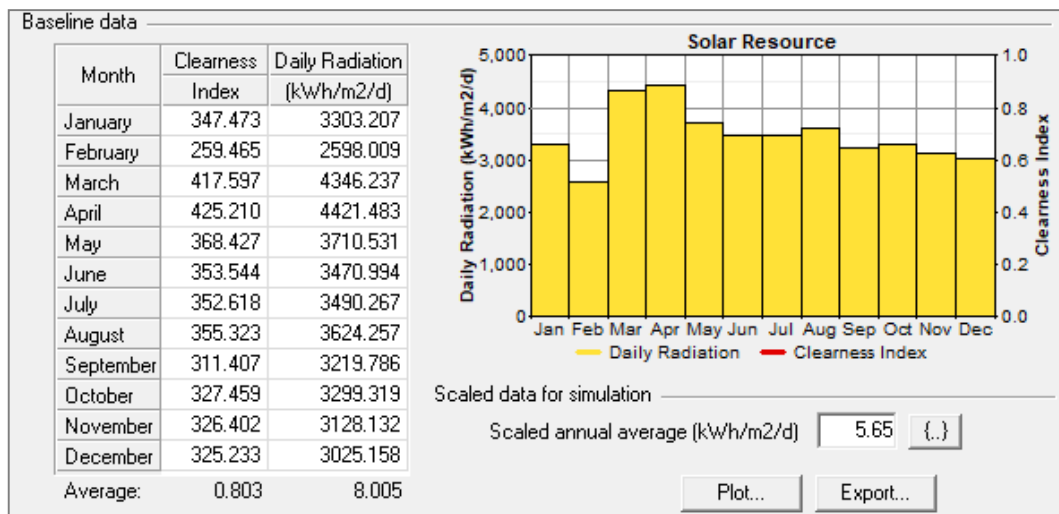


Figure 3. Solar energy resource availability based on sky clearness index and daily radiation.

2.2.2 Energy for spraying and system constraint

The assumption of electric spraying load is depicted in Figure 4. The previous study indicated that 138 200L water tank with chemical mixing and 150L per ha nozzle volume could complete a task within 40 to 50 minutes. The vehicle was required to return to the water source after the water depleted in the tank for refilling and mixing process. Therefore, it was assumed in the worst-case scenario that each spraying time is one hour and another one hour for refilling and mixing.



Figure 4. Assumption of the spraying load.

A medium pressure of up to 5 bars of a 12V electric diaphragm pump is attached to the system that provides spraying through two sets of low rate spraying nozzles. In terms of energy consumption of an electric sprayer, a small power utilisation about 22W on average was observed from a preliminary power test in a laboratory. The result of the test is depicted in Figure 5 and also indicated a variation of spraying rate between 2.25L/m to 2.40L/m due to diaphragm pump characteristic and with 1.5 bar pressure limitation by the pressure

regulator. The data were recorded by using a wattmeter and logged to a computer. Therefore, an average of 25Watt power was assumed to be used for the spraying system, as indicated in Figure 4.

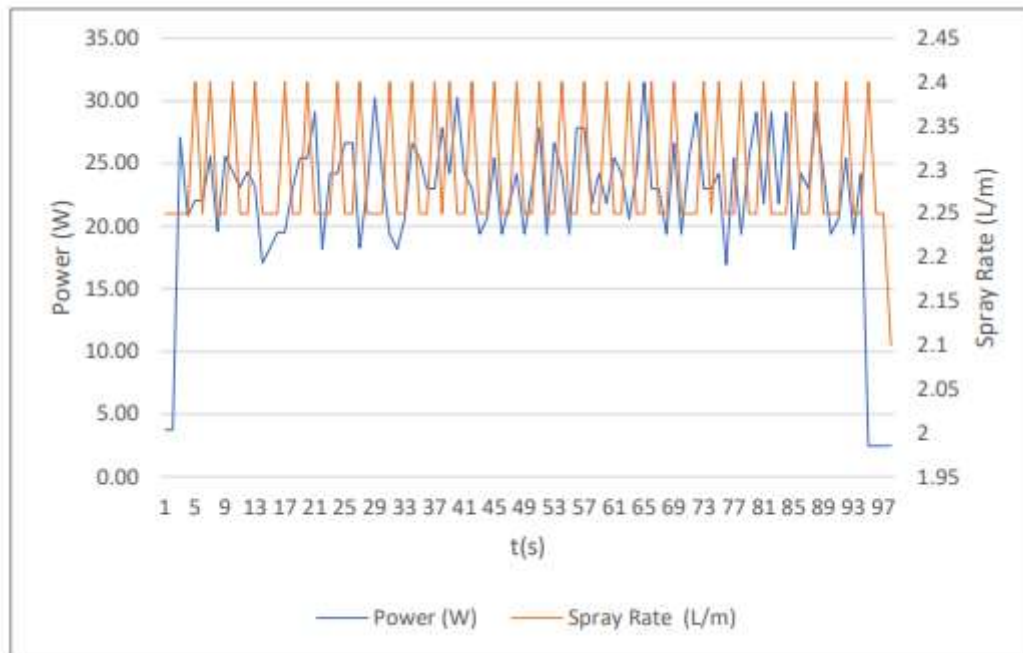


Figure 5. Preliminary energy test for spraying load with 1.5 bar nozzle pressure.

2.3. In-Field Test and validation

A study on the prototype performance in the actual field was carried out in a real oil palm plantation in Malaysia. The test period was about two months, from early May to the end of June 2018. The study was conducted in such a way that the prototype carried out a real task of herbicide spraying. A field contractor had been given the job by the estate's management to utilise the prototype and fed the necessary information. The information was the battery state of charge (SoC) and the productivity of the spraying activity. The analysis of battery performance was based on Equation 1 (Vermaak & Kusakana, 2014).

$$\text{DoD} = \text{SoC}_{\text{final}} - \text{SoC}_{\text{initial}} \quad (\text{Equation 1})$$

Where;

DoD is referred to as the depth of discharge (%).

SoC_{initial} is referred to as the reading of the state of charge (%) before the activity is carried out. SoC_{final} is referred to as the reading of the state of charge (%) after the activity is completed.

Battery performance is also related to the efficiency of the energy generator. The impact of solar panel efficiency is very much dependent on the intensity of the solar radiation strike on the solar panel (Rajput & Sudhakar, 2013) and characteristic of the solar panel itself as depicted in Equation 2. However, for the solar photovoltaic application on-board a vehicle, the solar radiation is varied mostly due to the movement of the vehicle. In a recent study of photovoltaic system on-board an electric vehicle, about 21% of solar energy can be captured for the application in an oil palm plantation in Malaysia (Azwan *et al.*, 2017). Meanwhile, for the electrical power obtained from a combustion engine vehicle, the efficiency of the rectifier generator is impacted by the crankshaft speed, drop voltage and leakage current. Thus, the effectiveness of both energy generators can be investigated through a state of charge reading in general and later could be compared to the environmental data available.

$$r = \frac{VOC \times I_{sc}}{A \times I} \times 100\% \quad (\text{Equation 2})$$

Where:

r = solar panel efficiency (%) V_{oc} = open circuit voltage

I_{sc} = short circuit current

A = total solar panel area (m^2)

I = average intensity of the solar radiation (W/m^2)

3. Results and Discussion

3.1. Simulation Analysis

HOMER software has provided significant simulation results, as depicted in Figure 6. The results obtained indicate that the highest energy fraction between solar power and engine rectifier output to serve the load is the renewable energy or solar energy up to 70%. The results also indicate that no energy shortage occurred, thus making the herbicide spraying feasible for this experimental setup. Further simulation analysis on battery's state of charge (SoC) versus DC primary load or spraying power as depicted in Figure 7 also shows that battery is always in the optimum percentage at capacity between 0.02 to 0.025kW. The depth of discharge is not more than 20% of its original state. The condition will ensure longer battery life or it is less damaging to battery health (Abdelhamid, Singh & Haque, 2012; Doerffel & Sharkh, 2006). Good battery condition will ensure this practice could be accepted and used substantially in the plantation. Besides, the approach could also promote sustainable development in agriculture. More advanced agriculture tools with sensors and

microprocessor could also later be incorporated into the system since the electrification platform is available.

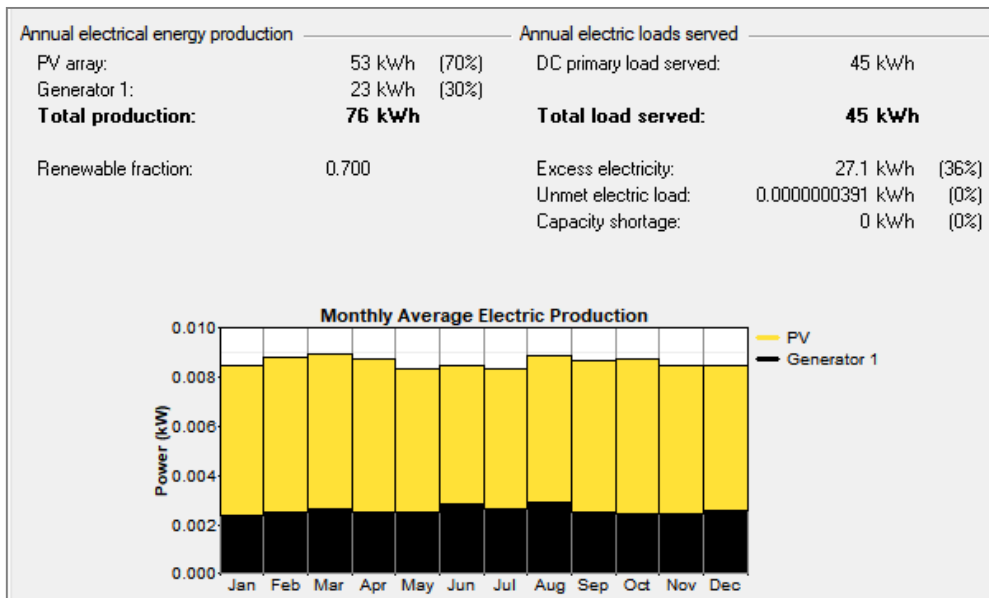


Figure 6. Result of the Simulation Analysis from HOMER interface.

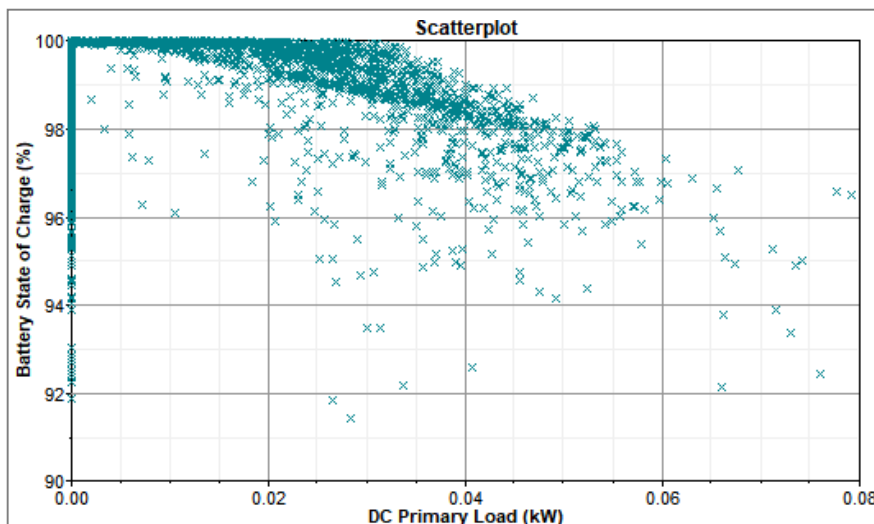


Figure 7. HOMER simulation result of soc vs. DC primary load or the spraying power.

In terms of economic analysis, HOMER had produced two optimisation results, as shown in Table 2, where both scenarios refer to the energy system with different equipment and sizing to serve the spraying load indicated previously. HOMER analysed the economic based on the input provided to the software. Table 3 indicates the economic assumption used for the analysis in Scenario 1 that certain parameters were quoted from previous studies. Scenario 1 comprised of energy equipment with 20W solar photovoltaic and 60W rectifier engine

output. Meanwhile, Scenario 2 is the energy system without solar photovoltaic and bigger size rectifier engine output of 100W. The capacity of rectifier engine output is more significant in Scenario 2 due to its massive size. Thus, it incurred slightly higher capital cost. Both scenarios utilised cost of diesel that is capped at RM2 per litre. The analysis shows that the price of energy for Scenario 1 was almost 70% lower as compared to Scenario 2. The result validates the previous study, which is 70% of the energy for electric spraying load is provided by solar energy. Thus, less diesel fuel was used in Scenario 1 that provided high impact to the energy cost.

Table 2. Optimisation result of system selection. 246

	Solar Energy Power	Rectifier Engine Output	Initial Capital (RM)	Cost of Energy (RM/kWh)
Scenario 1	20W	60W	3,100 ¹	37.64
Scenario 2	0	100W	5,000 ¹	106.00

*The cost quoted by the equipment supplier.

Table 3. Economic assumption for the selected optimisation result (Azwan *et al.*, 2017; Jorgensen, 2008; Vermaak & Kusakana, 2014).

SYSTEM	DETAILS	ASSUMPTION
Solar Photovoltaic 20Watt	Capital	200RM
	Operational & maintenance	0
	Lifetime	5 years
Battery 12V 100Ah	Capital	800RM
	Operational & maintenance	300RM/year
Engine Rectifier 60Watt	Capital	2,000RM
	Operational & maintenance	0.6RM/hour
	Fuel consumption	0.25RM/L/hour

3.2. In-Field Test Validation

The test was carried out in an actual oil palm plantation with herbicide spraying operation carried out based on the machine setup explained previously. The experiment was carried out to validate the simulation result. The actual field test was conducted within two months, with almost 150ha of the area covered.

Battery condition was monitored through the state of charge (SoC) meter. The operator logged the battery SOC before and after the work completed daily on the farm. The area covered for the daily operation was also recorded based on the estate's map provided.

The result, as Figure 8 shows that the battery was always in good condition since the depth of discharge (DoD) was in the range of 20% only. The percentage was obtained by subtracting SoC after the work completed with SoC before the work started, as stated in Equation 1. It indicates that the proposed setup enables the battery to be charged and

discharged effectively. The result is also consistent with the HOMER simulation result, where battery SoC usually felt up to only 20% of its original state as depicted in Figure 7.

The DoD is always dependent on the battery consumption in undertaking the fieldwork such as herbicide spraying. Besides that, initial battery condition also determines the SoC reading since lower initial battery voltage will result in higher current flow to achieve the desired power and subsequently increase the energy consumption since the current flow is also associated with more heat generated. Thus, one method to improve stability of the DoD is to ensure the battery voltage is at the optimum level before any work is carried out. In terms of machine productivity, it was found that on average, 8ha per day of the area can be covered for herbicide spraying activity. The result shows significant productivity as compared to the manual labour of only 1–2 ha per day per operator and almost similar productivity with the existing spraying technology employed in the field, where the pressure water is pumped through a secondary fossil fuel engine (Ludin *et al.*, 2014).

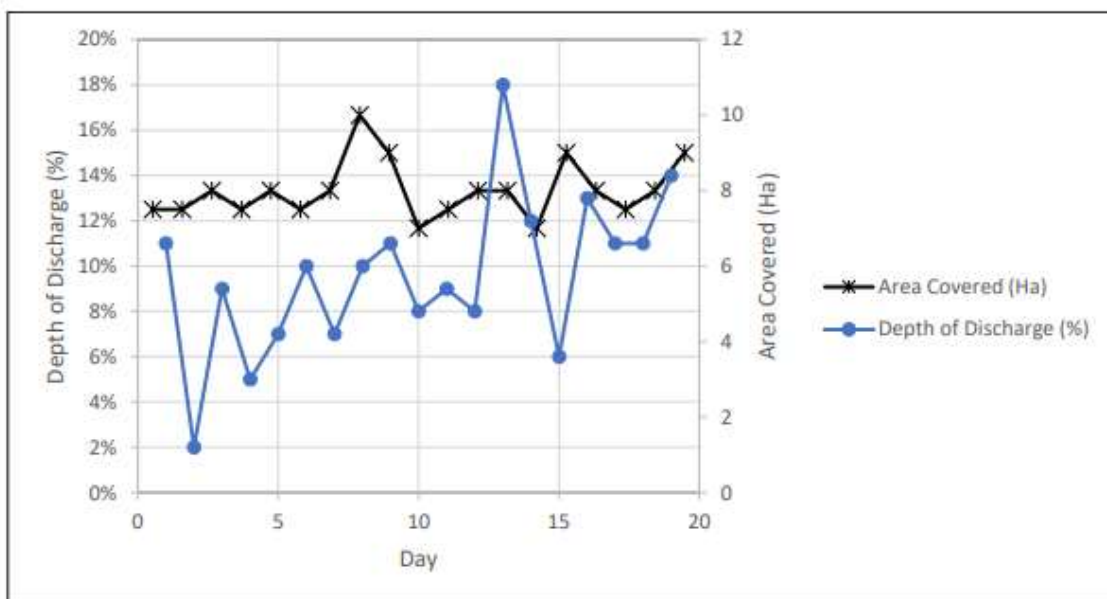


Figure 8. Results of the field validation (depth of discharge and area covered).

4. Conclusion

In general, the study indicates that renewable energy and energy efficiency technology is feasible to be incorporated into a mechanised oil palm plantation operation. The simulation result shows that renewable energy power fraction is almost 70% for the use of an electric medium pressure pump for herbicide spraying in the field. The analysis also indicates excellent battery performance in terms of the state of charge condition throughout the year. Reduction of fossil fuel utilisation of more than 70% will increase the sustainability of the farm operation. The simulation analysis by using HOMER also indicates the cost of energy is lower for the system proposed as compared to the full diesel fuel engine utilisation as the

primary energy for the herbicide spraying power. The lower energy cost is due to the smaller engine and photovoltaic system requirement. Besides that, the actual field test has validated the simulation analysis results and system performance. The test indicated that the system could work continuously and produce a significant effect in terms of productivity, which was about 8ha per day with a single man operation. The function of the hybrid power utility vehicle concept could be expanded to other farm tasks and definitely could improve the sustainability of the oil palm mechanisation operation.

Acknowledgement: The researchers would like to thank the management of MPOB, especially the Director-General of MPOB in supporting the research and granting permission for this publication.

Funding: MPOB funded this research under PAC Project allocation BD433-2015, Hybrid Power Vehicle for Herbicide Spraying.

Conflicts of Interest: The authors declare no conflict of interest for publication of the manuscript.

References

- Abdelhamid, M., Rhodes, K., Christen, E., *et al.* (2018). Analysis and opportunities for solar photovoltaics technologies on electrified vehicles. *SAE Technical Papers*, doi:10.4271/2018-01-0426
- Abdelhamid, M., Singh, R. & Haque, I. (2012). Role of PV generated DC power in transport sector: Case study of plug-in EV. *Renewable Energy*, 16(1), 1–7. doi:10.1016/j.rser.2010.07.062
- Awaludin, A., Salim, S., Salim, S., *et al.* (2015). Performance study of an oil palm fresh fruit bunch three wheeler evacuation machine. *The Online Journal of Science and Technology*, 5(2), 46–53.
- Azwan, M. B., Ludin, N. A., Abd Rahim, S., *et al.* (2016). Analysis of energy utilisation in Malaysian oil palm mechanisation operation. *Journal of Oil Palm Research*, 485–495.
- Azwan, M. B., Norasikin, A. L., Sopian, K., *et al.* (2017). Assessment of electric vehicle and photovoltaic integration for oil palm mechanisation practise. *Journal of Cleaner Production*, 140, 1365–1375. doi:10.1016/j.jclepro.2016.10.016
- Blackmore, B. S., Wang, M. & Runov, B. (2005). Robotic agriculture - the future of agricultural mechanisation?. *5th European Conference on Precision Agriculture*, 621–628. Uppsala, Sweden: Wageningen Academic Publishers.
- Daut, I., Zainuddin, F., Irwan, Y. M., *et al.* (2012). Analysis of solar irradiance and solar energy in Perlis, northern of peninsular Malaysia. *Energy Procedia*, 18, 1421–1427. doi:10.1016/j.egypro
- Rajput, D. S. & Sudhakar, K. (2013). Effect of dust on the performance of PV panels. *International Journal of ChemTech Research*, 5(2), 1083–1086.
- Doerffel, D. & Sharkh, S. A. (2006). A critical review of using the Peukert equation for determining the remaining capacity of lead-acid and lithium-ion batteries. *Journal of Power Sources*, 155(2), 395–400. doi:10.1016/j.jpowsour.2005.04.030
- Jorgensen, K. (2008). Technologies for electric, hybrid and hydrogen vehicles: Electricity from renewable energy sources in transport. *Utilities Policy*, 16(2), 72–79. doi:10.1016/j.jup.2007.11.005
- Kushairi, A., Singh, R. & Ong-Abdullah, M. (2017). The oil palm industry in Malaysia: Thriving with transformative technologies. *Journal of Oil Palm Research*, 29(4), 431–439. doi:10.21894/jopr.2017.00017
- Li, T., Baležentis, T. & Makutėnienė, D., *et al.* (2016). Energy-related CO₂ emission in European Union agriculture: driving forces and possibilities for reduction. *Applied Energy*, 180, 682–694. doi:10.1016/J.APENERGY.2016.08.031
- Li, Y., Huang, X., Liu, D., *et al.* (2019). Hybrid energy storage system and energy distribution strategy for four-wheel

- independent-drive electric vehicles. *Journal of Cleaner Production*, 220, 756–770. doi:10.1016/j.jclepro.2019.01.257
- Llorens, J., Gil, E., Llop, J., *et al.* (2010). Variable rate dosing in precision viticulture: Use of electronic devices to improve application efficiency. *Crop Protection*, 29(3), 239–248. doi:10.1016/j.cropro.2009.12.022
- Ludin, N. A., Bakri, M. A. M., Kamaruddin, N., *et al.* (2014). Malaysian oil palm plantation sector: Exploiting renewable energy toward sustainability production. *Journal of Cleaner Production*, 65, 9–15. doi:10.1016/j.jclepro.2013.11.063
- Shahidan, M. F. & Salleh, E. (2007). Effects of tree canopies on solar radiation filtration in a tropical microclimatic environment. *PLEA2007 - The 24th Conference on Passive and Low Energy Architecture*, 400–406.
- Somà, A. (2017). Trends and hybridization factor for heavy-duty working vehicles. *Hybrid Electric Vehicles*. doi:10.5772/intechopen.68296
- Vermaak, H. J. & Kusakana, K. (2014). Design of a photovoltaic-wind charging station for small electric Tuk-tuk in D.R.Congo. *Renewable Energy*, 67, 40–45. doi:10.1016/j.renene.2013.11.019



Copyright © 2020 by Azwan MB, *et al.* and HH Publisher. This work is licenced under the Creative Commons Attribution-Non-commercial 4.0 International Licence (CC-BY-NC4.0)

Original Research Article

Nutritional Properties of Orange-Fleshed Sweet Potato Juice

Nurul Ainina Zulkifli¹, Nurhanisah Mohammed Salleh¹, Mohd Zuhair Mohd Nor^{1, 2*}, Farah Nadia Omar¹, Alifdalino Sulaiman¹, Mohd Noriznan Mokhtar¹

¹Department of Process and Food Engineering, Faculty of Engineering, Universiti Putra Malaysia, 43400 Serdang, Selangor, Malaysia

²Laboratory of Halal Science Research, Halal Products Research Institute, Universiti Putra Malaysia, 43400 Serdang, Selangor, Malaysia

*Corresponding author: Mohd Zuhair Mohd Nor, Department of Process and Food Engineering, Faculty of Engineering, Universiti Putra Malaysia, 43400 Serdang, Selangor, Malaysia; zuhair@upm.edu.my

Abstract: Orange-fleshed sweet potato (OFSP) offers many health benefits and can be processed into different food forms including as a healthy drinking juice. However, the OFSP juice requires exploration on the juice properties, especially its nutritional elements before it can be marketed as a healthy drink. Hence, this study aims to address the detailed nutritional composition of the OFSP juice via analyses of proximate composition, amino acids, mineral, carotenoids and vitamins. Findings have shown that OFSP juice is proven to be high in beta-carotene with a value of 4916.06 µg/L which is almost 100 times the value of beta-carotene in orange juice, and also rich in vitamins, certain amino acids and minerals. By considering that, these phytochemicals can aid in the reduction of anti-mutagenic, immuno-enhancers, cancer, and free radical scavengers, in which this study has proven the potential of OFSP to be processed into a healthy juice based on its nutritional properties.

Keywords: *Ipomoea batatas* (L.) Lam; orange-fleshed sweet potato; carotenoid; healthy drinking juices

Received: 25th April 2020

Accepted: 14th August 2020

Published: 28th August 2020

Citation: Zulkifli NA, Salleh NM, Nor MZM, *et al.* Nutritional properties of orange-fleshed sweet potato juice. Adv Agri Food Res J 2020; 1(1): a0000104. <https://doi.org/10.36877/aafrij.a0000104>

1. Introduction

Fruits and vegetables are rich in nutrients and are considered vital for mankind which can help people who suffer from nutrient deficiency. Many people suffer from premature mortality and disability due to the low fruit and vegetable consumption (Management Association, Information Resources, 2018). In fact, inadequate fruit and vegetable intake was reported to be the cause of an estimated 3.9 million deaths worldwide in 2017 (Owolade *et al*, 2017).

Hence, proper consumption of fruits and vegetables is needed, as it can reduce the risk of cardiovascular diseases, stomach cancer, and colorectal cancer (Slavin & Lloyd, 2012). This is due to the benefits provided by many natural antioxidants that exist in fruits and vegetables. These compounds protect food from rancidity, as well as reduce oxidative damage in humans (Chiosa *et al.*, 2005). Among all the natural antioxidants, β - carotene is known for its benefits in the inhibition of initial stages of lipid peroxidation as well as play a protective role against cancer (Chiosa *et al.*, 2005).

One of the fruits and vegetables that contains high β -carotene is the orange-fleshed sweet potato (OFSP). Many studies have reported high β -carotene in OFSP, besides other nutritional elements including carbohydrate, vitamins, protein and minerals. Considering offers by OFSP, this crop holds great potential to be utilised into various food forms in various market segments. Sweet potato can be utilised to make a healthy juice, while the flesh/pulp can be used to make flour for bread and pastries which can cater to celiac disease patients (non-gluten tolerance) (Gaesser & Angadi, 2015). Detailed exploration and processing of sweet potato are needed in order to have OFSP juice to be considered as a healthy juice drink. A thorough nutrient and proximate analysis should have been performed in order to determine the potential of OFSP juice. To the best of the authors' knowledge, there is very limited information on detailed nutrient composition analysis of local sweet potato juice. Hence, this study is aimed to conduct a nutritional compositional study of the orange-fleshed sweet potato juice. Details of each nutrient are thoroughly discussed.

2. Materials and Methods

2.1. Preparation of OFSP

Fresh OFSP was purchased from the Malaysian Agricultural Research and Development Institute (MARDI) farm in Bachok, Kelantan, Malaysia. Tubers were stored in the chiller at a temperature of 10°C before the subsequent analyses. The tubers were washed with clean running tap water and finally rinsed with distilled water to remove dirt and soil before they were air-dried at room temperature. Once dried, tubers were carefully and manually peeled and cut into small pieces. The small cuts of peeled tubers were pressed using juice extractor (PSN-MJ70M, Panasonic, Malaysia) with a ratio 1:1 (w/w) of water and tuber samples. The pressed samples were ground using a wet mill (MX-SM1031S, Panasonic, Malaysia) and filtered through a cloth filter (mesh size 200) in order to separate crude juice and fibre residues prior to centrifuge (Hettich® Universal 320/320R Centrifuge, Andreas Hettich GmbH & Co. KG, Germany) for five minutes at 2500 rpm. The obtained supernatants were considered as the OFSP juice and were stored at -20°C until further analysis. The whole OFSP juice preparation steps are shown in Figure 1 below.

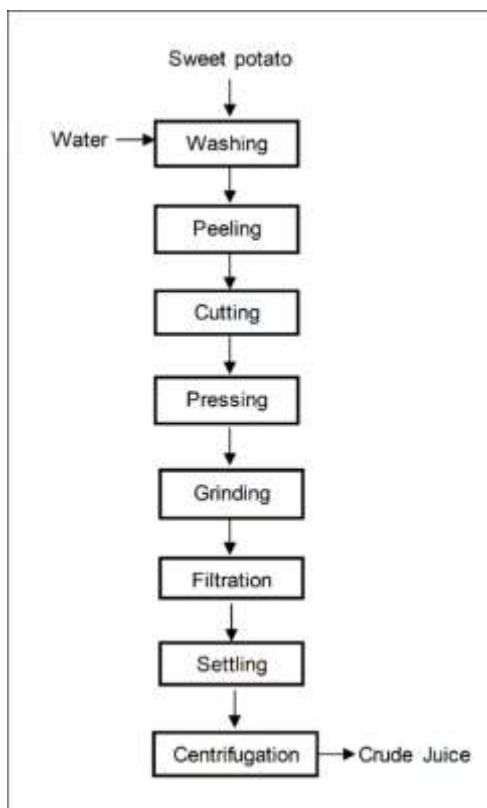


Figure 1. OFSP juice preparation steps

2.2. Proximate Analysis and Total Starch of OFSP Juice

OFSP juice was analysed for moisture content in an oven (Memmert, Germany) through the drying method at 105°C according to the procedure described in AOAC (1995). Crude fibre was determined according to AACC (2000) using Fibertec™ 2010 (Denmark). Crude fat was determined using Soxtec Extraction (Soxtec™ 2050, Denmark) for 24 hours. Crude protein content was tested by Kjeltac™ 2300, Denmark which involved protein digestion and distillation according to the Kjeldahl's method (FOSS Analytical AB., 2003). The ash was determined as a total inorganic matter by incineration of the samples at 600°C according to the method (AOAC., 1995). Total carbohydrate content was calculated by using the formula as Eq. (1):

$$\text{Carbohydrate (\%)} = 100 - (\% \text{ crude protein} + \% \text{ crude fibre} + \% \text{ total ash} + \% \text{ crude fat}) \quad (1)$$

Total energy content was obtained using Eq. (2), Atwater conversion factors 4, 9 and 4 for each gram of crude protein, crude fat and carbohydrate and expressed in calories, respectively (Dako *et al.*, 2016).

$$\text{Total energy } \left(\frac{\text{Kcal}}{100\text{g}} \right) = (9 \times \% \text{ crude fat}) + (4 \times \% \text{ crude protein}) + (4 \times \% \text{ total carbohydrate}) \quad (2)$$

Total starch content was determined by using UV-spectrophotometer (Ultrospec 3100 pro, Amershampharmacia Biotech, United Kingdom) read at 580nm (Xiao, Storms & Tsang, 2006).

2.3. Ascorbic Acid, Thiamine and Riboflavin Content

The determination of ascorbic acid was carried out by high-performance liquid chromatography (HPLC) (1100 Series, Agilent, Waldbronn, Germany). The samples were diluted with 4.5% metaphosphoric acid. Chromatographic separation was achieved on a reversed phase high-performance liquid chromatography (RP-HPLC) (Agilent ZORBAX Eclipse Plus C18, Munich, Germany) column through isocratic delivery of a mobile phase (A/B 33/67; A: 0.1M potassium acetate, pH = 4.9, B: acetonitrile: water [50:50]) at a flow rate of 1 mL/min. UV absorbance was recorded at 254nm at room temperature.

Then, thiamine and riboflavin content were determined by RP-HPLC column (Agilent ZORBAX Eclipse Plus C18, Munich, Germany; 250 × 4.6mm; 5 μm) through the isocratic delivery mobile phase (A/B 33/67; A: MeOH, B: 0.023M H₃PO₄, pH = 3.54) at a flow rate of 0.5 mL/min. Ultraviolet (UV) absorbance was recorded at 270nm at room temperature.

2.4. Total β-carotene Content

The β-carotene determination was carried out by dissolving samples in 95% (v/v) acetone. The supernatant was filtered using filter paper (Whatman filter paper grade 1) before being read with UV-Vis spectrophotometer at absorbance of 449nm (Biswas *et al.*, 2011). The concentration of β-carotene can be calculated using Beer-Lambert law as in Eq. (3):

$$A = \epsilon c l \quad (3)$$

Where A is the absorbance; c represents the concentration of carotene; ε is extinction coefficient; l is the thickness of cuvettes (path length) 1 cm; the ε of β-carotene extract using acetone is 134 × 10³ Lmol⁻¹cm⁻¹, while 536.88 g/mol of β-carotene molecular weight.

2.5. Determination of Amino Acids Content

A 10 mL HCl (6 mol L⁻¹) in acid hydrolysis tubes with air elimination by nitrogen-blowing at 110°C for 24h was hydrolysed with 160 mL of sample. The hydrolyte was diluted with ultrapure water to 50 mL after cooling, filtering and washing processes. Then, 1 mL diluent was placed in a bottle, dried with nitrogen flow and redissolved with 1 mL HCl (0.02 mol L⁻¹). For further analyses, the solutions were passed through 0.02-mesh

filter membranes. The amino acid composition of the samples was measured using amino acids automatic analyser (L-8900, Hitachi Ltd., Tokyo, Japan).

2.6. Determination of Mineral Elements Content

0.25 mL of sample was measured into a polytetrafluoroethylene digestion tube and 8 mL 65% (v/v) HNO₃ was added for pre-digestion. After 1 hour, 30% (v/v) H₂O₂ was added and digested using a microwave digestion system (MARS 5, CEM Co., Matthews, NC, USA). The digested solution was diluted to 100 mL with Milli-Q water (Bedford, MA, USA) and stored in plastic tubes at 4°C for further analysis. Inductively Coupled Plasma Mass Spectrometry (ICP-MS, 7700X; Agilent, USA) was used to measure twelve mineral elements at the operating conditions as such; cooling gas flow rate, 1.47 L/min; radio frequency power, 1280 W; auxiliary gas flow rate, 1 L/min, carrier gas flow rate, 1 L/min; nebulization chamber temperature, 20°C; and sampling depth, 8 mm.

3. Results

3.1. Proximate Analysis

Table 1 displays the proximate properties of OFSP juice. For the purpose of comparison with a more established fresh juice, the properties of orange juice reported by Yarkwan & Oketunde, (2016) are also being listed in Table 1. Based on Table 1, the moisture content of OFSP was recorded at 89.76%, almost similar to orange juice, indicating that OFSD juice in this study is comparable with the more established juice.

The crude fibre content of OFSP juice is displayed in Table 1. According to Table 1, the crude fibre content of OFSP juice was more than 175 times higher (3.49%) as compared to orange juice (0.02%). This finding shows the potential of OFSP juice to be promoted as a healthy drink since high fibre drink can be a source of energy for the human body while preventing constipation and reducing heart disease and diabetes (Rose & Vasanthakaalam, 2011; Alam *et al.*, 2016). Meanwhile, the crude fat of OFSP juice content was recorded as 1.13%, ten times higher than orange juice (0.120%) as shown in Table 1. This finding is in contrast with another study on the fat content of SP tuber which was reported at 0.2% (Alam *et al.*, 2016), that might be due to the properties alteration by processing variation.

Based on Table 1, the crude protein content of OFSP juice is 0.39% which is close to the protein content in orange juice (0.35%). The presence of protein in the OFSP juice signifies the existence of valuable essential amino acids which are important for the metabolism process in the human body. Hence, this could justify the potential of the OFSP juice as a healthy juice. Ash content of OFSP is shown as 0.68% (Table 1), much lower than orange juice in a range of 0.040–0.045%. This high value of ash content indicates a good measure of minerals preserved in juices (Rose & Vasanthakaalam, 2011). Low ash content in OFSP juice might be attributed to the solids extraction and processing process performed on the tubers during the samples preparation (Figure 1).

The total carbohydrate content of OFSP juice was determined at 5.04% which also reflects its energy content of 29.45 Kcal/100 g (Table 1). The carbohydrates are an important source of energy in human diets comprising some 40–80% of total energy intake (FAO/WHO, 1998). An optimum diet for all ages (except for children under the age of two) should consist of at least 55% of total energy from a variety of carbohydrate sources (FAO/WHO, 1998). In comparison, orange juice has a higher total carbohydrate and energy content. Nevertheless, OFSP juice can still provide energy supply for the human diet. This is proven by the amount of starch content of OFSP juice which is at 1.27% (Table 1). High starch content in the juice can be manipulated in many food applications such as for dessert and beverages.

Table 1. Proximate analysis of fresh juice.

Proximate Analysis	OFSP juice	Orange juice
Moisture (%)	89.76 ± 0.11	86.00 - 86.50
Crude Fibre (%)	3.49 ± 0.19	0.020
Crude Fat (%)	1.13 ± 0.03	0.120
Crude Protein (%)	0.39 ± 0.03	0.35 - 0.39
Ash (%)	0.68 ± 0.02	0.040 - 0.045
Total Carbohydrate (%)	5.04 ± 0.27	13.09 - 13.56
Starch (%)	1.27 ± 0.11	-nd-
Total Energy (Kcal/100g)	29.45 ± 1.07	54.84 - 56.88

*Data are mean values ± standard deviation.

3.2. Ascorbic Acid, Thiamine and Riboflavin, and β -carotene Content

Table 2 shows the vitamin composition of OFSP juice in this study as compared to orange juice reported by other studies. Based on Table 2, the OFSP juice contains 0.04 mg/100 g thiamine and 0.12 mg/100 g riboflavin reflecting the presence of vitamin B components in the juice. Vitamin B plays a role in the growth of the body as well as for lesions treatment (Ragunatha *et al.*, 2014). Meanwhile, vitamin C in the OFSP juice is 3.73 mg/100 g as shown in Table 2 which is in the lower range compared to the vitamin C in orange juice, 8 - 10 mg/100 g (Yarkwan & Oketunde, 2016). Although the value of ascorbic acid of OFSP juices is considered low, the value is still appreciable to provide health benefits to consumers. The recommended daily amount for vitamin C is 20 to 90 milligrams (mg) a day, and the upper limit is 2,000 mg a day (German Nutrition Society (DGE), 2015). Besides, the content of vitamin C in the juice might be affected by an oxidation process during the juice preparation. Interestingly, the amount of β -carotene in OFSP juice sample was 4916.06 μ g/L (Table 2), which is 92 times higher compared to orange juice ranging from 53–69 μ g/L

reported by Chiosa *et al.* (2005). This is expected as many studies have reported about the high β -carotene content in orange-fleshed sweet potato (Mamo *et al.*, 2014; Rodrigues *et al.*, 2016). β -carotene provides many health benefits such as to alleviate vitamin A deficiency which is good for children under age six (Rodrigues *et al.*, 2016). Moreover, vitamin A also helps in preventing night blindness (Alam *et al.*, 2016). By considering these benefits, OFSP juice can be promoted as a β -carotene-rich drink and can be marketed in the healthy beverages segment. The potential market of healthy beverages segment has been discussed by Mamo *et al.*, (2014), where the demand for high vitamin content drinks including β -carotene is expected to increase by 20% in the next five years. Hence, promoting OFSP juice in this segment is a wise choice.

Table 2. Vitamin composition of fresh juice.

Vitamins	OFSP juice
Vitamin B1 (Thiamine) (mg/100g)	0.04 \pm 0.18
Vitamin B2 (Riboflavin) (mg/100g)	0.12 \pm 0.03
Vitamin C (Ascorbic acid) (mg/100g)	3.73 \pm 0.06
β -carotene (μ g/L)	4916.06 \pm 0.73

*Data are mean values \pm standard deviation.

3.3. Amino acids Content

Table 3 exhibits the amino acids content of OFSP juice. Based on Table 3, histidine, arginine and aspartic content (0.50%, 0.42% and 0.20%) were recorded higher as compared to other types of amino acids. The other amino acid content such as glycine, isoleucine, alanine, lysine, glutamic, leucine, methionine, tyrosine, phenylalanine, serine, threonine and valine were found to be at lower content ranging from 0.01% until 0.09%. However, cysteine and proline were not detected from the analysis. Mohanty *et al.*, (2014) has discussed the role of each amino acid in detail including the roles of histidine in the protein interaction and is also a precursor of histamine. Besides, histidine is important for the repair of tissues and growth, for maintaining the myelin sheaths, and for the removal of heavy metals from the body. Meanwhile, arginine is needed in cell division, ammonia removal, immune function, wound healing and hormone release (Mohanty *et al.*, 2014). It also plays important roles in neurotransmission, maintenance of blood pressure and blood clotting which is the precursor for biological synthesis of nitric oxide. In addition, arginine is also essential for the recovery of a few diseases like hypertension, erectile dysfunction, sepsis, preeclampsia and anxiety. As amino acid deficiencies lead to several diseases, knowledge of its composition in foods is important as it will affect the preparation, processing and storage of foods and use as dietary guidance for healthy drink production.

Table 3. Amino acids content of juice.

Amino Acids (%)	OFSP juice
Alanine	0.06 ± 0.31
Lysine	0.05 ± 0.12
Arginine	0.42 ± 0.65
Aspartic	0.20 ± 0.88
Cystine	-nd-
Glutamic	0.09 ± 0.45
Glycine	0.04 ± 0.23
Histidine	0.50 ± 0.11
Isoleucine	0.04 ± 0.07
Leucine	0.06 ± 0.32
Methionine	0.01 ± 0.48
Phenylalanine	0.05 ± 0.01
Proline	-nd-
Serine	0.04 ± 0.17
Threonine	0.04 ± 0.05
Tyrosine	0.03 ± 0.06
Valine	0.06 ± 0.33

*Data are mean values ± standard deviation.

3.4. Mineral Element Content

Table 4 represents the mineral element composition of the OFSP juice compared to orange juice as reported by Yarkwan & Oketunde, (2016). The OFSP juice contains 147.77 mg/100 g of potassium, 30.06 mg/100 g of sodium, 10.03 mg/100 g of calcium, and 0.79 mg/100 g of iron which are higher as compared to orange juice, as shown in Table 4. The role of calcium is good for humans in particular cell physiology, mineralisation of bone and in making the teeth and bone very strong. Meanwhile, iron helps in transporting oxygen in the blood. In human diets, these minerals are important micronutrients (Danish *et al.*, 2019).

Besides, the other mineral element composition of OFSP juice such as phosphorus (44.74 mg/100 g), sulphur (32.66 mg/100 g), magnesium (32.64 mg/100 g), zinc (0.57 mg/100 g), manganese (0.31 mg/100 g), aluminium (0.30 mg/100 g), copper (0.17 mg/100 g), and boron (0.15 mg/100 g) were determined in Table 4. Subsequently, the appropriate Recommended Dietary Allowance (RDA) or adequate intake (AI), AI for females and males aged 31–50 is 1500 mg/day (sodium), 1000 mg/day (calcium) and 4700 mg/day (potassium) (Yarkwan & Oketunde, 2016; Koubová *et al.*, 2018). Iron has an RDA value of 8 mg/day and 18 mg/day for average men and women aged 31–50 respectively (Yarkwan & Oketunde, 2016; Koubová *et al.*, 2018). Thus, in reference to the AI and RDA, OFSP juice can provide high minerals to the consumers in order to cater to the required intake.

Table 4. Mineral element composition of fresh juice.

Minerals (mg/100g)	OFSP juice	Orange juice
Phosphorus	44.74 ± 0.13	-nd-
Potassium	147.77 ± 0.09	0.0181 - 0.021
Sulphur	32.66 ± 0.02	-nd-
Aluminium	0.30 ± 0.33	-nd-
Calcium	10.03 ± 0.15	0.0046 - 0.0048
Magnesium	32.64 ± 0.11	-nd-
Manganese	0.31 ± 0.46	-nd-
Iron	0.79 ± 0.04	0.0012 - 0.0014
Copper	0.17 ± 0.18	-nd-
Zinc	0.57 ± 0.01	-nd-
Boron	0.15 ± 0.03	-nd-
Sodium	30.06 ± 0.22	0.0052 – 0.0053

*Data are mean values ± standard deviation.

**Yarkwan & Oketunde, 2016

4. Conclusion

Based on the proximate analysis, vitamins, amino acids and mineral composition, OFSP juice shows a promising potential to be an alternative for a healthy drink. The highlight of the juice composition was the high content of β -carotene, which can provide many health benefits including prevent anti-mutagenic, immuno-enhancers, cancers and free radical

scavengers. Besides the vitamins, amino acids and mineral content of the OFSP juice are also considered sufficient to partly cater to the recommended daily intake of consumers.

Acknowledgments: Authors are thankful to the staff technician laboratory, Department of Processing and Food Engineering, Faculty of Engineering, for their considerable help to complete this research successfully.

Funding: The research was supported by GP-IPB/2018/9660302, University Putra Malaysia (UPM), Serdang, Selangor, Malaysia is acknowledged

Conflicts of Interest: The authors declare no conflict of interest, and also the funders had no role in the collection, analyses, or interpretation of data; design of the study; in the writing of the manuscript, or in the decision to publish the results.

References

- Alam, M., Rana, Z., & Islam, S. (2016). Comparison of the Proximate Composition, Total Carotenoids and Total Polyphenol Content of Nine Orange-Fleshed Sweet Potato Varieties Grown in Bangladesh. *Foods*, 5(4): 64.
- AOAC. (1995). *Association of Official Analytical Chemist*. Official methods of analysis, 17th edition. Washington, DC.
- AACC. (2000). *Approved Methods of the American Association of Cereal Chemists*, Vol. 1 (Method No. 30–25, 44–15A), USA: American Association of Cereal Chemists.
- Biswas, A. K., Sahoo, J., & Chatli, M. K. (2011). A simple UV-Vis spectrophotometric method for determination of β -carotene content in raw carrot, sweet potato and supplemented chicken meat nuggets. *LWT – Food Science and Technology*, 44(8): 1809–1813.
- Chiosa, V., Mandravel, C., Kleinjans, J. C. S., *et al.* (2005). Determination of B-Carotene Concentration in Orange and Apple Juice and in Vitamin Supplemented Drinks. *Analele Universităţii din Bucureşti – Chimie, Anul XIV (serie nouă)*; Vol. I–II, 253–258.
- Dako, E., Retta, N., & Desse, G. (2016). Comparison of Three Sweet Potato (*Ipomoea Batatas* (L.) Lam) varieties on Nutritional and Anti-Nutritional Factors. *Global Journal of Science Frontier Research: D Agriculture and Veterinary*. 16(4): 63–71.
- Danish, A.Z., Rozaihan, M., Mohd, M.M.A., *et al.* (2019). Differentiation of Malaysian Farmed and Commercialised Edible Bird's Nests through Nutritional Composition Analysis. *Pertanika J. Trop. Agric. Sc.* 42(3): 871–881.
- FAO/WHO (1998). *Carbohydrate in Human Nutrition*. Report of a Joint Expert FAO/WHO Consultation. FAO Food and Nutrition Paper 66. Food and Agriculture Organization, Rome. 140 p.
- Foss Analytical AB. (2003). *Manual for Kjeltac System 2300 Distilling and Titration Unit*.
- Gaesser, G.A., & Angadi, S.S. (2015). Navigating the gluten-free boom. *Journal of American Academy of Physician Assistants*, 28(8): 1–8.
- German Nutrition Society (DGE) (2015). New Reference Values for Vitamin C Intake. *Ann Nutr Metab*, 67:13–20. doi: 10.1159/000434757.

- Koubová, E., Sumczynski, D., Šenkárová, L., *et al.* (2018). Dietary Intakes of Minerals, Essential and Toxic Trace Elements for Adults from Eragrostis tef L. *A Nutritional Assessment. Nutrients*, 10(4): 479.
- Mamo, T.Z., Mezgebe, A.G., & Haile A. (2014). Development of orange-fleshed sweet potato (*Ipomoea batatas*) juice: Analysis of physico-chemical, nutritional and sensory property. *International Journal of Food Science and Nutrition Engineering*, 4(5): 128–137.
- Management Association, Information Resources. (2018). *Food Science and Nutrition: Breakthroughs in Research and Practice: Breakthroughs in Research and Practice*. Book. IGI Global, Medical.
- Mohanty, B., Mahanty, A., Ganguly, S., *et al.* (2014). Amino Acid Compositions of 27 Food Fishes and Their Importance in Clinical Nutrition. *Journal of Amino Acids*. 7.
- Owolade, S.O., Akinrinola, A.O., Popoola, F.O., *et al.* (2017). Study on physico-chemical properties, antioxidant activity and shelf stability of carrot (*Daucus carota*) and pineapple (*Ananas comosus*) juice blend. *International Food Research Journal*, 24(2): 534–540.
- Ragunatha, S., Kumar, J.V., Muruges, S.B., *et al.* (2014). Therapeutic Response of Vitamin A, Vitamin B Complex, Essential Fatty Acids (EFA) and Vitamin E in the Treatment of Phrynoderma: A Randomized Controlled Study. *Journal of Clinical Diagnostic Research*, 8(1): 116–118.
- Rodrigues, N. da R., Barbosa Junior, J.L., & Barbosa, M.I.M.J. (2016). Determination of physico-chemical composition, nutritional facts and technological quality of organic orange and purple-fleshed sweet potatoes and its flours. *International Food Research Journal*, 23(5): 2071–2078.
- Rose, I. M., & Vasanthakalam, H. (2011). Comparison of the Nutrient composition of four sweet potato varieties cultivated in Rwanda. *American Journal of Food and Nutrition*, 1(1): 34–38.
- Slavin, J. L., & Lloyd, B. (2012). Health Benefits of Fruits and Vegetables. *Advances in Nutrition*, 3(4): 506–516.
- Xiao, Z., Storms, R., & Tsang, A. (2006). A quantitative starch–iodine method for measuring alpha-amylase and glucoamylase activities. *Analytical Biochemistry*, 146–149.
- Yarkwan, B., & Oketunde, O. (2016). A Study of the Nutritional Composition of Freshly Squeezed and Processed Orange Juices. *Food Science and Quality Management*, 48, 126–132.



Original Research Article

Optimisation of parameters laser cutting of oil palm fronds using fibre pulsed laser of 1064 Nm wavelength system

Mohd Ikmal Hafizi Azaman^{1*}, Mohd Adzir Mahdi², Mohd Rizal Ahmad¹, Abd Rahim Shuib¹, Mohd Ramdhan Khalid¹, Mohd Azwan Bakri¹, Mohd Khairul Fadzly Md Radzi¹ and Ahmad Syazwan Ramli¹

¹Malaysian Palm Oil Board, 6, Persiaran Institusi, Bandar Baru Bangi, 43000 Kajang, Selangor, Malaysia

²Department of Computer and Communication System Engineering, Faculty of Engineering, Universiti Putra Malaysia, 43400 Serdang, Selangor, Malaysia

*Corresponding author: Mohd Ikmal Hafizi Azaman, Malaysian Palm Oil Board, 6, Persiaran Institusi, Bandar Baru Bangi, 43000 Kajang, Selangor, Malaysia, ikmalhafizi@mpob.gov

Abstract: Oil palm plantations produce fresh fruit bunches (FFB) as their primary output. Over the years, several technologies for cutting oil palm fronds and FFB have been developed and only a few of these technologies have been taken up by the industry. A study to explore the potential of fibre lasers as an alternative technology to cut oil palm fronds has been initiated where in this study laser cutting parameters using a 250 mm focus lens by manipulating power, speed and frequency are being optimised. The pulse fibre laser system used in this work operates at the wavelength and power of 1064 nm and 50 kW respectively where it is equivalent to 2 mJ of energy. Characterising and optimising the laser system with the 250 mm lens, an optimisation study is conducted in order to find a suitable working range for the fibre pulsed laser system to perform oil palm frond cutting. This study concludes that all three parameters; frequency, power and speed play huge roles in determining the quality and efficiency of the laser cutting. High frequency and speed with power above 80 % and 1 mm-1 will yield the desired results.

Keywords: oil palm harvesting; laser technology; pulse fibre laser; laser optimisation

Received: 2nd August 2020

Accepted: 2nd September 2020

Published: 24th September 2020

Citation: Azaman MIH, Mahdi MA, Ahmad MR, *et al.* Optimisation of parameters laser cutting of oil palm fronds using fibre pulsed laser of 1064 Nm wavelength system. *Adv Agri Food Res J* 2020; 1(1): a0000108. <https://doi.org/10.36877/aafjr.a0000108>

1. Introduction

Oil palm plantations produce the fresh fruit bunches (FFB) as their primary output. A hectare of a plantation yields an average of 18 tonnes of FFB in a year (Kushairi *et al.*, 2019). Good estate management generally will produce FFB above the mean value. Malaysia is targeting to increase the national FFB yield up to 25 tonnes per hectare per year by implementing good plantation management practices across all estates around the country.

Among good estate management practices are by improving the harvesting activity which includes cutting only ripe bunches, collecting all loose fruit, and prompt delivery of FFB to mill. Many different tools have been developed for harvesting oil palm. Over the years, several technologies for cutting oil palm fronds and fresh fruit bunch (FFB) have been designed, developed and tested. Most of the technologies developed are directed towards mechanical concepts such as pneumatic and hydraulic circular saw, chainsaw cutter and shear-type cutter. Some of these technologies were not well taken up by the industry due to many reasons such as bulkiness in size, difficulty, and high capital requirement. The Malaysian Palm Oil Board (MPOB) has taken the initiative to venture into a new approach for cutting technology. One of the possibilities of new technology is the laser. The aim of this research study is to explore the potential of the laser as an alternative technology to cut oil palm fronds. The potential laser as a harvesting tool in oil palm plantations is based on scientists' reports, laser cutting can be used for tomato stalk cutting based on two essential aspects. One is the power density at the focusing spot of this device which is decided by both laser beam quality and properties of the focusing system. The other aspect is the tomato stalk that can be cut through under certain defocusing distance due to enough depth of focus of laser cutting device and the lower burn temperature of tomato stalks (Ji-Zhan Liu *et al.*, 2011). The specific objective is to optimise the laser cutting system using a 250 mm focus lens by manipulating power, speed and frequency. This study proposes the implementation of pulse fibre laser technology that has yet, to be explored for oil palm frond optimisation for the next laser cutting. The success of this work will give a significant effect on the optimisation of the parameter that will be used on another fibre pulse laser cutting.

2. Materials and Methods

2.1. Laser Technology and types in industry

The laser is a device that emits light through an optical amplification process based on the stimulation emission of electromagnetic radiation. Based on findings, the term "laser" originated as an acronym for "light amplification by stimulated emission of radiation". The theory behind the operation of a laser was explained by Einstein in 1917 using the Plank's law of radiation, where the absorption and spontaneous stimulated emission of electromagnetic radiation are based on Einstein's coefficients (Gould, R. Gordon, 1959). Laser technology has been widely used in several industries. The wide range of laser applications relies on the output power of which the laser emits. In the manufacturing industry, for example, lasers have found its sole purpose in metal cutting (Ji-Zhan Liu *et al.*, 2011), while in the medical field, lasers are used for eye surgery, kidney stone treatment, ophthalmoscopy and cosmetic procedures.

Among the leading industrial lasers today are carbon dioxide (CO₂) laser, solid-state (Nd: YAG) laser, and fibre lasers (Niyibizi *et al.*, 2013). CO₂ laser is commonly used in the manufacturing industry for laser cutting (Ji-Zhan Liu *et al.*, 2011). Fibre laser is a single-

mode beam that is converted from the multimode beam quality. Fibre laser is a less complex laser compared to other laser types. The fibre laser is using the single emitter diodes that pump the active fibre with other elements, like Ytterbium (Yb), Erbium (Er) or Thulium (Tm). The features of fibre lasers are no power limit, best of the quality beam, overall of high efficiency, the lifetime of pump diodes, small footprint, mobile and point of economical view is low investment and maintenance costs. In fibre lasers, there are no parts to be exchanged permanently (Westphäling, 2010). The advantages of fibre lasers are due to their high beam quality, high wall-plug efficiency and their ability to process high reflective materials such as copper and copper alloys.

2.2. Pulse fibre laser with an operation wavelength at 1064 nm

In this work, pulsed fibre laser system was used as its temporal pulse profile is more suitable for frond cutting. A continuous wave laser emits continuous energy that will cause excessive burning of fronds which may damage the quality of FFB. The pulse fibre laser system used in this work operated at the wavelength and power of 1064 nm and 50 kW (2 mJ) respectively. The experimental setup is as shown in Figure 1 while Figure 2 depicts the actual setup at the photonics lab. The focusing lens was fixed on a laser scanning head by a fastening ring that allows control of the distance between the targeted material and the focusing lens. The system was controlled using a central processing unit (CPU) and software known as EZCAD which gives the users control over crucial laser marking parameters such as speed, frequency and power.

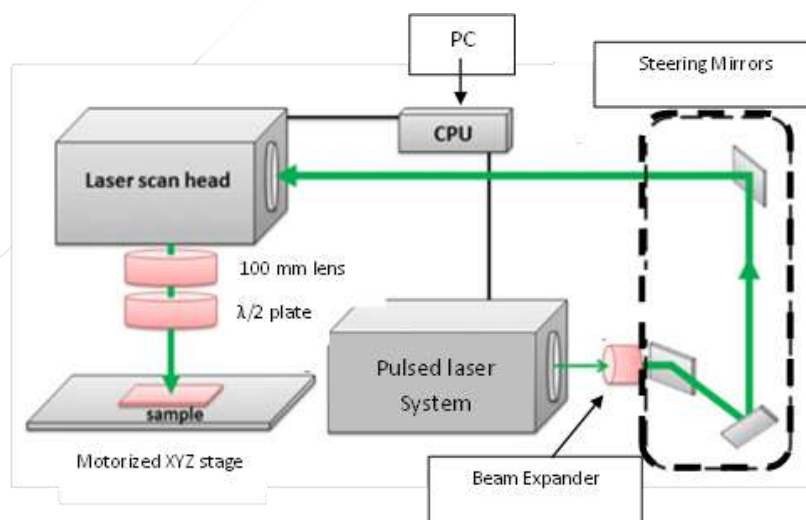


Figure 1. Experimental setup of oil palm frond cutting using a pulsed laser

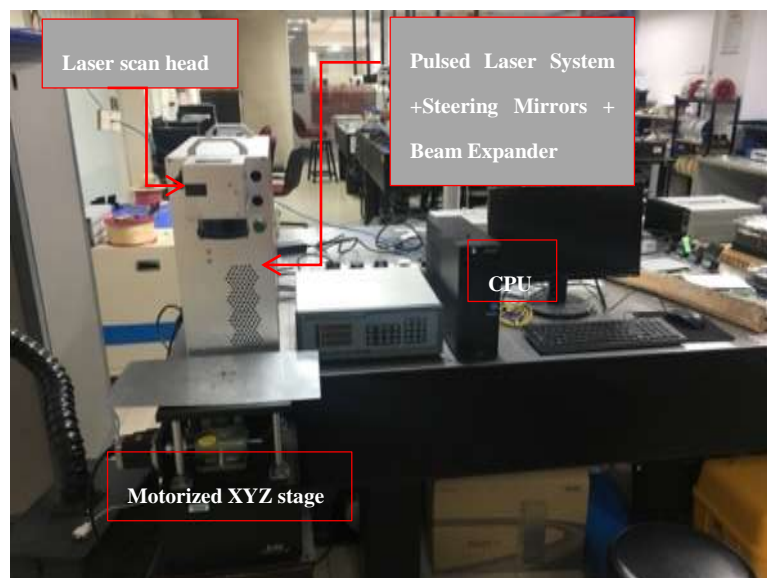


Figure 2. Installation of an equipment laser system

Dawson *et al.* (1998) investigated the optical properties and characteristics of the oil palm fronds and discovered similarities to other vegetation leaf material. Looking into the leaf composition, water contributes the most to the leaf weight. The remainder of leaf weight is a dry matter that is mainly composed of cellulose, lignin, protein, starch and minerals. The optical absorbance of these constituents increases with increasing concentration, thereby reducing leaf reflectance and transmittance. Ahmad *et al.* (2012) had reported that the oil palm fronds' composition consists of cellulose, hemicelluloses, lignin and others (water moisture, chlorophyll and protein). All these constituents have different optical properties with absorption ranging from the visible region and beyond the mid-infrared region (400 nm –2400 nm).

This understanding of the cellulose absorption peaks will help in optimising the laser parameters for ablating and cutting these oil palm fronds. When high energy laser beams are directed at the sample of fronds, the energy will be absorbed by the cellulose (material content in oil palm fronds), converting the high-energy laser pulses to thermal energy in a short burst, leading to material removal (ablation and cutting).

2.3. Optimisation with 250 mm of focal distance

One optical focus lens with 250 mm of focal distance was tested for the optimisation of the laser system. This section focuses on characterising the laser beam that was produced and its quality in cutting frond samples by looking at speed of the laser beam (mm s^{-1}), frequency (kHz), power (%), and time taken to complete the task of cutting. The frond samples were prepared by collecting randomly harvested fronds which were cut to 1 foot in length. The thickness, however, differed from one another which was an uncontrollable variable. The samples were tested with different power, frequency, and speed. Here, power refers to the energy of the laser system where 100% of power is equivalent to 50 W or 2 mJ.

To characterise the pulse fibre laser system, certain parameters must be identified first. Several parameters can be easily measured and used for calculation as follow;

2.3.1 Measured Parameters:

- Average Power (%); This is the average power measured from the laser output. The power is set in percentage via the EZCAD software with a total output power of 50 W at 100%.
- Repetition Rate (Frequency - kHz); This is the total number of laser pulses per second.
- Pulse Duration (nanosecond); This defines the pulse width ranging from 10 ns and up to 200 ns. The pulse duration can be set via the EZCAD software.

All the parameters above can be measured using a standard optical power meter with a thermopile sensor head and a fast photodetector connected to an oscilloscope. The parameters can be set directly using the laser software described earlier.

2.3.2 Calculated Parameters:

- Energy per Pulse; Energy per pulse is determined by dividing the average power by the repetition rate. The resultant quantity is the energy, in Joules, contained in each laser pulse.

$$E = \frac{P_{Av}}{R_{Rate}}, \quad (1)$$

where: E = Energy in Joules

P_{Av} = Average power in Watts

R_{Rate} = Repetition rate in pulses per Second

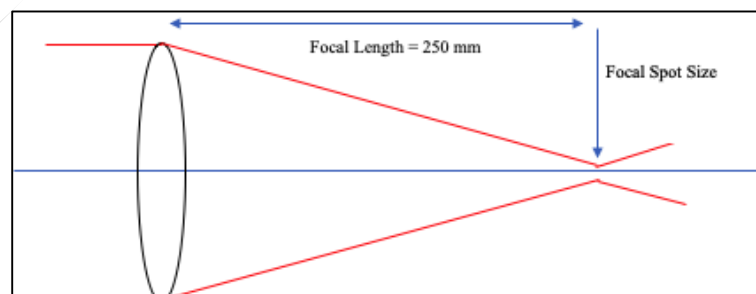


Figure 3. The diagram of focal length by lens at 250 mm

Prior to optimisation with the lenses, studies were conducted to see the effects of each parameter (power, speed, and frequency) on cutting depth. To test the effect of power, different power levels within the range of 40 % - 100 % were tested while keeping the other two parameters at a constant; speed and frequency at 1 mm s^{-1} and 800 kHz, respectively. The laser was let to run for 60 seconds, and the cutting depth was recorded. To test the effect of frequency, 200 kHz, 400 kHz, and 600 kHz were tested while power and speed remained 100 % and 1 mm s^{-1} , respectively. The laser was set to run for 90 seconds, and the cutting depth was recorded. Lastly, to assess the effect of speed, two different speeds were applied; 5 mm s^{-1} and 1 mm s^{-1} , while power and frequency remained at 100 % and 600 kHz. The main idea was to characterise and optimise the parameter of the laser cutting using 250 mm of focus lens. The several parameters have been used randomly and based on the various properties and characteristic of the fibre pulse laser (Westphäling, 2010). The study was conducted based on a preliminary study in which the result showed the deepest cutting has a cutting efficiency of 1 mm s^{-1} in the frequency range of 800 to 3000 kHz (Azaman *et al.*, 2018).

The main challenge is to ensure that the laser beam maintains the beam quality and the beam spot size when travelling across a distance to the target which is the oil palm frond. The success rate is high with the aim of removing the main material of oil palm fronds that is the cellulose and lignin out from the fronds and thus weakens the structure. On the system's side, there are no anticipating issues since these are commercially available systems. The focus should be on the beam delivery or focusing aspects and the laser beam interaction with the oil palm fronds. Theoretically, laser technology has the potential as a cutting tool in oil palm harvesting.

3. Results and Discussions

3.1. Characterisation and optimisation of laser cutting with 250 mm focus lenses

Prior to characterising and optimising the laser system with the 250 mm lenses, an optimised study was conducted in order to find a suitable working range for the laser system to perform oil palm frond cutting. To determine the working range, the power, frequency and speed of the laser were manipulated.

Firstly, four different power levels (40 %, 60 %, 80 % and 100%) were tested by cutting the same frond sample (Figure 4) for 60 seconds and maintaining the frequency and speed at 800 kHz and 1 mm s^{-1} . This is to assess the effect of varied power onto cutting depth with constant frequency and speed. Figure 4 shows the average cutting depth attained from each power level that was tested with a standard deviation of $\pm 0.13 \text{ mm}$. Based on Figure 5, 100 % of power resulted in the deepest cutting-depth of 3.02 mm with an average 0.063 mJ of energy per pulse while 40 % with an average 0.025 mJ of energy per pulse attained the shortest cutting-depth at 1.07 mm. The result also shows that cutting depth is directly proportional to the power of the laser. This correlates with the absorption theory as more

energy is emitted on the targeted material, more will be absorbed by the frond and cause deeper ablation. Also, the results suggest that efficient laser cutting can only be achieved with power > 80% as any length of depth below 2 mm per minute will not follow the standard time of cutting oil palm fronds.

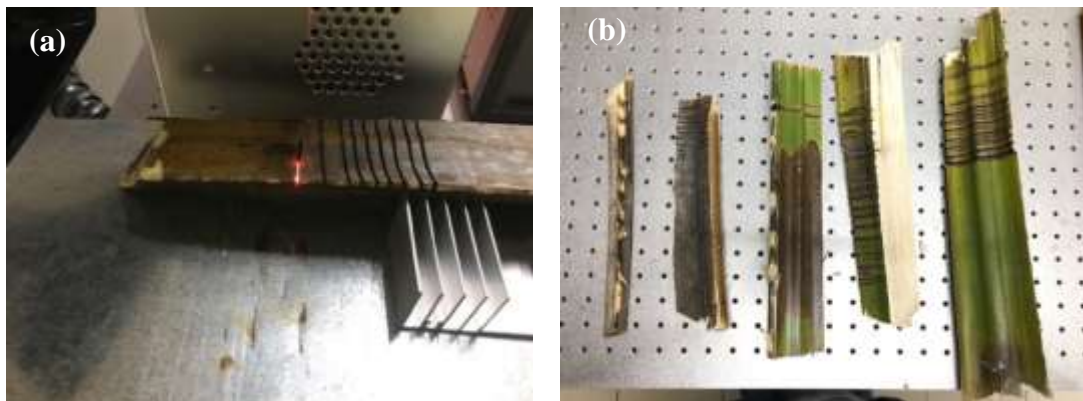


Figure 4. (a) Laser cutting for optimisation parameters, (b) Sample of oil palm fronds

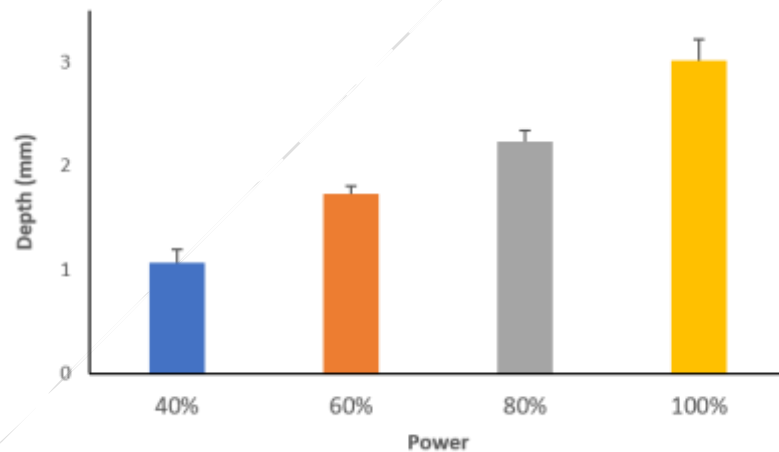


Figure 5. Effect of laser power to the cutting depth of oil palm frond

Figure 6 exhibits the relationship between cutting depth and average frequency taken from 3 data sets when the different frequency was applied to the system (200 kHz, 400 kHz, and 600 kHz) while power and speed remained constant at 100 % and 1 mm s^{-1} , respectively, and cutting time was set to 60 s. Among the tested frequencies, 600 kHz managed to attain the deepest cutting depth with $16.3 \text{ mm} \pm 1.26 \text{ mm}$ with an average energy of 0.063 mJ per pulse while 200 kHz achieved the shortest cutting depth at $3.3 \text{ mm} \pm 0.25 \text{ mm}$ with an average energy of 0.25 mJ per pulse. From here, a distinct trend can be seen between frequency and cutting depth where higher frequency will yield deeper cuts. This is in good agreement with the fact that as more pulses hit the targeted material, more energy will be absorbed to create

greater ablation. When the higher frequency was applied in the system, the energy per pulse hitting the samples was more frequent than the lowest frequency.

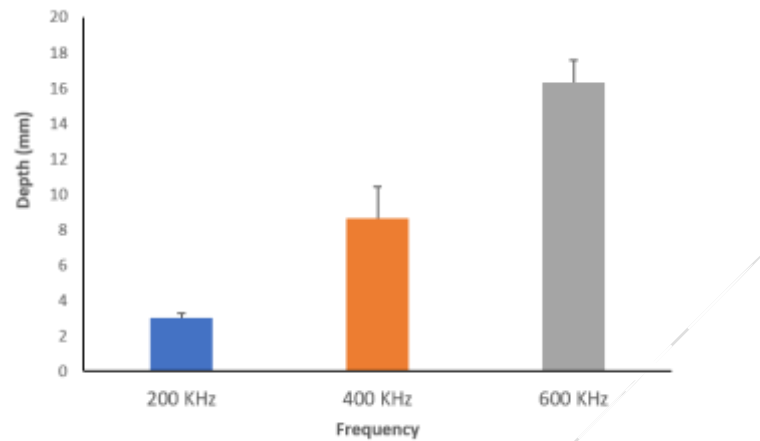


Figure 6. Effect of laser frequency to the cutting depth of oil palm frond

In Figure 7, the average cutting depth of two different laser speeds; 1 mm s^{-1} and 5 mm s^{-1} were compared with constant power and frequency at 100% and 600 kHz, respectively. The best average cutting depth was attained by 1 mm s^{-1} at $9.4 \text{ mm} \pm 1.86 \text{ mm}$, while 5 mm s^{-1} achieved $6.8 \text{ mm} \pm 1.53 \text{ mm}$ with both the energy per pulse at 0.083 mJ . The slowest speed gave more energy per pulse to spot on the surface of the samples. Laser speed here refers to the distance it can cover within a second. It is postulated that less speed attains better cutting depth because the laser beam is focused longer on a particular spot of the material which allows greater absorption and ablation.

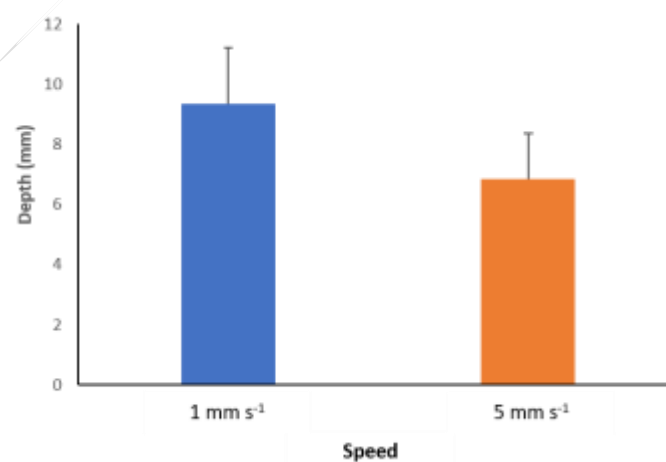


Figure 7. Effect of laser speed towards the cutting depth of oil palm frond

The results obtained show that all three parameters; frequency, power and speed; play huge roles in determining the quality and efficiency of the laser cutting. High frequency and lowest speed with power above 80 % and 1 mm s^{-1} respectively will yield the desired results. The energy per pulse reflecting the frequency of the system was applied in laser cutting. The lowest speed with high frequency, the energy per pulse hitting the spot on the surface of the sample gives more precise cutting and ablation.

4. Conclusion

Overall, it has been learned that a pulsed laser system operating at 1064 nm is capable to cut oil palm fronds. The main parameters that were looked into were frequency, power, and speed as these parameters determine the intensity of the laser at a given time and also time taken to cut through the fronds. Based on the results obtained, higher power and frequency at low speed will give better laser cutting performance. The main focus of this work is to optimise the parameter of using pulsed fibre laser technology in cutting oil palm fronds. This was achieved by assessing optimisation effects of power, speed, and frequency on time taken to cut through a frond sample. Overall, it was a successful attempt at using pulsed fibre laser technology to cut oil palm fronds. It is undeniable that using this alternative, precise cuts can be made with less man energy and less machinery which should boost production efficiency. Further experiments are encouraged to look into better ways in enhancing the laser cutting performance.

Acknowledgement: The researchers would like to thank the MPOB and UPM for their assistance.

Funding: This research was supported by MPOB.

Conflicts of Interest: The authors declare no conflict of interest, and also the funders had no role in the design of the study; in the collection, analyses, or interpretation of data; in the writing of the manuscript, or in the decision to publish the results.

References

- Ahmad, T.Y. and Tsuyoshi, H. (2012). Efficacy of hydrothermal treatment for production of solid fuel from oil palm wastes. *Resource Management for Sustainable Agriculture (V Abrol and P Sharma eds.)*. InTech.
- Azaman, M.I.H., Mahdi, M.A., Jelani, A.R., *et al.* (2018). The potentials of laser cutting technologies for oil palm harvesting. *Oil Palm Bulletin*, 77, 19–25.
- Dawson, T. P., Curran, P. J. and Plummer, S. E. (1998). Liberty - Modelling the effects of leaf biochemistry on reflectance spectra. *Remote Sensing of Environment*, 65, 50–60.
- Gould, R. and Gordon. (1959). The LASER, Light amplification by stimulated emission of radiation. In Franken, P.A., Sands, R.H. (eds.). *The Ann Arbor Conference on Optical Pumping*, the University of Michigan, 15 June through 18 June 1959, 128.
- Kushairi, A., Meilina, O-A., Balu, N., *et al.* (2019). Oil palm economic performance in Malaysia and R&D progress in 2018. *Journal of Oil Palm Research*, 31, 165–194.
- Liu, J-Z., Hu, Y., Xu, X-Q., *et al.* (2011). Feasibility and influencing factors of laser cutting of tomato peduncles for robotic harvesting. *African J. Biotechnology*, 10(69), 15552–15563.

Niyibizi, A., Kioni, P.N., and Ikua, B.W. (2013). Recent developments in laser sources for industrial applications. *Proc. of the 2013 Mechanical Engineering Conference on Sustainable Research and Innovation*, 5, 24–26.

Westphäling, T. (2010). Pulsed fiber lasers from ns to ms range and their applications. *Physics Procedia* 5 (2010), 125–136.



Copyright © 2020 by Azaman MIH, *et al.* and HH Publisher. This work is licenced under the Creative Commons Attribution-Non-commercial 4.0 International Licence (CC-BY-NC4.0)

Original Research Article

Anaerobic Co-digestion of Pineapple Wastes with Cow Dung: Effect of Different Total Solid Content on Bio-methane Yield

Adila Fazliyana Aili Hamzah^{1*}, Muhammad Hazwan Hamzah^{1,2}, Fauzan Najmi Ahmad Mazlan¹, Hasfalina Che Man^{1,2}, Nur Syakina Jamali³, Shamsul Izhar Siajam³

¹Department of Biological and Agricultural Engineering, Faculty of Engineering, Universiti Putra Malaysia, 43400 UPM Serdang, Selangor, Malaysia

²Smart Farming Technology Research Centre, Faculty of Engineering, Universiti Putra Malaysia, 43400 UPM Serdang, Selangor, Malaysia

³Department of Chemical and Environmental Engineering, Faculty of Engineering, Universiti Putra Malaysia, 43400 UPM Serdang, Selangor, Malaysia, syakina@upm.edu.my, shamizhar@upm.edu.my

*Corresponding author: Muhammad Hazwan Hamzah, Department of Biological and Agricultural Engineering, Faculty of Engineering, Universiti Putra Malaysia, 43400 UPM Serdang, Selangor, Malaysia; hazwanhamzah@upm.edu.my

Abstract: The abundance of agricultural wastes produced from pineapple processing and livestock industries has resulted in the difficulties of disposing of a large amount of waste. Anaerobic digestion is a way to reduce waste and generate renewable energy sources including biogas. In this study, pineapple waste is co-digested with cow dung in batch experiments under mesophilic temperature at $38\pm 1^\circ\text{C}$ at a working volume of 100 ml in 125 ml serum bottle. The effects of the total solid on methane yields are investigated at a different substrate ratio. The batch study is conducted at 3 different total solid which are 12%, 20% and 28% and at three different substrate ratio cow dung to pineapple waste (CD: PW) (1:1, 1:2 and 1:3). Daily biogas collection for 28% total solid at 1:1 ratio results in the highest cumulative biogas production of 313 ml, followed by 28% total solid at 1:3 ratio with 246 ml biogas yield. The highest methane yield is achieved at 12% total solid with a 1:2 ratio (17.19 $\text{CH}_4/\text{g VS}$). Results show that at 12% total solid produces the highest methane yield at all ratios compared to other total solid percentages. Moreover, methane yield decreases as the total solid percentage increases from 12% to 28%. Overall, the production of methane from pineapple wastes co-digested with cow dung is proven to be a good strategy to minimise solid wastes.

Keywords: Biogas; co-digestion; cow dung; methane; pineapple; total solid

Received: 8th August 2020

Accepted: 10th September 2020

Published: 30th September 2020

Citation: Aili Hamzah AF, Hamzah MH, Ahmad Mazlan FN, *et al.* Anaerobic co-digestion of pineapple wastes with cow dung: Effect of different total solid content on bio-methane yield. *Adv Agri Food Res J* 2020; 1(1): a0000109. <https://doi.org/10.36877/aafj.a0000109>

1. Introduction

Malaysians generated about 38,142 tons of waste daily in 2018 according to The Star Online and there was a tremendous upsurge in the amount of waste generated in Malaysia in 2018 compared to 19,000 tons waste per day in 2005 in which 44.5% of them were food waste (Chu, 2019). Through anaerobic digestion, renewable resources especially food waste can be utilised as energy and nutrient. In an anaerobic environment, anaerobic digestion process works by decomposing the organic matter by microbes and produces 50–75% methane (CH₄), 19–34 % carbon dioxide (CO₂) and less than 1% biohydrogen (H₂) (Elina, 2016; Jehan *et al.*, 2017). During anaerobic digestion, through the metabolic action of methanogenic bacteria, wastes are converted biochemically into methane. The reactions are carried out by various groups of microbes at four different stages named hydrolysis, acidogenesis, acetogenesis and methanogenesis (Deressa *et al.*, 2015; Mata-Alvarez *et al.*, 2000; Ogunleye *et al.*, 2016).

Nowadays, there are few methods that are subjected to anaerobic digestion: single-phase digestion, two-phase digestion, dry fermentation and co-digestion (Deressa *et al.*, 2015). Three major issues or difficulties have been reported, namely; the effect operational factors, the nutritional imbalance and lack of diversified microorganisms via direct utilisation of substrates or mono-substrates in anaerobic digestion (Hagos *et al.*, 2017). Here, it is suggested that the co-digestion process can be performed to reduce the aforementioned problem, like incorporating agricultural by-products with livestock manure. Several lines of evidence have established that co-digestion is an economically feasible and promising technology in terms of good synergism in the digestion reactor and the ability to improve stability of the process, as well as to improve the biogas production rates (Astals *et al.*, 2013; Giuliano, 2013; Mata-Alvarez *et al.*, 2000). Anaerobic digestion is often categorised based on total solids (TS) content classes. Three of the foremost classes based on substrate total TS content — wet for TS lower than 15%; dry for TS lower than 25%; and solid-state operated at up to 40% TS content (Abbassi-Guendouz *et al.*, 2012; Rabii *et al.*, 2019; Yi *et al.*, 2014).

In the pineapple sector, a lot of agricultural waste from pineapple is produced from various harvesting activities (Chakravarty, 2016; Chan, 2000). Currently, according to Rani and Nand (2004), lack of the appropriate method of managing these wastes has become an environmental concern. Converting pineapple wastes into value-added products is one of the promising ways to handle these wastes without destroying the environment (Khai *et al.*, 2014; Maneeintr *et al.*, 2018). Biogas can be produced from peel, core, pulp and crown of pineapple waste, but the amount of nitrogen in these wastes is insufficient to produce a high amount of biogas. A high amount of carbohydrates in pineapple wastes can be used as a carbon source

for microbial fermentation to produce bio-methane (Khai *et al.*, 2014). Livestock such as cows and buffaloes produce lots of manure and most of the manure ends up as waste. Livestock manure is the main organic waste that contains a high quantity of nitrogen (N) and phosphorus (P), a high percentage of these substances causes nutrient imbalance and failure to properly manage these wastes leads to environmental pollution (Chakravarty, 2016; Deressa *et al.*, 2015). Bacteria found in cow dung are known to produce a high yield of methane gas (Gupta *et al.*, 2016). According to Neshat *et al.* (2017), facultative and obligative bacteria are responsible for hydrolysis and acidogenesis and several bacterial genera including *Corynebacterium*, *Lactobacillus*, *Escherichia coli* and *Actinomyces* were isolated from an anaerobic digester.

Lignocellulosic wastes are ineffective to be used as the sole substrate and hard to digest due to their complex structure that hinders their biodegradability. While manure contains useful microorganisms that can enhance biological activity and about 10 pounds of nitrogen were found in per ton of cow dung (Neshat *et al.*, 2017). However, the carbon insufficiency in cow dung cannot completely fulfil the anaerobic digestion requirements. Temperature is one of the important parameters in anaerobic co-digestion. Thus, it has been suggested to be incorporated with carbon-rich wastes. Higher operational temperature requires higher energy demand and that makes mesophilic temperature preferable compared to thermophilic (Alemahdi *et al.*, 2015). The mesophilic temperature should be maintained at 20°C to 40°C. Hydraulic retention time, total solid (TS), volatile solids (VS), initial cultivation pH, temperature, C/N ratio and the ratio of pineapple waste to cow dung are some of the common operational parameters that need to be considered when operating anaerobic digester. To ensure high biogas yield, optimisation of these parameters is necessary, but it depends on the type of waste and operation used. Thus, all of these facts suggest for us to optimise the biogas production process from pineapple waste and cow dung using anaerobic co-digestion in mesophilic condition but due to several limitations, only TS factor is chosen as a preliminary study. The current study aims at investigating the effect of TS added in anaerobic co-digestion of pineapple waste with cow dung at different ratios. Hence, incorporating lignocellulosic materials such as pineapple waste and nitrogen-rich waste like cow dung has been seen as a good strategy in managing waste.

2. Materials and Methods

2.1. Substrate Preparation

The wastes of Sarawak pineapple were collected from sundry supermarkets around Serdang, Selangor area. The pineapple wastes consisting of pulp, core, peel and crown were ground using an electric blender. The cow dung was collected from Ladang 16 at UPM, Selangor. The cow dung and pineapple wastes were stored at 4°C and later used as substrates

for anaerobic co-digestion. The substrates were first characterised on their total solid (TS), volatile solids (VS), carbon (C) and nitrogen content (N) and pH. The carbon and nitrogen were analysed by using CHN628 Series Carbon, Hydrogen, Nitrogen Determinator (LECO, United States) and the values were used to determine the C/N ratio of the substrate. Meanwhile, TS and VS were conducted based on the standard method (APHA, 1998). Then, the pH of the substrates was measured using pH5SS Spear pH Tester (IONIX, Singapore).

2.2. Experimental Setup

The anaerobic co-digestion experiment was conducted at 100 ml working volume with 25 ml headspace in 125 ml serum bottles as shown in Figure 1. Pure nitrogen gas was flushed into the serum bottles for 2 minutes to remove oxygen traces as well as to ensure the anaerobic condition and the bottles were enclosed with rubber stoppers. Co-digestion was conducted at mesophilic temperature ($38\pm 1^\circ\text{C}$) in water bath WNB 45 (Mettler, Germany) for 30 days. The gas was collected for 30 days to observe the difference of gas produced in each day. The water displacement method was used to measure cumulative biogas production (Jehan *et al.*, 2017). Abbassi-Guendouz *et al.* (2012) stated that the threshold value of the TS solid of the feedstock is 30% since the methanogenic activity was strongly inhibited above that value. Meanwhile Fernández *et al.* (2008) observed that the reactor had significantly high performance when TS content was adjusted to 20%. Ardaji *et al.* (2016) observed that biogas production increased when TS increased from 5 to 25%. Thus, this study was conducted at TS at 12% to 28%. The bottles containing the mixture of pineapple waste and cow dung were at 3 different ratio CD: PW of 1:1, 1:2 and 1:3, respectively. The pineapple waste slurry was first diluted to 3 different total solids (TS) of 12%, 20 % and 28 % of pineapple waste added using distilled water (Abbassi-Guendouz *et al.*, 2012; Ardaji *et al.*, 2016; Fernández *et al.*, 2008). The initial pH of both substrates was low; the final pH after mixing both substrates was still insufficient to be maintained around the optimal pH. Thus, the pH of substrates was adjusted to 7 ± 1.0 using sodium hydroxide (NaOH) (Jehan *et al.*, 2017). In order to produce methane and biogas effectively, it is crucial to maintain pH, C/N ratio and temperature at the optimal condition to provide better growth conditions for methanogenic bacteria. Hence, pH value must be maintained at 6.5 to 8.0 (Ogunleye *et al.*, 2016; Sibiya *et al.*, 2014). The experiments were triplicate, and biogas was collected daily and its composition was analysed.

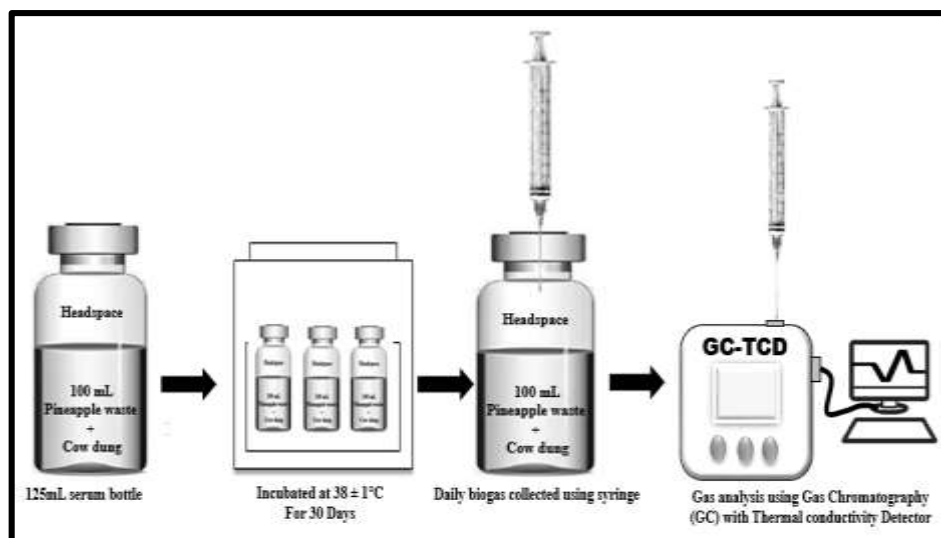


Figure 1. The co-digestion of pineapple waste and cow dung process.

2.3. Biogas Measurement and Analysis

The composition of the daily biogas produced was determined by a gas chromatograph (GC) (Agilent 6890) with thermal conductivity detector (TCD). Methane (CH₄) gas quantity in 1 ml sample was calculated using Equation 1 (Alemahdi *et al.*, 2015; Khairul *et al.*, 2018). The methane yield was expressed as the volume of methane produced based on the initial total VS of the feedstock.

$$\text{CH}_4 \text{ area} / 2291.67 = \text{qCH}_4 \text{ quantity in 1ml gas sample} \quad (1)$$

3. Results and Discussions

3.1. Characteristics of Pineapple Waste and Cow Dung

It is crucial to examine the characteristic of the waste before conducting the co-digestion process, pineapple waste and cow dung were first characterised based on their TS, VS, carbon content, nitrogen content, C/N ratio and pH, and the results are summarised in Table 1. It can be seen from the characterisation results, the TS, VS and pH of the pineapple were 79.35%, 4.95% and 4.82%, respectively while 81.86%, 6.25 % and 6.81% for cow dung, respectively. In accordance with that, cow dung had the highest TS, VS and pH compared to pineapple waste. Formerly, Rani and Nand (2004) reported that the TS, VS and pH of pineapple as 72.57%, 95.90% and 4.7% whereas Anhuradha and Mullai (2010) stated that TS and VS of cow dung were 15.32% and 77.50 %, respectively. High TS value suggests that there is low water content in the wastes (Ardaji *et al.*, 2016; Liotta *et al.*, 2014). Apart from that, pineapple waste has high carbon content compared to cow dung. The C/N ratio of pineapple waste and cow dung were 44.95 and 55.51, respectively, in which the ratio was

determined from the carbon and nitrogen content from the CHNS analyser. C/N ratio in this study was relatively higher than other studies (Anhuradha & Mullai, 2010; Arelli *et al.*, 2018; Bardiya *et al.*, 1996; Dahunsi, 2019). Low nitrogen value in waste contributes to the higher C/N ratio (Arelli *et al.*, 2018; Dahunsi, 2019). Based on the literature, C/N of anaerobic digestion should be maintained at a ratio range of 20–30, and unsuitable C/N ratio can contribute to the increase of total ammonia nitrogen (TAN), free ammonia or high volatile fatty acids (VFAs) accumulation (Kainthola, Kalamdhad, & Goud, 2019). Excessive ammonia concentration inside anaerobic digester contributes to elevated pH in the digester, which is toxic to methanogens as well as leads to microbial growth inhibition (Rabii *et al.*, 2019).

Table 1. Characterisation of pineapple waste and cow dung.

Parameter	Pineapple Waste	Cow Dung
Total Solid (TS)	79.35%	81.86%
Volatile Solid (VS)	4.95%	6.25%
Carbon content	39.79%	8.90%
Nitrogen Content	0.89%	0.16%
C/N ratio	44.95	55.51
pH	4.82	6.81

3.2. Cumulative Biogas Production

The cumulative biogas production for all TS at different CD: PW ratio is shown in Figure 2 (a)–(c). According to the results, the highest cumulative biogas was produced by 28% TS at 1:1 ratio of CD: PW followed by 28% TS at 1:3 ratio. In contrast, the lowest cumulative biogas was produced by 12% TS at 1:3 ratio of the substrate. Comparing the cumulative biogas production for 12%, 20% and 28% at all CD: PW ratio of the substrate, 28% of TS produced the highest biogas after 30 days compared to the other TS. According to Ardaji *et al.* (2016), at high TS, the amount of organic matter increase could benefit the degradation process. The higher the TS percentage added, the higher the biogas produced. As observed in Figure 2(a), initially the biogas produced by 28% was lower than 20% and 12% but biogas produced kept increasing after day 3 as more substrates were degraded by the microbes. The same trends were showed by 28% TS in Figure 2 (b), where the amount of biogas produced was lower than 20% but the biogas produced was higher than all TS after day 23. Meanwhile, in 1:3 ratio as shown in Figure 2 (c), the biogas produced in 28% was always higher than all TS from the beginning until the end of the fermentation period. Even so, the composition of biogas is essential to be examined as the biogas produced contains methane and other gas components.

This finding was in accordance with those reported by Ardaji *et al.* (2016) who observed the effect of TS adjustment on biogas production from co-digestion of pomegranate waste,

poultry manure and cow dung sludge. They found out that biogas production increased from 0.273 L/day to 0.736 L/day with an increase in TS from 5% to 25% and the highest TS which was 25% produced the highest biogas production. Complementary to this, it has also been reported that co-digestion of pineapple, orange, apple, banana and jackfruits produce more biogas (975ml) compared to pineapple alone (900 ml) due to the high concentration of solids and total viable count of microbes than the sole fruit substrate (Chakravarty, 2016).

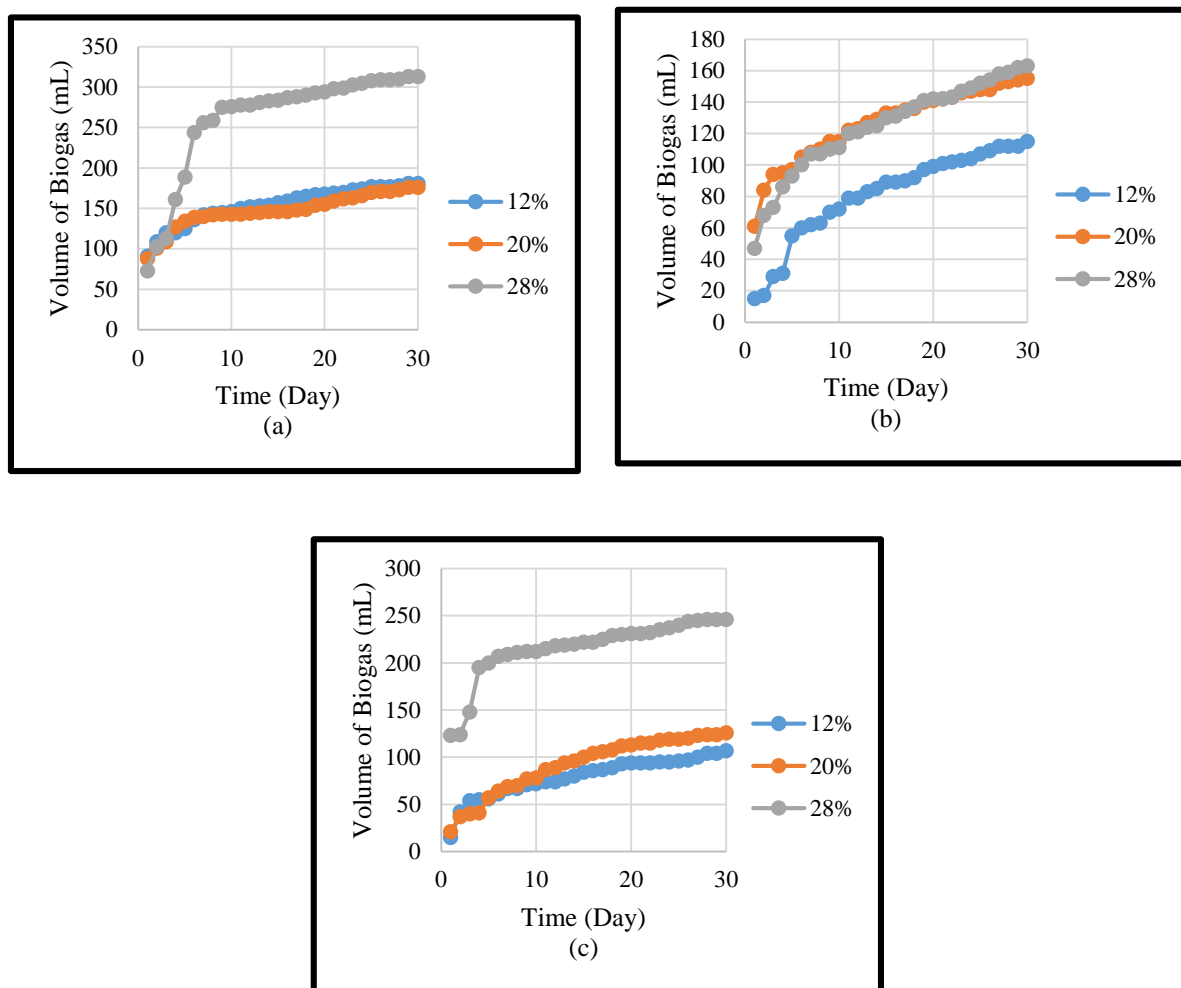


Figure 2. Cumulative biogas production for CD:PW ratio (a) 1:1; (b) 1:2; (c) 1:3.

3.3. Methane Yield from Batch Fermentation

The effect of TS on the cumulative methane yield at different ratio over 30 days of fermentation is shown in Figure 3 (a)–(c). According to Figure 3 (a), at 1:1 CD:PW ratio, 12% TS showed a constant increase in methane yield over 30 days of the fermentation period. Whereas at 20% and 28% TS, methane production was slower towards the end after 5 days. At 1:2 ratio CD:PW, all TS showed increasing trends in methane production (Figure 3 [b]). For 12% TS, methane produced higher methane compared to 20% and 28% TS and increased

to the maximum yield after 5 days. Then, as illustrated in Figure 3 (c), 12% and 20% TS showed a constant increase. However, after 23 days, there was no methane produced for 20% TS while for 12% TS, methane was still being produced after 27 days. On the other hand, the amount of methane produced was the lowest and slow since the start for 28% TS since, at high TS, the substrate content was high in lignocellulosic materials thus making it harder for the microbes to degrade it (Abbassi-Guendouz *et al.*, 2012; Fernández *et al.*, 2008).

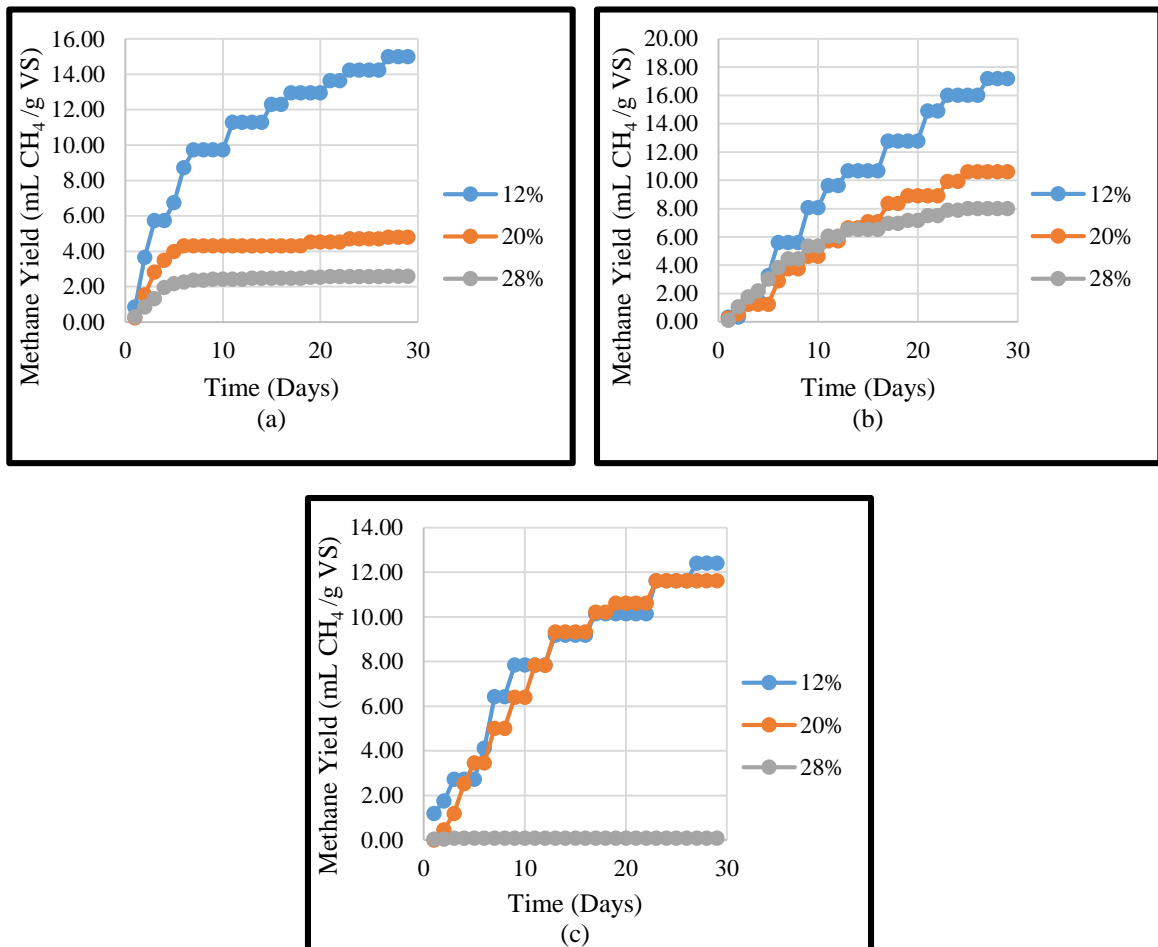


Figure 3. Cumulative methane production for CD:PW ratio (a) 1:1; (b) 1:2; (c) 1:3.

Low methane content suggests slow hydrolysis and low biodegradability of the substrate. To which at higher TS content, the amount of substrate increases while water content decreases, thus contributing to the aforementioned problems (Ardaji *et al.*, 2016; Orhororo, Egunilo & Sadjere, 2017). High pineapple wastes in the substrate mixture also make it hard for the microbes to degrade the wastes. According to Jehan *et al.* (2017), a slow rate of degradation of the substrates is due to the complex structure of lignocellulosic biomass such as pineapple that makes it hard for the microbe to digest the substrate. Dahunsi (2019) also pointed out that due to the lignin-cellulose matrix in lignocellulosic biomass, there are limits in the process efficacy during hydrolysis where microbial enzymes fail to degrade these substrates. Lignin-cellulose matrix presence in the lignocellulosic wastes itself makes its

structure very complex and resistant to deconstruction. The exposure of cellulose and hemicellulose to microbial attack during hydrolysis to convert it into simple sugar is interrupted by its cell structure support named lignin (Karuppiah & Azariah, 2019). The lignin layer protects the cellulose and hemicellulose and makes it inaccessible for degradation.

Overall, 12% TS of 1:2 ratio CD:PW resulted in the highest methane yield with 17.19 ml CH₄/g VS followed by 12 % TS at 1:1 ratio with 15 ml CH₄ /g VS after 30 days. Conversely, the lowest methane yield was produced by 28% TS at a 1:3 ratio with only 0.08 ml CH₄/g VS. In this study, it was observed that methane yield decreases as the TS percentage increases at all ratio in which TS of 28 % contributes to the lowest methane yield at all ratio. Even if 28% TS gives the highest biogas produced compared to 12% and 20%, the methane content is low. This is due to the other biogas composition such as carbon dioxide and hydrogen that contribute more in terms of its composition (Khairul *et al.*, 2018; Neshat *et al.*, 2017). Biogas that contains high methane makes it a useful fuel to replace natural gas or can be transformed into heat and electricity (Jafari-Sejahrood *et al.*, 2019).

Similar findings were reported by Ogunleye *et al.* (2016) using animal waste and fruit wastes where the yield of methane decreased with an increase in TS content from 8% to 40%. Liotta *et al.* (2014) also mentioned that increasing TS of food waste from 4.5% to 19.2% contributes to the reduction in methane production. The drop in methane yield as TS increases is due to the amount of water. Water reduces the restriction of mass transfer of the particulate substrate and promotes hydrolysis, making it possible for bacteria growth and movement as well as nutrient transportation (Ejiroghene *et al.*, 2017; Liotta *et al.*, 2014). Thus, at higher TS, low water content causes the transport process to be slower which on the other hand, reduces the level of microbial activity, hence, lowering the methane produced (Liotta *et al.*, 2014).

4. Conclusion

It can be concluded that the co-digestion of pineapple waste and cow dung has proved that the addition of pineapple waste has the potential of increasing biogas. This study focused on the effect of the TS percentage on the biogas and methane yield from the co-digestion process. Co-digestion of pineapple waste at high TS content produces high biogas yield. On the contrary, high methane yield is observed at low TS percentage although, at low TS content, the amount of biogas is low. A decreasing trend of methane yield is observed when increasing the TS content. Low methane content suggests low water content at high TS which inhibits the microbial activity, thus, reducing the digestion process. Moreover, the presence of complex structure due to the lignin layer that binds cellulose and hemicellulose in pineapple wastes makes it harder for microbes to degrade the substrate and consequently slows down the hydrolysis process. Further improvement should be implemented and developed to improve the efficacy of the process such as pretreatment of pineapple waste itself and make it accessible for the microbe to degrade the wastes. Thus, it was proven that

successful implementation of the anaerobic co-digestion as a method of waste treatment has the potential to change the concept of ‘waste to wealth’ which will lead to total utilisation of renewable energy resources in reducing energy requirement, making it readily available and minimising environmental pollution.

Author Contributions: Conceptualization, AFAH and FNAM; Formal analysis, AFAH and FNAM; Investigation, AFAH and FNAM; Methodology, AFAH and FNAM; Supervision, MHH, HCM, NSJ and SIS; Validation, MHH, HCM, NSJ and SIS; Writing — original draft, AFAH; Writing — review & editing, MHH and HCM All authors have read and agreed to the published version of the manuscript.

Funding: This research was financially supported by Geran Putra — Inisiatif Putra Muda (GP-IPM) through Universiti Putra Malaysia Grant (Grant No: GP-IPM/2018/9669700).

Acknowledgments: Thanks and appreciation are acknowledged to the Department of Biological and Agricultural Engineering, Department of Chemical and Environmental Engineering and Smart Farming Technology Research Centre, Faculty of Engineering, Universiti Putra Malaysia, Selangor, Malaysia.

Conflicts of Interest: The authors declare that there is no conflict of interest in this work.

References

- Abbassi-Guendouz, A., Brockmann, D., Trably, E., *et al.* (2012). Total solids content drives high solid anaerobic digestion via mass transfer limitation. *Bioresource Technology*, *111*, 55–61. <https://doi.org/10.1016/j.biortech.2012.01.174>
- Alemahdi, N., Che Man, H., Abd Rahman, N., *et al.* (2015). Enhanced mesophilic bio-hydrogen production of raw rice straw and activated sewage sludge by co-digestion. *International Journal of Hydrogen Energy*, *40*(46), 16033–16044. <https://doi.org/10.1016/j.ijhydene.2015.08.106>
- Anhuradha, S. & Mullai, P. (2010). Mesophilic biodigestion of cowdung and mango peel in relation to bioenergy-batch study. *An Indian Journal*, *5*(5), 320–324.
- Ardaji, V., Radnezhad, H. & Nourouzi, M. (2016). Improving biogas production performance from pomegranate waste, poultry manure and cow dung sludge using thermophilic anaerobic digestion: Effect of total solids adjustment. *Journal of Earth, Environment and Health Sciences*, *2*(3), 97. <https://doi.org/10.4103/2423-7752.199293>
- Arelli, V., Begum, S., Anupoju, G. R. *et al.* (2018). Dry anaerobic co-digestion of food waste and cattle manure: Impact of total solids, substrate ratio and thermal pre treatment on methane yield and quality of biomanure. *Bioresource Technology*, *253*, 273–280. <https://doi.org/10.1016/j.biortech.2018.01.050>
- Astals, S., Nolla-Ardèvol, V. & Mata-Alvarez, J. (2013). Thermophilic co-digestion of pig manure and crude glycerol: Process performance and digestate stability. *Journal of Biotechnology*, *166*(3), 97–104. <https://doi.org/10.1016/j.jbiotec.2013.05.004>
- Bardiya, N., Somayaji, D., & Khanna, S. (1996). Biomethanation of banana peel and pineapple waste. *Bioresource Technology*, *58*(1), 73–76. [https://doi.org/10.1016/S0960-8524\(96\)00107-1](https://doi.org/10.1016/S0960-8524(96)00107-1)
- Chakravarty, G. (2016). Evaluation of fruit wastes as substrates for the production of biogas. *Scholars Research Library Annals of Biological Research*, *7*(3), 25–28. Retrieved from <http://scholarsresearchlibrary.com/archive.html>
- Chan, Y. K. (2000). Status of the pineapple industry and research and development in Malaysia. *Acta Horticulturae*, *529*, 77–83. <https://doi.org/10.17660/actahortic.2000.529.7>
- Chu, M. M. (2019, July). Generating more waste than ever. *The Star Online*. Retrieved from <https://www.thestar.com.my/news/nation/2019/07/30/generating-more-waste-than-ever#1cbSCyx1wuM8MyGX.99>
- Dahunsi, S. O. (2019). Liquefaction of pineapple peel: Pretreatment and process optimization. *Energy*, *185*, 1017–1031. <https://doi.org/10.1016/j.energy.2019.07.123>

- Deressa, L., Libsu, S., Chavan, R. B., *et al.* (2015). Production of biogas from fruit and vegetable wastes mixed with different wastes. *Environment and Ecology Research*, 3(3), 65–71. <https://doi.org/10.13189/eer.2015.030303>
- Elina, T. (2016). *Utilization of Food Waste via Anaerobic Digestion*. Tampere, Finland: Tampere University of Technology.
- Fernández, J., Pérez, M. & Romero, L. I. (2008). Effect of substrate concentration on dry mesophilic anaerobic digestion of organic fraction of municipal solid waste (OFMSW). *Bioresource Technology*, 99(14), 6075–6080. <https://doi.org/10.1016/j.biortech.2007.12.048>
- Giuliano, A., Bolzonella, D., Pavan, P., *et al.* (2013). Co-digestion of livestock effluents, energy crops and agro-waste: Feeding and process optimization in mesophilic and thermophilic conditions. *Bioresource Technology*, 128, 612–618. <https://doi.org/10.1016/j.biortech.2012.11.002>
- Gupta, K. K., Aneja, K. R., & Rana, D. (2016). Current status of cow dung as a bioresource for sustainable development. *Bioresources and Bioprocessing*, Vol. 3, pp. 1–11. <https://doi.org/10.1186/s40643-016-0105-9>
- Hagos, K., Zong, J., Li, D., *et al.* (2017). Anaerobic co-digestion process for biogas production: Progress, challenges and perspectives. *Renewable and Sustainable Energy Reviews*, 76, 1485–1496. <https://doi.org/10.1016/j.rser.2016.11.184>
- Jafari-Sejathood, A., Najafi, B., Faizollahzadeh Ardabili, S., *et al.* (2019). Limiting factors for biogas production from cow manure: energy-environmental approach. *Engineering Applications of Computational Fluid Mechanics*, 13(1), 954–966. <https://doi.org/10.1080/19942060.2019.1654411>
- Jehan, O. S., Sanusi, S. N. A., Sukor, M. Z., *et al.* (2017). Biogas production from pineapple core — A preliminary study. *AIP Conference Proceedings*, 1885(1), 020246. <https://doi.org/10.1063/1.5002440>
- Kainthola, J., Kalamdhad, A. S., & Goud, V. V. (2019). Optimization of methane production during anaerobic co-digestion of rice straw and hydrilla verticillata using response surface methodology. *Fuel*, 235, 92–99. <https://doi.org/10.1016/j.fuel.2018.07.094>
- Karuppiyah, T. & Azariah, V. E. (2019). Biomass pretreatment for enhancement of biogas production. *Anaerobic Digestion*. <https://doi.org/10.5772/intechopen.82088>
- Khai Lun, O., Bee Wai, T. & Siew Ling, L. (2014). Pineapple cannery waste as a potential substrate for microbial biotransformation to produce vanillic acid and vanillin. *International Food Research Journal*, 21.
- Khairul Anuar, N., Che Man, H., Idrus, S. *et al.* (2018). Biochemical methane potential (BMP) from anaerobic co-digestion of sewage sludge and decanter cake. *IOP Conference Series: Materials Science and Engineering*, 368(1), 012027. <https://doi.org/10.1088/1757-899X/368/1/012027>
- Liotta, F., D'Antonio, G., Esposito, G., *et al.* (2014). Effect of total solids content on methane and volatile fatty acid production in anaerobic digestion of food waste. *Waste Management and Research*, 32(10), 947–953. <https://doi.org/10.1177/0734242X14550740>
- Maneeintr, K., Leewisuttikul, T., Kerdsuk, S., *et al.* (2018). Hydrothermal and enzymatic treatments of pineapple waste for energy production. *Energy Procedia*, 152, 1260–1265. <https://doi.org/10.1016/j.egypro.2018.09.179>
- Mata-Alvarez, J., Macé, S., & Llabrés, P. (2000). Anaerobic digestion of organic solid wastes. An overview of research achievements and perspectives. *Bioresource Technology*, 74(1), 3–16. [https://doi.org/10.1016/S0960-8524\(00\)00023-7](https://doi.org/10.1016/S0960-8524(00)00023-7)
- Neshat, S. A., Mohammadi, M., Najafpour, G. D. *et al.* (2017). Anaerobic co-digestion of animal manures and lignocellulosic residues as a potent approach for sustainable biogas production. *Renewable and Sustainable Energy Reviews*, 79, 308–322. <https://doi.org/10.1016/j.rser.2017.05.137>

- Ogunleye, O. O., Aworanti, O. A., Agarry, S. E., *et al.* (2016). Enhancement of animal waste biomethanation using fruit waste as co-substrate and chicken rumen as inoculums. *Energy Sources, Part A: Recovery, Utilization and Environmental Effects*, 38(11), 1653–1660. <https://doi.org/10.1080/15567036.2014.933286>
- Orhorhoro, E. K., Ebunilo, P. O., & Sadjere, G. E. (2017). Experimental determination of effect of total solid (ts) and volatile solid (vs) on biogas yield. *American Journal of Modern Energy*, 3(6), 131–135. <https://doi.org/10.11648/j.ajme.20170306.13>
- Rabii, A., Aldin, S., Dahman, Y., *et al.* (2019). A review on anaerobic co-digestion with a focus on the microbial populations and the effect of multi-stage digester configuration. *Energies*, 12(6). <https://doi.org/10.3390/en12061106>
- Rani, D. S. & Nand, K. (2004). Ensilage of pineapple processing waste for methane generation. *Waste Management*, 24(5), 523–528. <https://doi.org/10.1016/j.wasman.2003.10.010>
- Sibiya, N. T., Muzenda, E., & Tesfagiorgis, H. B. (2014). Effect of temperature and pH on the anaerobic digestion of grass silage. *6th International Conference on Green Technology, Renewable Energy and Environmental Engineering*, 27–28.
- Yi, J., Dong, B., Jin, J., *et al.* (2014). Effect of increasing total solids contents on anaerobic digestion of food waste under mesophilic conditions: Performance and microbial characteristics analysis. *PLoS ONE*, 9(7). <https://doi.org/10.1371/journal.pone.0102548>



Copyright © 2020 by Aili Hamzah AF, *et al.* and HH Publisher. This work is licenced under the Creative Commons Attribution-NonCommercial 4.0 International Licence (CC-BY-NC4.0)

Original Research Article

Effect of Different Jackfruit Puree Concentrations on the Mechanical Properties of Jackfruit Frozen Confection

Amiruddin Mat Johari¹, Nur Aliaa Abd Rahman^{1*}, Roseliza Kadir Basha¹, Azhari Samsu Baharuddin¹, Mohd Afandi P. Mohammed¹, Ahmad Tarmeze Talib¹, Minato Wakisaka²

¹Department of Process and Food Engineering, Faculty of Engineering, Universiti Putra Malaysia, 43400 UPM Serdang, Selangor

²Graduate School of Life Science and Systems Engineering, Kyushu Institute of Technology, 2-4 Hibikino, Wakamatsu-ku, Kitakyushu, 808-0196, Japan

*Corresponding author: Nur Aliaa Abd Rahman, Department of Process and Food Engineering, Faculty of Engineering, Universiti Putra Malaysia, 43400 UPM Serdang, Selangor, Malaysia; nuraliaa@upm.edu.my

Abstract: Jackfruit frozen confection has been mechanically characterised in situ by using compression tests. There are no available studies on the mechanical behaviour of jackfruit frozen confection. The aim of this study is to identify the mechanical properties of jackfruit frozen confections formulated with different concentrations of jackfruit puree. In this study, the experimental analyses are conducted using a compression test device made from LEGO Mindstorms EV3. The portable device is placed inside a freezer to enable the measurements to be done in low temperatures (-20°C). This is to overcome the limitation of an actual texture analyser which can only be operated at room temperature. The mechanical properties of jackfruit frozen confections at different jackfruit puree concentrations (10%, 20% and 30%) are obtained using the tester and analysed. The tests conducted are uniaxial compression, stress relaxation test and multi-step stress relaxation test. It has been observed that frozen confection with 20% jackfruit puree concentration (JF20) is able to withstand a higher force of compression (27.79kPa) compared to the ones with 10% (JF10) and 30% (JF30) concentrations, at 21.15kPa and 10.48kPa, respectively. For stress relaxation test, JF30 has the highest increasing stress for a strain of 0.05 to 0.2 but it decreases at a strain of 0.3 to 0.4. The results of the multi-step relaxation test on JF30 show agreement with the other two tests where the stress decays starting from the 3rd step until the 5th step of the test. This study provides information on the behaviour of jackfruit frozen confection when subjected to compression and stress that imitates the movement during consumption.

Keywords: Mechanical characterisation; jackfruit; frozen confection; dairy processing

Received: 28th June 2020

Accepted: 10th September 2020

Published: 30th September 2020

Citation: Mat Johari A, Abd Rahman NA, Kadir Basha R, *et al.* Effect of different jackfruit puree concentrations on the mechanical properties of jackfruit frozen confection. *Adv Agri Food Res J* 2020; 1(1): a0000110. <https://doi.org/10.36877/aafjr.a0000110>

1. Introduction

Ice cream refers to frozen creamy dessert with a fat content of more than 10% while frozen confection contains fat of less than 10% (Johari *et al.*, 2020). In this study, a study on jackfruit frozen confection is conducted. The complex physical structure of frozen confection presents challenges to the producers during production, distribution and consumption. Specifically, jackfruit frozen confection properties need to be properly studied to solve these challenges. Jackfruit is the main ingredient in frozen confection as it influences the overall flavour. Therefore, its addition would also play a role in the structure of frozen confection. The shelf life of jackfruit may affect the texture and the physico-chemical properties of frozen confection such as the mix viscosity, melting characteristics and overrun. The fruit concentration may also affect the mechanical behaviour of frozen confection such as its viscosity, compressive strength, hardness and stress relaxation. However, certain experiments need to be performed under subfreezing temperature as frozen confection in general, is sensitive to temperature fluctuation just like ice cream. This prevents frozen confection from deforming due to melting. A change in temperature could affect the physical and chemical properties of ice cream (Leducq *et al.*, 2015). The same issue that would affect frozen confection too.

Just like ice cream, the frozen confection is a temperature-sensitive product. Temperature fluctuation during sample preparation and experimental work could change the physical and chemical properties of ice cream (Leducq *et al.*, 2015). Performing mechanical tests on frozen confection would require a controlled environment and proper laboratory instruments. The main limitation is due to the temperature-sensitive properties of frozen confection which require experimental procedures performed at sub-freezing temperature, i.e., -10 to -18°C. This is to prevent frozen confection from deforming due to melting. Thus, a compression tester was designed to fit into a controlled temperature freezer. By using the miniature compression tester from LEGO Mindstorms EV3 (Rahman *et al.*, 2019), mechanical tests could be performed in the limited space freezer. LEGO Mindstorms EV3 consists of microprocessors, motors and sensors that could be programmed to perform complicated tasks. MATLAB programming was used to navigate and synchronise the movements of the plate, sensors and the load cell to obtain data easily and systematically.

Mechanical loading tests differ according to the sample tested. The types of tests that are suitable to be used for frozen confection are the uniaxial compression, stress relaxation and cyclic compression. A compression test is important as it provides analytical insights on the properties of ice cream/frozen confection. It stimulates the forces imparted on the product

during eating, and also in extrusion and packaging of ice cream during its processing stage. Research showed that a strong compressive strength was needed for ice cream with high milk fat percentage (Casarotto *et al.*, 2015). In order to achieve true uniaxial stress without shear deformation, the platen interface and samples need to be properly staged. The inability to do so will produce friction between the sample and loading platen interface which causes inhomogeneous uniaxial stress. This effect is also known as the “friction hill” that causes the barrelling of the sample. A cylindrical shape sample through compression may exhibit this phenomenon whereby the diameter half through the length of the compressed sample is larger than the diameter at the top and bottom edges (Çetinarslan, 2007).

Stress relaxation is a time-dependent process that allows a material to slowly relax at a constant strain that leads to a decrease in stress performed on the sample. This test provides valuable information specifically on the rheological parameters of viscoelastic foods (Heldman *et al.*, 2006). Ideal viscous substances relax instantaneously while ideal elastic materials show no relaxation. Viscoelastic materials relax gradually and stop depending on the molecular structure of the material. Stress in viscoelastic solids would decay to equilibrium stress that is greater than zero, but residual stress in viscoelastic liquids would decrease to zero (Banes, 2016). In the stress relaxation of the ice cream/confection sample, the stress will decay as it remains at a certain strain. Therefore, proper relaxation time is important as it influences the stress-strain measurements. The aim of this study is to identify the mechanical properties of jackfruit frozen confections formulated with different concentrations of jackfruit puree.

2. Materials and Methods

2.1. Preparation of Jackfruit Frozen Confection

The base formulation of frozen confection had the following composition (%w/w): 29.1% water, 46.5% full cream milk, 16.5% sugar, 3.6% whey powder, 3.6% creamer, 0.4% emulsifier and 0.3% stabiliser. This was based on the formulation used by Rahman *et al.* (2019) with some modifications. The wet and dry ingredients were thoroughly agitated by manual mixing at room temperature. The mix was batch pasteurised at 80°C for 15 seconds and later homogenised using a laboratory-scale homogeniser. The liquid mixes were then aged overnight at 0–5°C. Jackfruit puree was incorporated into the aged mixes as suggested by Goff and Hartel (2013), and the jackfruit frozen confection mixes were then frozen using an ice cream machine (Model BCI600XL, Breville, USA). The produced frozen confections

were stored in a deep freezer at -18°C . Based on Goff and Hartel (2013), the recommendation of fresh and frozen fruit required to impart the desired flavour varies from 10 to 25% of the mass of the finished product. Therefore, the jackfruit puree added was 10% (JF10), 20% (JF20) and 30% (JF30) of the total mass of the mix in this experiment.

2.2. The Setup of LEGO Mechanical Testing System

The mechanical testing system was comprised of a custom-built LEGO Mindstorms EV3 Robotic Kit, load cell (FUTEK LSB200, USA) and an endoscope (Rahman *et al.*, 2019). The robotic kit was designed with a microcontroller programmed through a USB connection. The structure of LEGO was built with pegs that allows modification when needed as shown in Figure 1. Load cell could operate at sub-freezing temperature (-20°C) which is suitable with the low-temperature condition needed in frozen confection mechanical testing. The endoscope was used to record and obtain live feeds of the tests. The movement of the LEGO compression tester was set accordingly to specific tests i.e. the uniaxial compression and stress relaxation.

The motor and load cell were controlled by written programming scripts (MATLAB 2014a, USA) to synchronise the movement of the actuator and data acceptance from the load cell. The compression tester was made portable with its small dimension (L: 17.2cm, W: 14.8cm, H: 31.2cm). The small size of the compression tester allows convenient placement inside the freezer along with the ice cream samples. A portable compression tester is also important so that it can be moved in and out of the freezer easily. This ensures minimum exposure of the machine to sub-freezing temperature especially during the gaps between testing and loading of the sample. Several challenges were encountered throughout the testing phase. These challenges were the preparation of frozen confection sample, development of the LEGO compression tester and the temperature conditioning of experiments.

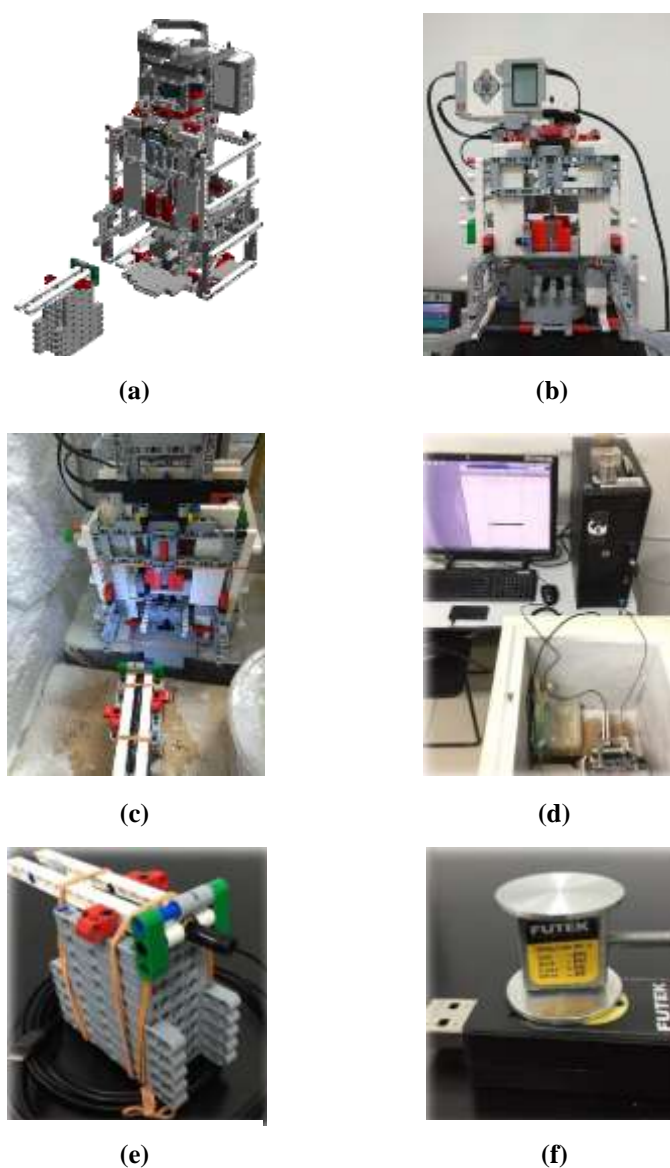


Figure 1. LEGO Mindstorms EV3 compression tester; (a) LEGO drawing of prototype, (b) Front image of prototype, (c) Prototype in freezer, (d) Wiring of prototype attached to CPU, (e) Endoscope mounted on LEGO holder, (f) FUTEK load cell.

2.3. Frozen Confection Sample for Mechanical Testing

The frozen confection samples were produced from the formulation explained previously. Jackfruit puree concentrations were added at 10%, 20% and 30% of the total mass of liquid mix. After the dynamic freezing of jackfruit frozen confection, the samples were then piped into a cylindrical plastic container (d: 1.5 cm). The frozen confections were hardened overnight. After that, the frozen confection samples were cut to a height of 0.75 cm to produce tablet shape samples (Figure 2). The cutting of samples was done in a freezer to prevent melting.



Figure 2. Frozen confection sample with a diameter of 1.5 cm and height of 0.75 cm.

2.4 Compression Tests on Jackfruit Frozen Confection

Compression tests were performed to determine the mechanical properties of jackfruit frozen confection under subfreezing temperature. This prevents further melting of frozen confection which could affect the tests conducted. The compression tests were conducted using a compression tester (LEGO Mindstorms kit) equipped with a load cell (FUTEK LSB200, USA). The tests initiated were uniaxial compression, stress relaxation and step-stress relaxation. The tests were adapted according to Mohammed (2012) with simplifications and performed under sub-freezing temperature and low space of the experimental area. Jackfruit frozen confection samples were transferred from the storage freezer (-18°C) to a controllable freezer set to -10°C. The compression tester and load cell were placed in the controllable freezer 10 minutes earlier before the experiment started. The sample was then placed onto the load cell.

i. Uniaxial compression test

The uniaxial compression test provides true uniaxial stress without any shear deformation taking place. Jackfruit frozen confection sample was compressed at a speed of 0.2 mm/s and a strain of 0.4 (3 mm). The stress and strain were computed from the load and displacement obtained. The experiments were performed in triplicate.

ii. Stress and multi-step stress relaxation test

The stress relaxation test was done to investigate the time-dependent behaviour of jackfruit frozen confection. The speed was set at 0.2mm/s and strain of 0.4 (3 mm). Relaxation time was set to 30 seconds. Step-stress relaxation test was also conducted with a 5-step compression at a speed of 0.2mm/s and strain of 1mm. The relaxation time was five seconds in between steps. The experiments were performed in triplicate.

The data of all mechanical tests were analysed in terms of stress (kPa) and strain. The stress is defined as the applied force divided by the original cross-sectional area of the sample. It is

calculated using equation 1:

$$\sigma_e = \frac{P}{A_0} \quad (1)$$

where σ_e is the stress, P is the applied load and A_0 is the initial cross-sectional sample normal to the loading direction. The strain expresses the length of the deformed sample divided by the initial height of the sample. It is calculated based on equation 2:

$$\varepsilon_e = \frac{\Delta L}{L_0} \quad (2)$$

where ε_e is the strain, ΔL is the measured displacement and L_0 is the initial sample length along a single axis.

3. Results and Discussions

3.1. Mechanical Tests on Jackfruit Frozen Confection at Different Jackfruit Puree Concentrations Using LEGO Mindstorms Compression Tester

Compression tests on jackfruit frozen confection were performed to obtain the ideal jackfruit puree concentration needed in the sample as a flavouring. Ideal, in this case, means that the frozen confection produced from the puree has an acceptable texture and taste. Mechanical tests were conducted in a controlled temperature freezer using a compression tester made from LEGO Mindstorms kit (EV3 Core Set). This prevented the melting of jackfruit frozen confection which could affect its mechanical properties.

3.2. Uniaxial Compression Test on Jackfruit Frozen Confection

The compressive strength of frozen confection indicates significant importance to manufacturers as it relates to handling and extruding of the product. Besides that, the compressive strength also affects consumer preference in terms of its textural characteristics. Uniaxial compression tests were carried out on three different jackfruit puree concentrations. The concentrations were 10%, 20% and 30% of the total mass of liquid mix. Different concentrations were used to determine the ideal jackfruit puree needed based on the mechanical properties of jackfruit frozen confection. Figure 3 shows the deformation of jackfruit frozen confection at different puree concentrations that were penetrated to a 0.4 (3 mm) strain at 0.2 mm/s.

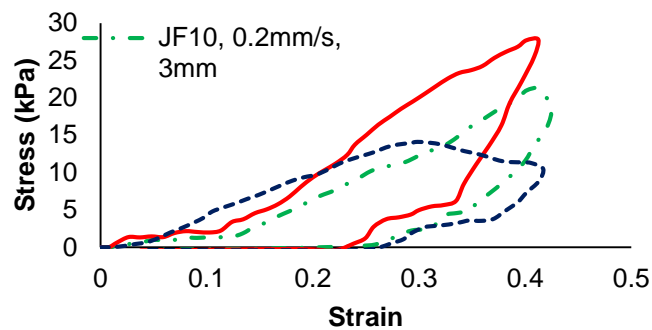


Figure 3. Uniaxial compression test result of jackfruit frozen confection at different jackfruit concentrations.

The graph shows the effect of increasing stress for all three types of jackfruit frozen confections. As the speed increased, the slope of stress versus time increased. At 0.4 (3 mm) strain, JF10 produced a stress of 21.15 kPa, JF20 had the stress of 27.79 kPa while JF30 with the stress of 10.48 kPa. JF20 had higher stress compared to JF10 due to the effect of jackfruit puree concentration. Jackfruit bulb contains carbohydrates, protein, minerals and fibres (Swami *et al.*, 2012), therefore it would affect the mechanical structure of the frozen confection. In terms of sugar concentration from the fruit puree, the effects were contrasted to the findings of Guinard *et al.* (1997) which stated that high sugar causes low hardness of frozen confection. Sugar content coming from jackfruit bulbs may not be the main factor in affecting the mechanical properties of jackfruit frozen confection as it opposes the finding stated beforehand. However, water content increases as a higher amount of jackfruit puree was added. Hartel (1996) stated that increasing water in ice cream increases its hardness. Higher water content could also dilute the sugar content provided by the jackfruit puree. Besides that, fibre content reduces the whipping capacity of the ice cream mix. This reduces the overrun of ice cream which subsequently produces harder ice cream. Carbohydrate-based fat replacers had also shown to prevent air incorporation as reported by Adapa *et al.* (2000).

JF30 had the highest increasing stress for a strain of 0.05 to 0.2 but it decreased at a strain of 0.3 to 0.4. The high increasing amount of stress in the early stage of compression may be due to the amount of jackfruit moisture content of around 70 to 80%. This contributes more water to the frozen confection as jackfruit puree concentration increases. Increased water would produce larger ice crystals and this will subsequently increase the hardness of ice confection as also stated by Hartel (1996). However, the decrease of stress at a strain of 0.3 to 0.4 is due to the solid-like structure of frozen confection that breaks at certain strains.

3.3. Stress-Relaxation Test on Jackfruit Frozen Confection

Stress relaxation tests were conducted in order to illustrate the viscoelasticity of frozen confection. Results of jackfruit frozen confection at different jackfruit concentrations are shown in Figure 4.

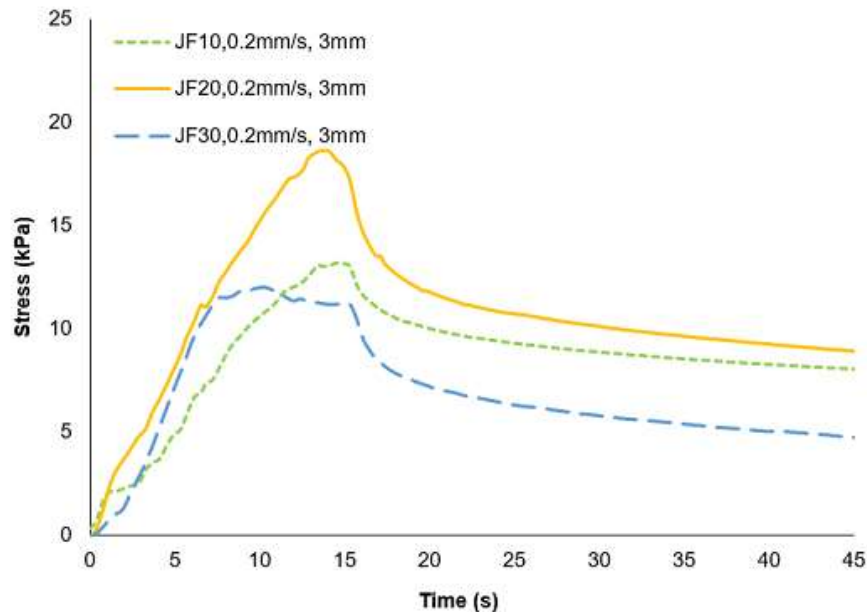


Figure 4. Relaxation test result of jackfruit frozen confection at different jackfruit concentrations.

The jackfruit frozen confection showed viscoelasticity characteristics during the tests. JF10 had increasing stress until 15 seconds of compression with peak stress of less than 15 kPa. A similar trend was seen for JF20 that showed a higher peak of the stress of more than 15 kPa. A higher amount of jackfruit concentration increases stress during compression. This is similar to the results obtained for uniaxial compression tests of JF10 and JF20. The effect of stress was likely due to the increase in water content which hardens the frozen confection. However, JF30 exhibited a plateau characteristic from five seconds to 15 seconds of compression. This could explain why JF30 exhibited lesser elastic properties compared to JF10 and JF20. The higher amount of fibre, sugar and pectin from the jackfruit pulp increases the stiffness of JF30 frozen confection. Thus, this solid-like structure would break faster upon reaching a certain strain. The addition of jackfruit puree affects the overrun and consequently hardness of jackfruit frozen confection.

3.4. Multi-step relaxation test on jackfruit frozen confection

A multi-step stress relaxation graph is presented in Figure 5. The 5-step relaxation was applied to each sample. It was observed that JF10 graph trend was lower than JF20. Similar

trends were also observed in the uniaxial compression test and stress relaxation test. The graph for JF30 followed similar curves as JF10 and JF20 up to its third step which was at its 0.4 (3 mm) strain. The highest amount of fibre, pectin and sugar in the sample increased the stiffness of JF30, thus showing a solid-like structure and broke at an earlier compression time and strain. This was presented with the dropping decay of stress starting from the third step until the fifth step of the test.

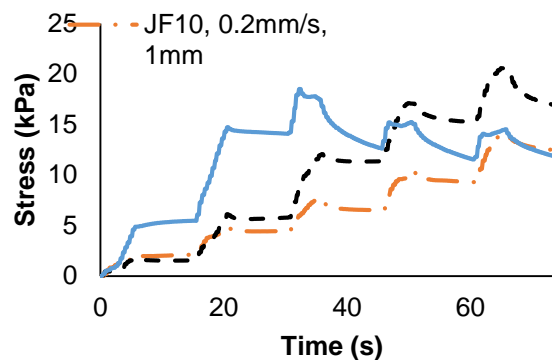


Figure 5. Multi-step stress relaxation test result of jackfruit frozen confection at different jackfruit concentrations.

4. Conclusion

Mechanical tests were conducted in a controlled temperature freezer using a compression tester made from LEGO Mindstorms kit (EV3 Core Set). For the uniaxial compression test, JF20 had higher stress compared to JF10 due to the effect of jackfruit puree concentration. For stress relaxation test, JF30 had the highest increasing stress for a strain of 0.05 to 0.2 but it decreased at a strain of 0.3 to 0.4. JF30 exhibited lesser elastic properties compared to JF10 and JF20. The higher amount of fibre, sugar and pectin from the jackfruit pulp increases the stiffness of JF30 frozen confection. The results of the multi-step relaxation test on JF30 showed agreement with the other two tests where the stress decayed starting from the third step until the final step of the test. JF30 had a solid-like structure and broke at an earlier compression time and strain. Based on the results, it can be concluded that jackfruit frozen confection with 20% jackfruit puree concentration (JF20) had the desired texture compared to JF10 and JF30 samples.

Acknowledgements: The authors would like to thank Universiti Putra Malaysia (GP/IPS/9518100) for the funding and Pahang State Farmers Association (PASFA) for working closely with us to make this study a success.

Conflicts of Interest: The authors declare that there is no conflict of interest in this work.

References

Adapa, S., Dingeldein, H., Schmidt K.A. *et al.*, (2000). Rheological properties of ice cream mixes and frozen ice creams containing fat and fat replacers. *Journal of Dairy Science*, 83(10), 2224–2229.

- Banes, P., (2016). Viscoelastic behavior. European Medical Alliance.
- Casarotto, A.M., Wolfgang, E. & Lundgren, K.J. (2015). Effects of composition and flavor on viscoelastic properties of ice cream. In *Department of Mechanical Engineering*. Worcester Polytechnic Institute.
- Çetinarslan, C.S. (2007). Effect of aspect ratio on barreling contour and variation of total surface area during upsetting of cylindrical specimen. *Materials & Design*, 28(6), 1907–1913.
- Goff, H.D. & Hartel, R.W. (2013). *Ice cream* (7th ed.). US: Springer.
- Guinard, J.-X., Zoumas-Morse, C., Mori, L., *et al.* (1997). Sugar and fat effects on sensory properties of ice cream. *Journal of Food Science*, 62(5), 1087–1094.
- Hartel, R.W. (1996). Ice crystallization during the manufacture of ice cream. *Trends in Food Science & Technology*, 7(10), 315–321.
- Heldman, D.R., Lund, D.B. & Sabliov, C. (2006). *Handbook of food engineering* (2nd ed.). CRC Press.
- Johari, A.M., Rahman, N.A.A., Baharuddin, A.S., *et al.*, (2020). Effects of low temperature storage of *Mastura* (J37) jackfruit bulbs on the physical quality of jackfruit frozen confection. *Journal of Agricultural and Food Engineering*, 1, 1–6.
- Leducq, D., Ndoye, F.T., Charriau, C., *et al.*, (2015). Thermal protection of ice cream during storage and transportation. 24ième Congrès International du Froid ICR 2015.
- Mohammed, M.A.P. (2012). *Mechanical characterisation, processing and microstructure of wheat flour dough* [Doctoral dissertation, Imperial Collage London]. Mechanical Engineering, Imperial College London.
- Rahman, N.A.A, Parid, D.M., Abdul Razak, S.Z., *et al.*, (2019). *In-situ* viscoelastic characterization and modelling of ice cream. *Journal of Food Engineering*, 263, 96–101.
- Swami, S.B., Thakor, N.J., Haldankar, P.M., *et al.*, (2012). Jackfruit and its many functional components as related to human health: A review. *Comprehensive Reviews in Food Science and Food Safety*, 11(6), 565–576.



Original Research Article

Pemantauan Tanaman Padi Menggunakan Sistem Maklumat Geografi dan Imej Multispektral

Rowena Mat Halip¹, Nik Norasma Che'Ya^{1*}, Wan Fazilah Fazlil Ilahi¹, Rhushalshafira Rosle¹, Nor Athirah Roslin¹, Mohd Razi Ismail², Zulkarami Berahim³ dan Mohamad Husni Omar³

¹ Department of Agriculture Technology, Faculty of Agriculture, Universiti Putra Malaysia, 43400 Serdang, Selangor, Malaysia

² Department of Crop Science, Faculty of Agriculture, Universiti Putra Malaysia, 43400 Serdang, Selangor, Malaysia

³ Laboratory of Climate-Smart Food Crop Production, Institute of Tropical Agriculture and Food Security, Universiti Putra Malaysia, 43400 Serdang, Selangor, Malaysia

*Corresponding author: Nik Norasma Che'Ya, Department of Agriculture Technology, Faculty of Agriculture, Universiti Putra Malaysia, 43400 Serdang, Selangor, Malaysia; niknorasma@upm.edu.my

Abstract: *This study is focused on paddy growth monitoring using Geographic Information System (GIS) and multispectral imagery via unmanned aerial vehicle (UAV). The objective of the study is to identify the best treatment that produces the highest yield. This combined technology is an effective farming management known as precision farming. UAV was used as a tool for field data capturing to produce orthophoto which will be a source for vegetative index and also for vector data digitizing purposes using ArcGIS 10.2. Data will be used as a source to analyze and monitor paddy growth. Geographical features that are digitized will able to provide farmer a full visual of their crop area such as crop layout, treatment type and also vegetative index. As a result, plot with treatment type Compost with Inoculum is able to produce the highest yield with 24947.73 kg/ha yield comparing to other treatment plots. Treatment - U Grow producing the highest NDVI reading which is 0.4327 with yield producing only 2411.31 kg/ha lower than the plot with treatment type Compost with Inoculum. Analytical images have shown that the high NDVI reading rate indicates that the paddy is still actively carrying out photosynthesis activities and is not yet ready to be harvested. Therefore, this research has shown that vegetative index value is able to become a benchmark for paddy growth monitoring while spatial analysis is able to make farming management more efficient. Other factors such as terrain model and effectiveness of current irrigation system can be a next sub topic for the research.*

Abstrak: Kajian ini memfokuskan kepada pemantauan pertumbuhan tanaman padi menggunakan sistem maklumat geografi (GIS) dan imej multispektral dengan menggunakan kaedah alatan pemanduan tanpa pesawat (UAV). Ianya bertujuan untuk mengenal pasti jenis rawatan yang mampu memberi hasil pengeluaran padi yang tinggi. Kombinasi teknologi ini merupakan kaedah pengurusan ladang yang lebih efektif dikenali sebagai pertanian tepat. UAV diguna pakai sebagai alatan untuk pencerapan data lapangan untuk menghasilkan peta ortofoto yang seterusnya digunakan untuk menghasilkan indeks tumbuhan dan pendigitan data vektor menggunakan perisian ArcGIS 10.2. Data vektor dan indeks tumbuhan ini seterusnya dapat digunakan untuk analisis pemantauan pertumbuhan tanaman padi.

Maklumat geografi yang didigitalkan dalam bentuk pemetaan dapat memberi visual penuh kepada peladang tentang tanaman padi mereka seperti susun atur petak sawah, jenis pembajaan dan juga bacaan indeks tumbuhan. Hasil kajian mendapati bahawa plot rawatan jenis kompos dengan inokulum mengeluarkan hasil yang paling tinggi iaitu 2494.73 kg/ha berbanding plot dengan rawatan yang lain. Plot rawatan *U Grow* memberi bacaan nilai maksimum NDVI yang paling tinggi iaitu 0.4677 dan mengeluarkan hasil tuaian hanya 2411.31 kg/ha lebih rendah daripada plot rawatan kompos dengan inokulum. Imej analisis telah menunjukkan bahawa kadar bacaan NDVI yang tinggi menandakan pokok padi tersebut masih aktif menjalankan aktivi fotosintesis dan masih belum sedia untuk dituai. Justeru, kajian menunjukkan bahawa indeks bacaan tumbuhan boleh dijadikan sebagai penunjuk aras untuk pemantauan pertumbuhan tanaman padi dan analisis spatial mampu memudahkan tadbir urus ladang.

Keywords: GIS; UAV; imej multispektral; NDVI; indeks tumbuhan

Received: 28th May 2020

Accepted: 4th September 2020

Published: 30th September 2020

Citation: Mat Halip R, Che Ya NN, Fazlil Ilahi WF, *et al.* Pemantauan tanaman padi menggunakan sistem maklumat geografi dan imej multispektral. *Adv Agri Food Res J* 2020; 1(1): a0000118. <https://doi.org/10.36877/aafmj.a0000118>

1. Pengenalan

Lembaga Kemajuan Pertanian Kemubu (KADA) merupakan satu badan kerajaan yang diwujudkan pada tahun 1972. Salah satu fungsi kewujudan lembaga ini adalah untuk memenuhi keperluan beras nasional (Kementerian Pertanian dan Industri Asas Tani, 2019). Beras merupakan makanan ruji bagi rakyat Malaysia dan kerajaan harus memastikan pengeluaran beras mampu menampung keperluan negara. Berdasarkan Statistik Tanaman (Sub-Sektor Tanaman Makanan) 2019 yang dikeluarkan oleh Jabatan Pertanian Semenanjung Malaysia, hasil pengeluaran KADA tidak menunjukkan hasil pengeluaran padi dari tahun 2015 hingga 2019 (Gambar rajah 1).

Berdasarkan statistik yang diterima, hasil pengeluaran beras masih tidak memenuhi sasaran kerajaan sebanyak 8 hingga 12 t/ha setahun (Abd Mutalib, 2019). Faktor penyumbang kepada hasil pengeluaran padi yang rendah adalah seperti keadaan cuaca, bekalan air, serangga dan penyakit. Seseengah peladang didapati menghadapi kesukaran pada kerja-kerja tadbir urus ladang dalam skala yang besar (Norasma *et al.*, 2018). Pada tahun 2019, kerajaan telah melancarkan program yang dikenali sebagai Halatuju Kementerian Pertanian dan Industri Asas Tani: Prioriti & Strategi 2019–2020. Antara agenda yang disarankan adalah perlaksanaan pertanian tepat dengan memperkenalkan penggunaan teknologi baharu dan juga pengukuhan sistem tadbir urus ladang yang lebih sistematik. Ianya bertujuan untuk meningkatkan hasil pengeluaran padi pada peringkat nasional.



Gambar rajah 1. Purata hasil pengeluaran padi KADA yang dicatat (Jabatan Pertanian, 2019)

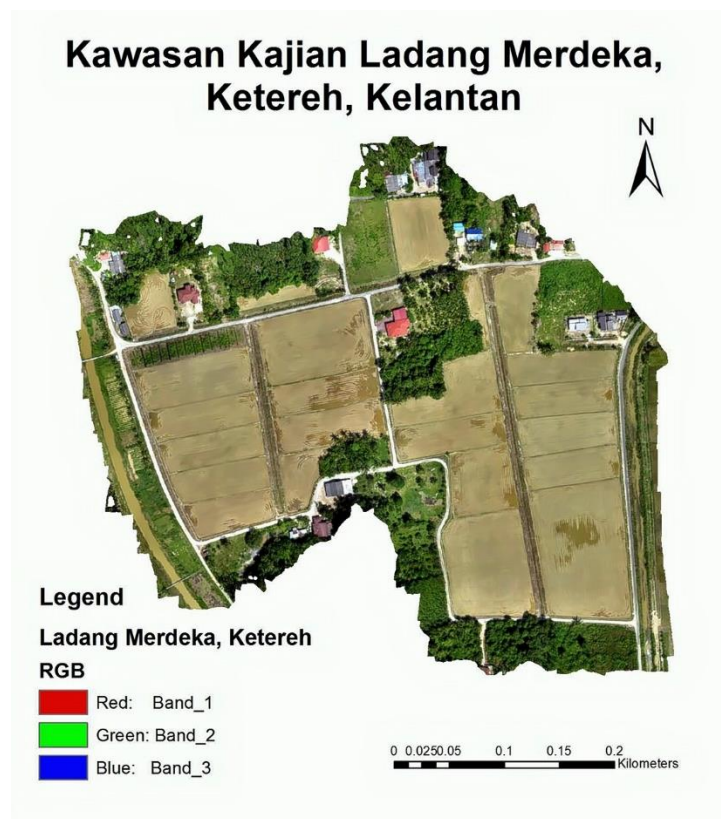
Pertanian tepat memberi kelebihan kepada peladang dari segi mengurangkan kos operasi, mengoptimumkan hasil dan kualiti serta mampu memberi informasi yang lebih terperinci untuk pengurusan yang lebih baik (Srinivasan, 2006). Ketepatan data bagi tujuan pertanian tepat hanya boleh dicapai melalui analisis dari data yang tepat juga (Sabarina & Priya, 2015). Penggunaan alatan pemanduan tanpa pesawat (UAV) disarankan dalam agenda kerajaan. UAV yang dilengkapi dengan kamera mampu memberi gambaran plot tanaman secara menyeluruh (Murugan *et al.*, 2016). Sistem maklumat geografi (GIS) dan teknologi penginderaan jarak jauh (*Remote Sensing* atau RS) diguna pakai dalam kajian ini sebagai elemen bantuan untuk penambahbaikan pengurusan ladang. Pengambilan data menggunakan UAV dan kamera multispektral mampu menghasilkan bacaan *Normalized Difference Vegetation Index* (NDVI) yang beresolusi tinggi.

Bacaan NDVI ini banyak diguna pakai dalam bidang pertanian untuk tujuan anggaran pengeluaran padi dan juga keberkesanan rawatan yang diberi (Guan *et al.*, 2019). Bacaan indeks tumbuhan digunakan secara meluas dalam bidang pertanian untuk mengukur kadar pertumbuhan tanaman sama ada tanaman dalam keadaan baik atau tidak (Ghobadifar, 2015). Pigmen daun pada tanaman akan memantulkan '*near infrared light*' (NIR) dan menyerap '*visible wavelength*'. Kadar kepekatan warna hijau memberi indikasi bahawa tanaman adalah sihat (Mahajan & Bundel, 2017). Setiap tanaman mempunyai nilai julat NDVI yang unik. Dengan menggunakan sistem GIS, julat NDVI yang dihasilkan terbukti mampu untuk mengklasifikasikan tanaman yang berbeza (Bhumika *et al.*, 2019). Kajian ini menggabungkan penggunaan UAV untuk pengambilan imej multispektral dan juga sistem GIS yang bertujuan untuk mengukur kadar keberkesanan rawatan yang diberi pada tanaman padi.

2. Metodologi

2.1. Kawasan Kajian dan Informasi Plot Kajian

Kajian ini meliputi sebahagian kawasan seliaan Lembaga Kemajuan Pertanian Kemubu (KADA) yang terletak di Ladang Merdeka, Ketereh, Kelantan dengan keluasan 20 hektar. Gambar rajah 2 di bawah menunjukkan kawasan kajian secara menyeluruh.



Gambar rajah 2. Gambaran menyeluruh kawasan kajian Ladang Merdeka, Ketereh, Kelantan

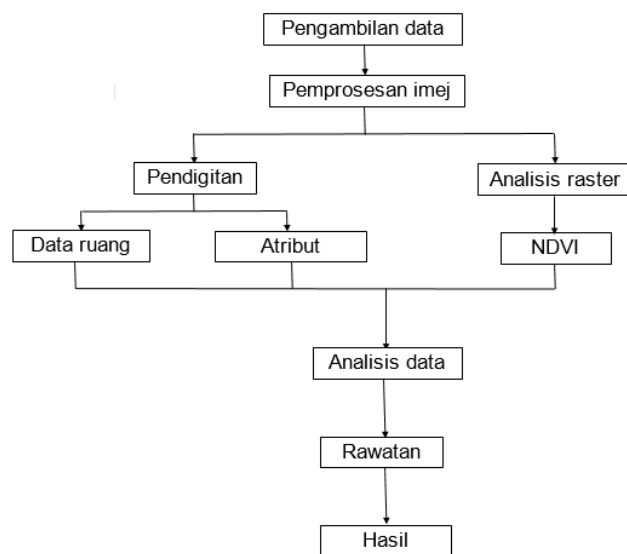
Kajian ini menggunakan benih dari PadiU Putra. Terdapat enam jenis plot kawalan yang menggunakan enam jenis pembajaan yang berbeza. Kajian ini menggunakan beberapa jenis pembajaan ke atas petak-petak sawah seperti formulasi di bawah:

1. **Kawalan (*Control*):** tanpa sebarang penambahan pembajaan, hormon atau bakteria.
2. **Kompos Komersil (*Commercial compost*):** pembajaan penambahan baja kompos sebanyak 3 t/ha yang dilakukan sewaktu persediaan tapak sawah dari kompos sekam padi dari Kilang Beras Bernas, Kelantan.
3. **Kompos dengan Inokulum (*Compost with Inoculum*):** kompos dengan penambahan inokulasi bakteria sewaktu persediaan tapak sawah (Mohd Zainudin *et al.*, 2019).

4. **U Grow**: aplikasi silikon baja foliar (2500 ppm) pada umur pokok padi 35 dan 55 hari selepas tuai.
5. **Mikrob**: aplikasi baja foliar bagi merangsang pertumbuhan *rhizobakteria* pada umur pokok padi 35 dan 55 hari selepas tuai (Mohamad Halid *et al.*, 2019).
6. **U-Filler**: aplikasi baja foliar bagi hormon berasaskan tumbuhan pada umur pokok padi 35 dan 55 hari selepas tuai (Farooq *et al.*, 2009).

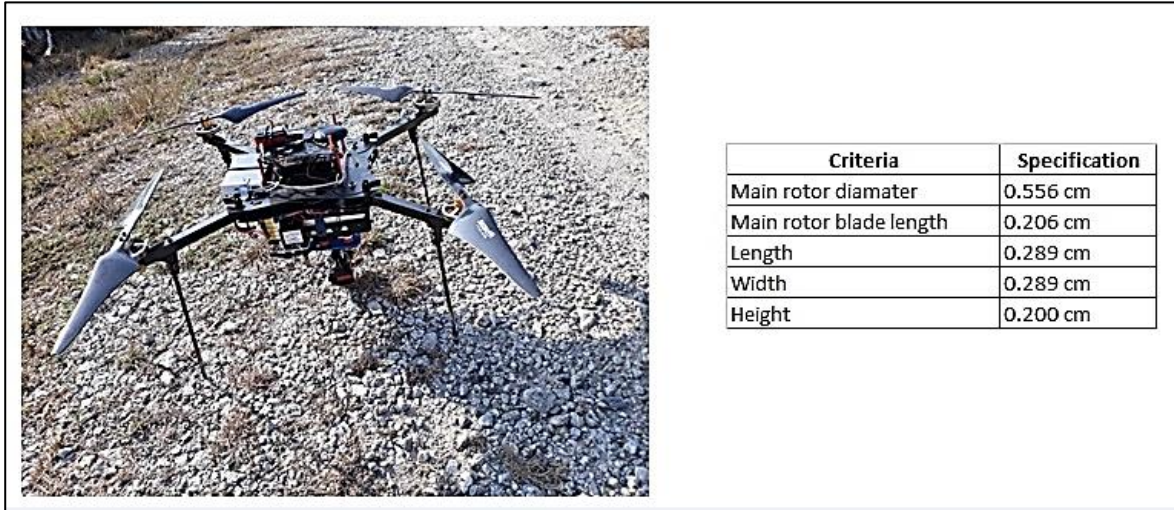
2.2. Pengambilan Data dan Analisis

Kajian ini menggunakan data yang diambil menggunakan UAV pada tarikh 28 Mei 2018 iaitu pada hari ke-117 umur tanaman padi. Data diambil pada waktu pagi di antara 8:30 pagi hingga 12:00 tengah hari untuk mengelakkan gangguan angin dan bayang-bayang. UAV diterbangkan pada ketinggian 70 meter dengan nisbah pertindihan imej melebihi 75%. Gambar rajah 3 di bawah menunjukkan carta alir proses yang digunakan dalam kajian ini.



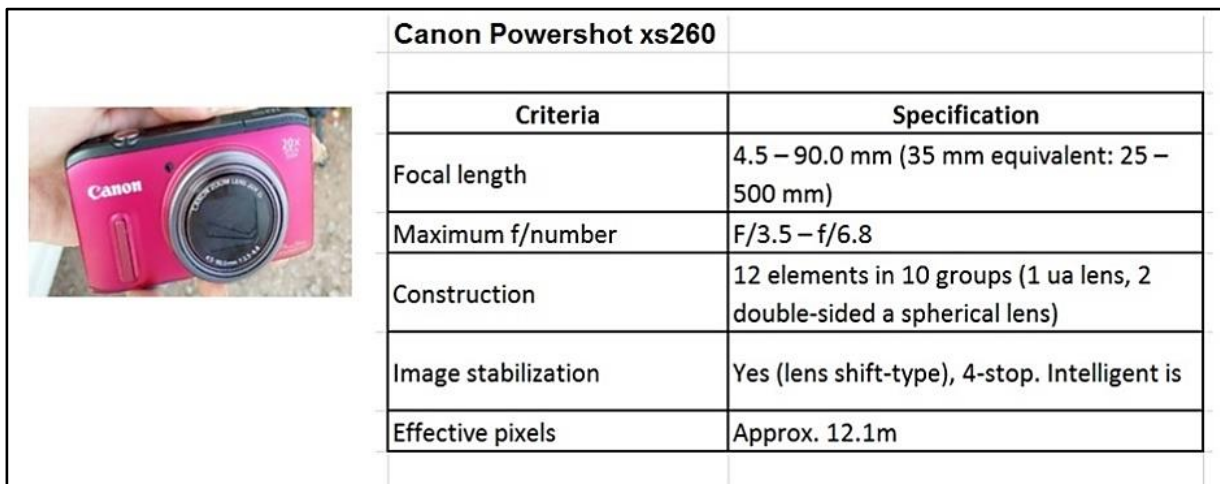
Gambar rajah 3. Carta alir proses yang digunakan dalam kajian

Kajian ini menggunakan UAV jenis XR q350 Pro UAV untuk tujuan pengambilan data. Spesifikasi UAV adalah seperti Gambar rajah 4 di bawah:

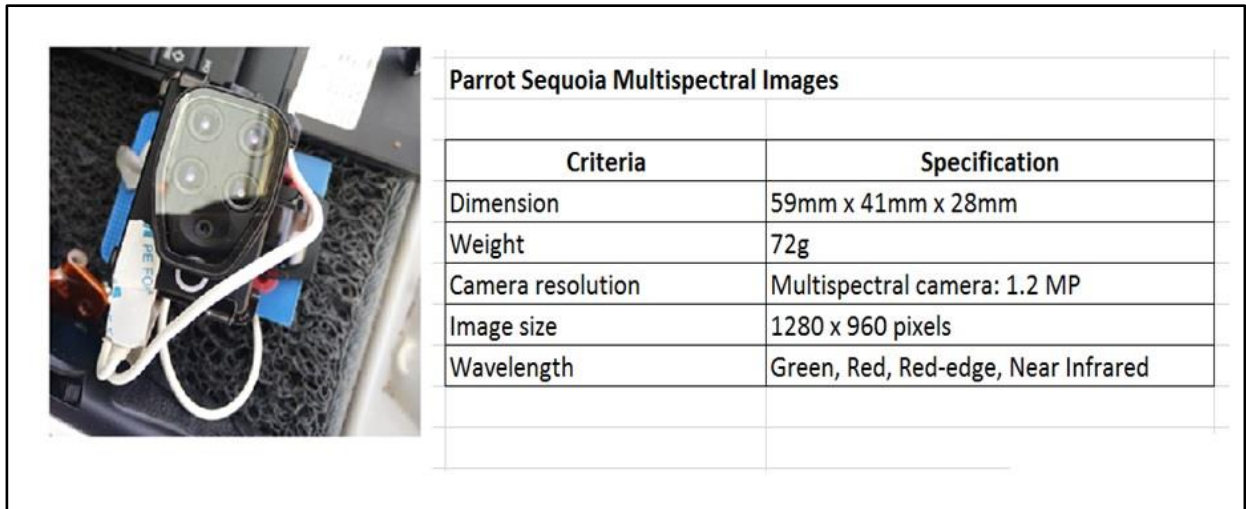


Gambar rajah 4. Spesifikasi XR q350 Pro UAV (Lee, 2019)

Pengambilan data untuk kajian dilakukan sebanyak dua kali iaitu yang pertama alatan UAV disertakan dengan Canon Powershot xs260 untuk pengambilan imej RGB seperti Gambar rajah 5 dan *Parrot Sequioa Multispectral Camera* untuk pengambilan imej multispektral seperti Gambar rajah 6.



Gambar rajah 5. Spesifikasi Canon Powershot xs260 (Lee, 2019)

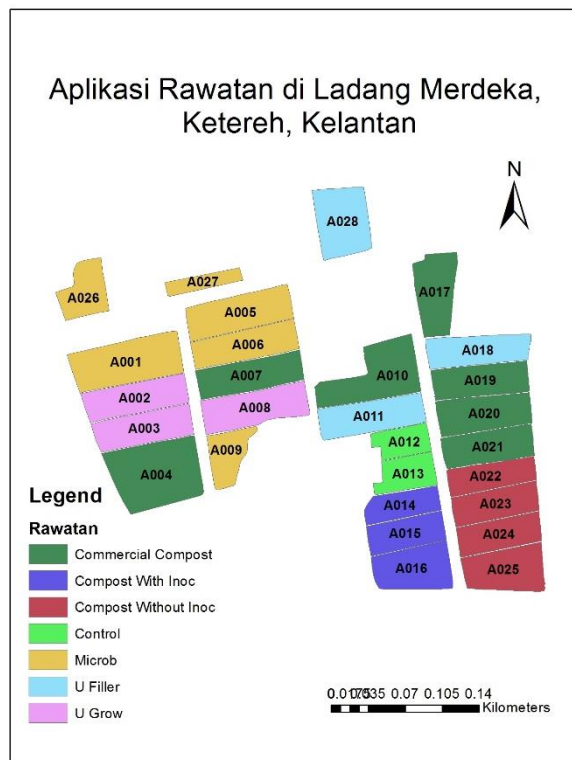


Gambar rajah 6. Spesifikasi *Parrot Sequoia Multispectral Camera* (www.parrot.com, 2019)

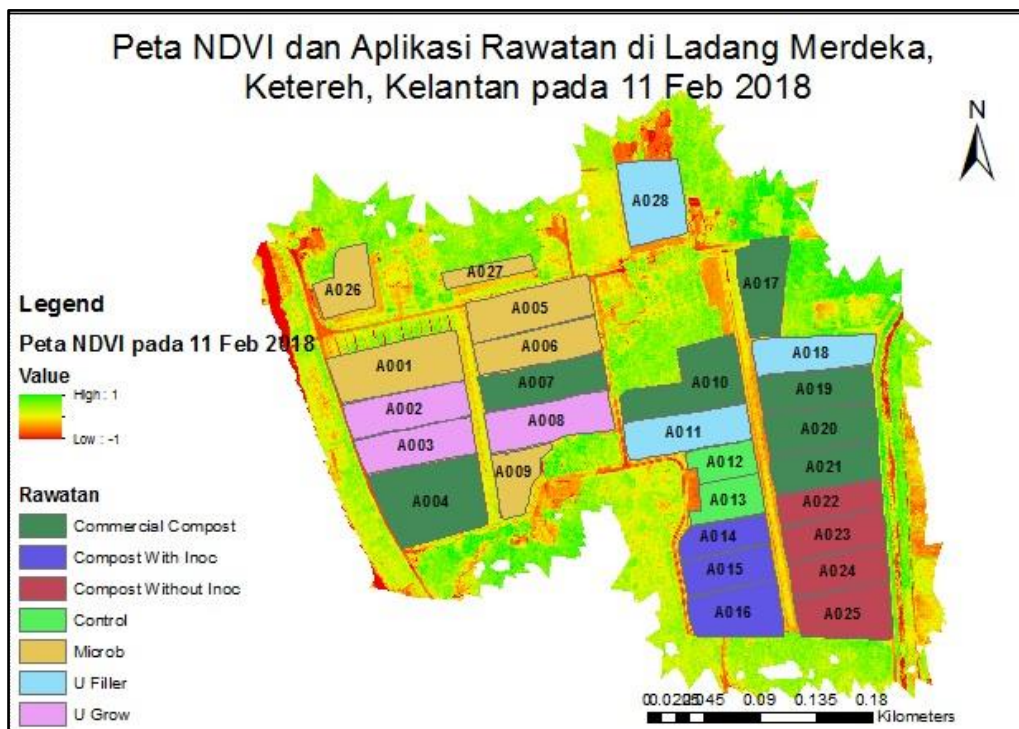
Imej-imej yang diambil kemudiannya diproses menggunakan perisian Agisoft Photoscan untuk menghasilkan ortofoto RGB dan juga imej multispektral. Imej RGB ini akan dipaparkan di dalam perisian ArcGIS 10.2 untuk tujuan penghasilan peta NDVI dan juga pendigitan data vektor seperti Gambar rajah 7, 8 dan 9 di bawah:



Gambar rajah 7. Gambaran keseluruhan kawasan kajian Ladang Merdeka dalam bentuk ortofoto RGB.



Gambar rajah 8. Data vektor rawatan pada plot kajian yang didigit dari imej RGB menggunakan perisian ArcGIS 10.2.



Gambar rajah 9. Peta NDVI yang dihasilkan dari imej multispektral berserta data vektor keseluruhan kawasan kajian.

2.3. Indeks Tumbuhan

Kajian ini menggunakan analisis indeks tumbuhan dengan formula seperti di bawah:

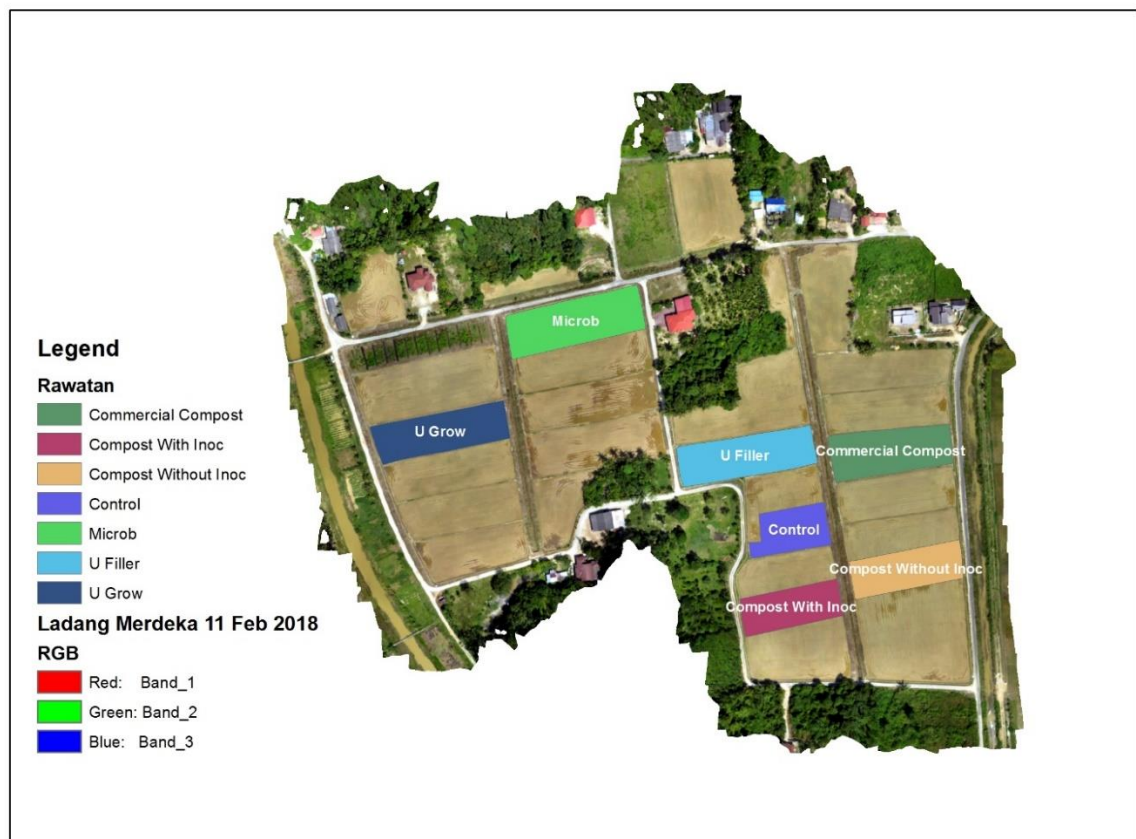
$$NDVI = (NIR - Red)/(NIR + Red) \quad (1)$$

di mana NIR mewakili nilai pantulan jalur infra merah dan nilai R adalah nilai pantulan dari jalur merah (Vergara-Diaz *et al.*, 2016). Julat bacaan NDVI adalah di antara -1.0 ke +1.0. Bacaan indeks tumbuhan 0 hingga +1.0 memberi indikasi tanaman dalam keadaan sihat atau tidak sihat. Semakin tinggi nilai NDVI semakin sihat keadaan tanaman (Kazuki *et al.*, 2017).

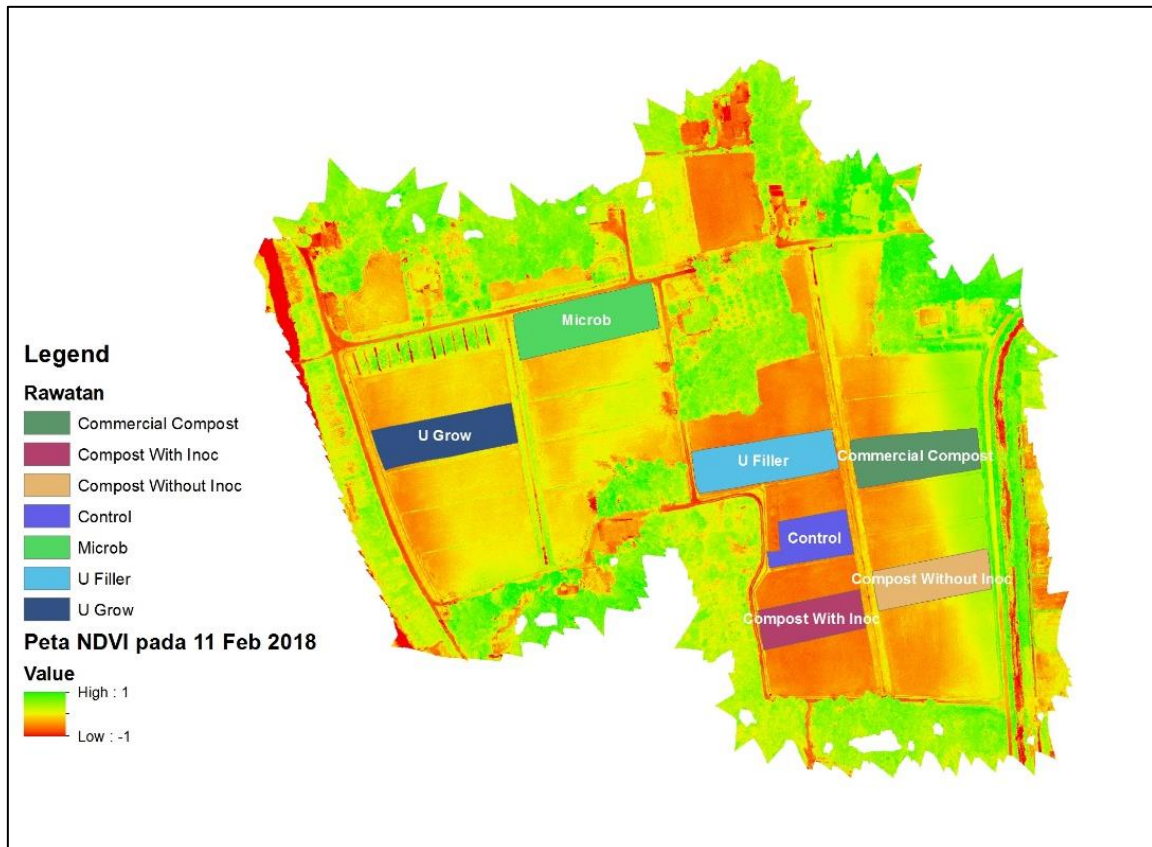
3. Hasil Kajian dan Perbincangan

3.1. Analisis Imej RGB dan Multispektral

Pertindihan data spatial dan imej RGB memberi gambaran yang lebih jelas mengenai susun atur petak sawah. Gambar rajah 10 di bawah menunjukkan susun atur petak sawah di kawasan kajian berserta label rawatan yang diberi. Dengan menggunakan perisian ArcGIS 10.2, imej multispektral digunakan untuk menghasilkan peta NDVI seperti Gambar rajah 11 di bawah.



Gambar rajah 10. Kawasan kajian beserta pilihan plot dijana dari imej


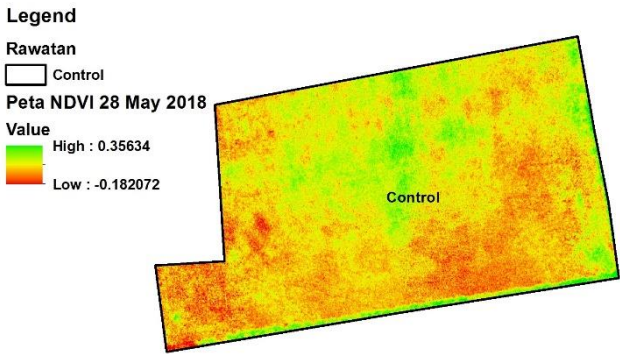



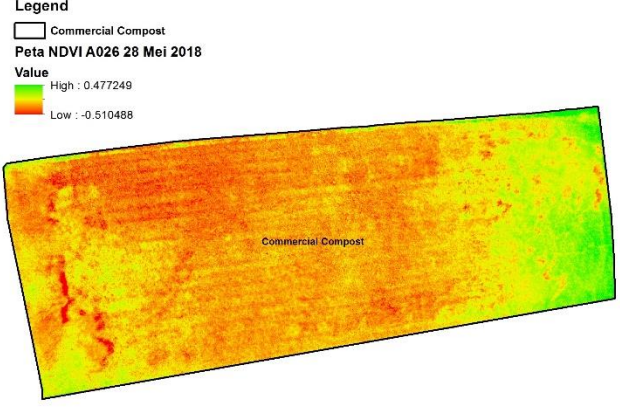
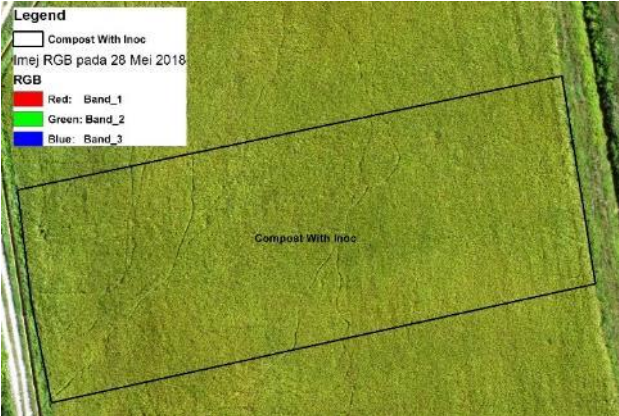
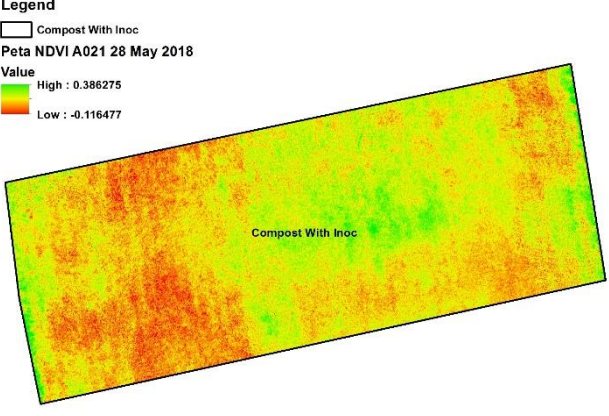
Gambar rajah 11. Peta NDVI yang multispektral berserta pilihan plot

3.2. Perbandingan Imej RGB dan Peta NDVI Pada Rawatan yang Berbeza

Keputusan menunjukkan setiap petak sawah menghasilkan nilai bacaan NDVI yang berbeza. Dalam kajian ini, dengan menggunakan data vektor yang dihasilkan dari perisian ArcGIS tadi, imej tersebut dapat diperincikan secara berasingan mengikut jenis rawatan yang diterima pada plot sawah. Pengguna hanya perlu memilih sama ada untuk memaparkan imej RGB atau imej NDVI dari perisian tersebut. Imej RGB dan NDVI bagi jenis rawatan yang berbeza pada plot pada umur pokok padi 117 hari seperti Jadual 1 di bawah.

Jadual 1. Menunjukkan perbandingan imej RGB dan peta NDVI pada plot rawatan

Jenis Rawatan: Kawalan (Control)	
Imej RGB	Peta NDVI
	
<p>Perbincangan:</p> <p>Nilai NDVI yang dihasilkan adalah di antara -0.1821 hingga 0.3563. Secara keseluruhan, imej RGB menunjukkan kawasan plot dalam keadaan yang padat, sihat dan sedia untuk dituai. Bacaan NDVI yang dihasilkan daripada imej dron adalah signifikan kerana pada usia 117 hari, pokok padi telah memasuki fasa sedia untuk dituai dan proses penghasilan makan melalui fotosintesis tidak giat dijalankan. Penggunaan peta NDVI boleh digunakan sebagai rujukan untuk tujuan pemantauan pertumbuhan pokok padi yang lebih menyeluruh dan pada masa yang sama dapat mengenal pasti kawasan plot yang mengalami kerosakan dengan merujuk kepada nilai NDVI yang dihasilkan (Rosle, <i>et al.</i> 2019). Dengan ini, petani mampu untuk mendapatkan pandangan menyeluruh kawasan tanaman padi dan mendapatkan maklumat kesihatan pokok yang tidak boleh dilihat secara pandangan mata kasar (Kazuki <i>et al.</i>, 2017).</p>	

Jenis rawatan: Kompos Komersil (Commercial Compost)	
Imej RGB	Peta NDVI
	
<p>Perbincangan: Nilai NDVI yang dihasilkan adalah di antara -0.5105 hingga 0.4772. Peta NDVI menunjukkan pertumbuhan tanaman padi adalah tidak seragam. Daripada peta NDVI yang dihasilkan, kawasan hijau masih belum sedia untuk dituai kerana aktiviti fotosintesis masih giat dijalankan untuk menghasilkan benih padi. Ini merupakan kelebihan peta NDVI dalam memantau pertumbuhan tanaman di dalam plot yang mana tidak dapat dilihat dengan jelas dari imej RGB (Kazuki <i>et al.</i>, 2017). Namun, sebahagian besar daripada plot juga mengalami kerosakan atau tumbang. Dengan bantuan dari peta NDVI ini, petani boleh melakukan pengawasan di ladang dan merancang hari yang sesuai untuk menuai hasil tanaman.</p>	
Jenis rawatan: Kompos Dengan Inokulum (Compost With Inoculum)	
Imej RGB	Peta NDVI
	
<p>Perbincangan: Nilai NDVI yang dihasilkan adalah di antara -0.1165 hingga 0.3863. Secara keseluruhan, kadar pertumbuhan tanaman pada plot ini yang ditunjukkan dari imej RGB agak memuaskan dan seragam. Kawasan plot dilihat padat dengan padi. Namun peta NDVI menunjukkan sebahagian daripada plot</p>	

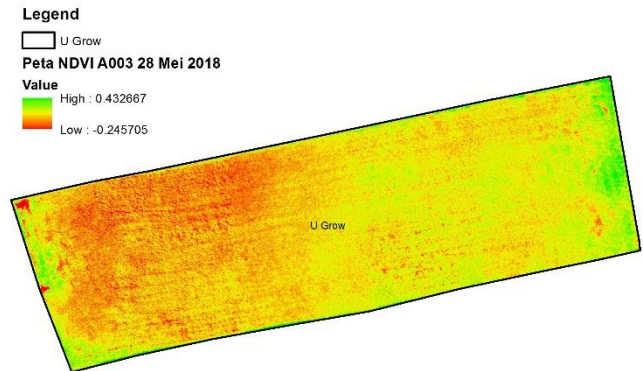
masih menjalankan aktiviti fotosintesis untuk menghasilkan benih padi. Justeru, pemerhatian terus ke atas plot sawah harus dilakukan oleh petani.

Jenis rawatan: *U Grow*

Imej RGB



Peta NDVI

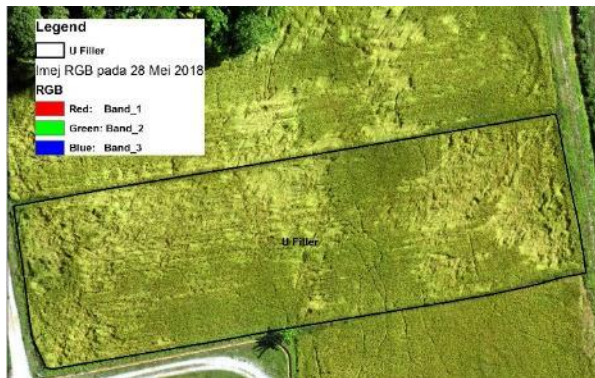


Perbincangan:

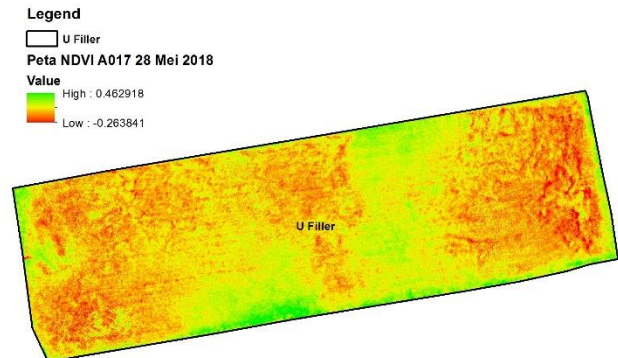
Nilai NDVI yang dihasilkan adalah di antara -0.2457 hingga 0.4327. Imej RGB yang diceraap menunjukkan tahap kerosakan pada plot padi dalam kadar yang agak minimum. Kadar pertumbuhan padi pada bahagian kiri plot adalah baik namun sedikit terjejas pada bahagian kanan dan sudut kiri plot. Indikasi warna kuning dan jingga pada peta NDVI menunjukkan kadar pertumbuhan yang normal. Maka, petani boleh menghadkan kawasan pemantauan hanya pada kawasan yang berindikasi warna hijau dari peta NDVI.

Jenis rawatan: *U-Filler*

Imej RGB



Peta NDVI



Perbincangan:

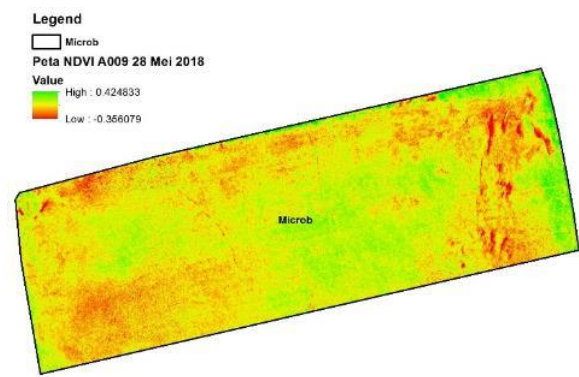
Nilai NDVI yang dihasilkan adalah di antara -0.2638 hingga 0.4629. Imej RGB menunjukkan jelas kadar kerosakan tanaman yang melebihi 50% daripada plot. Trend tanaman tidak sihat ini dapat juga dilihat melalui peta NDVI yang dihasilkan dengan merujuk kepada warna kuning dan jingga hampir di keseluruhan plot. Kerosakan yang diekstrak dari peta NDVI adalah signifikan dengan imej cerapan RGB.

Jenis rawatan: *Mikrob*

Imej RGB



Peta NDVI



Perbincangan:

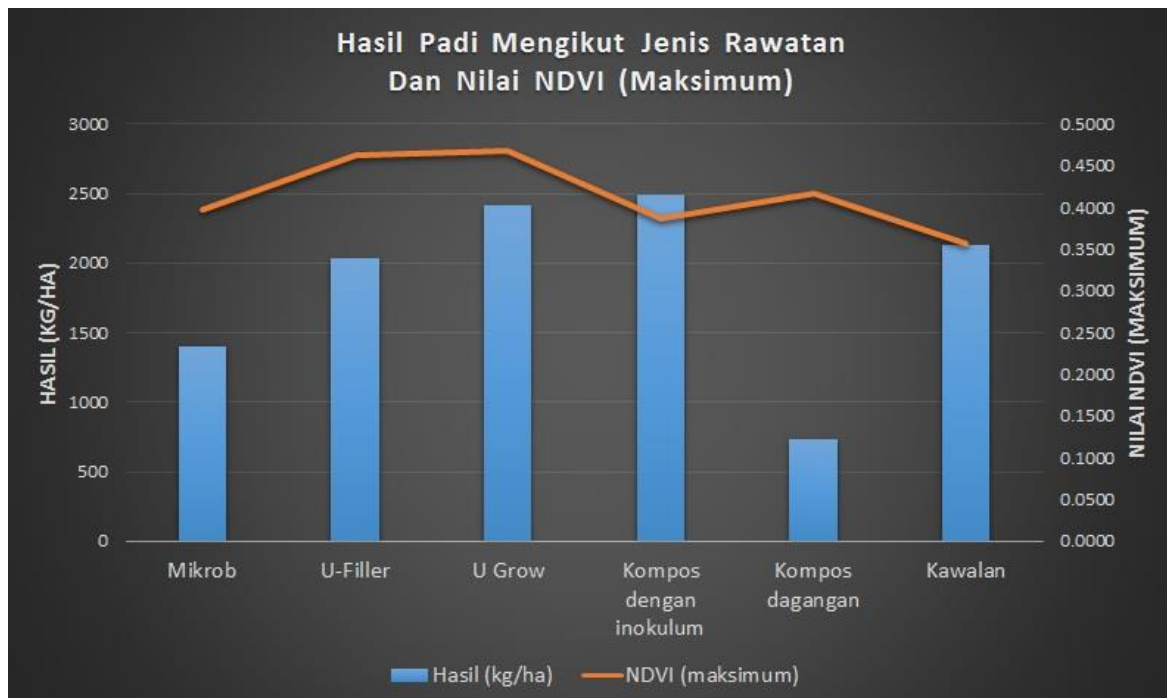
Nilai NDVI yang dihasilkan adalah di antara -0.3561 hingga 0.4248. Secara keseluruhan plot ini menunjukkan pertumbuhan yang agak baik yang boleh dilihat dari imej RGB kecuali di bahagian penjuru kanan plot. Sebahagian plot berindikasi warna kuning dan merah pada peta NDVI menunjukkan tanaman telah matang dan telah memasuki fasa sedia untuk dituai. Ianya juga boleh dilihat dengan jelas dari imej RGB. Dengan ini, petani boleh meminimumkan aktiviti penyelenggaraan pada bahagian tertentu sahaja.

3.3. Hasil Padi Daripada Mesin Penuai

Setelah pokok padi mencapai tahap kematangan bijian sehingga 80%, setiap petak sawah padi akan dituai secara berasingan. Pada akhir kajian, hasil padi dapat ditentukan daripada tiga replikasi dari rawatan yang digunakan (120 hari selepas tanam). Hasil padi akan dituai berasingan mengikut tapak sawah menggunakan mesin penuai, diangkut dari sawah menggunakan lori yang berasingan dan berat hasil tuaian akan ditimbang di kilang padi secara berasingan di Padiberas Nasional Berhad (BERNAS Sdn Bhd). Hasil dari jumlah tuaian dikira dengan menggandakan hasil padi ($t\ ha^{-1}$) dengan harga petani (RM 1,200.00 t^{-1}).

3.4. Korelasi Antara NDVI Dan Rawatan

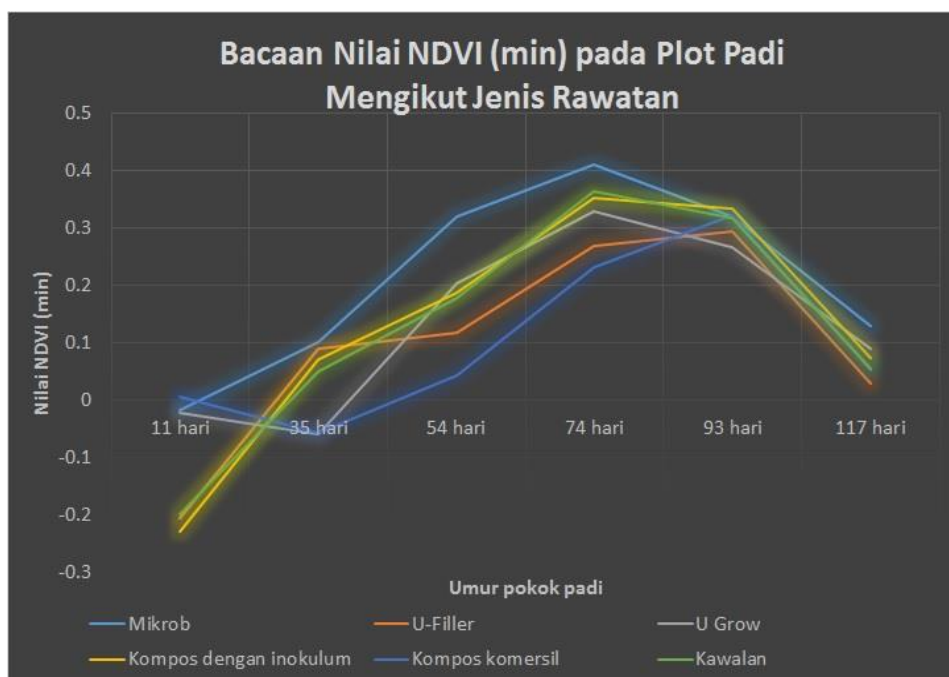
Analisis dan hasil menunjukkan bahawa hasil yang paling tinggi adalah dari plot rawatan kompos dengan inokulum dengan hasil 2494.73 kg/ha manakala plot dari rawatan kompos komersil mempunyai hasil tuaian yang paling rendah iaitu 732.10 kg/ha. Ianya diikuti dengan *U Grow*, kawalan, *U-Filler* dan Mikrob. Kajian imej analisis menunjukkan bahawa kadar bacaan NDVI yang tinggi menandakan pokok padi tersebut masih aktif menjalankan aktivi fotosintesis dan masih belum bersedia untuk dituai. Nilai NDVI pada tanaman adalah berbeza-beza mengikut tahap kesihatan dan pertumbuhan tanaman itu sendiri (Wakamori, *et al.*, 2017). Peta NDVI sesuai digunakan sebagai rujukan untuk memantau pertumbuhan tanaman serta mengesan lokasi sebarang kerosakan pada plot tanaman (Rosle, *et al.*, 2019). Daripada hasil kajian mendapati bahawa bacaan maksimum NDVI pada plot kompos komersil mempunyai nilai NDVI maksimum 0.4177 iaitu lebih tinggi daripada bacaan NDVI pada plot kompos dengan inokulum dengan bacaan NDVI maksimum 0.3863. Kedua-dua plot ini mempunyai perbezaan nilai bacaan NDVI maksimum sebanyak 0.0313. Namun perbezaan hasil antara kedua-dua plot ini sangat tinggi sehingga melebihi 1700 kg/ha.



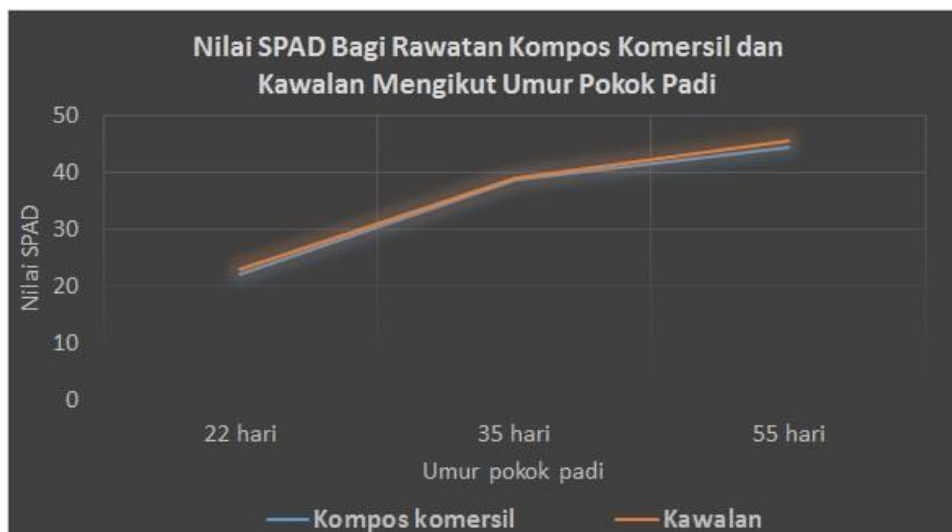
Gambar rajah 12. Graf hasil tuaian dan nilai NDVI (maksimum) bagi setiap rawatan

Gambar rajah 13 di bawah menunjukkan bacaan nilai NDVI (min) pada plot padi mengikut jenis rawatan dan umur pokok padi. Secara keseluruhannya, nilai NDVI akan beransur meningkat dari awal pertumbuhan dan semakin meningkat pada peringkat

pembungaan. Nilai NDVI akan kembali menurun menjelang tempoh penuaian (Mosleh, *et al.*, 2015). Untuk kajian ini, data lapangan yang dicerap dari *Soil Plant Analysis Development (SPAD) chlorophyll meter* adalah terhad seperti gambar rajah 14. Nilai bacaan SPAD yang diperolehi menunjukkan bacaan berkadar terus pada awal pertumbuhan padi di mana ianya adalah selari juga dengan nilai bacaan NDVI pada awal pertumbuhan tanaman. Nilai NDVI semakin meningkat selari dengan kadar kandungan klorofil pada tanaman. Semakin tinggi kandungan klorofil dalam tanaman semakin tinggi bacaan NDVI (Hashemi & Chenani, 2011).



Gambar rajah 13. Bacaan nilai NDVI (min) pada plot padi mengikut jenis rawatan



Gambar rajah 14. Bacaan nilai SPAD bagi rawatan jenis kompos komersil (*Commercial Compost*) dan kawalan (*Control*) mengikut umur pokok padi

4. Kesimpulan

Analisis menunjukkan rawatan jenis kompos dengan inoculum adalah rawatan paling berkesan dalam meningkatkan hasil tanaman padi berbanding lima jenis rawatan yang lain. Imej analisis pula menunjukkan kadar bacaan NDVI yang tinggi menandakan pokok padi tersebut masih aktif menjalankan aktivi fotosintesis dan masih belum sedia untuk dituai. Bacaan NDVI ini boleh dijadikan sebagai penanda aras untuk tujuan pemantauan tahap pertumbuhan tanaman padi. Peta NDVI perlu dilihat secara menyeluruh melalui indikasi warna yang dihasilkan untuk memastikan tahap pertumbuhan tanaman. Hasil menunjukkan bahawa imej RGB dapat mempamerkan plot tanaman secara menyeluruh dan peta NDVI dapat memberi indikasi sekiranya berlaku kerosakan di dalam kawasan tanaman padi tersebut dan pada masa yang sama memantau sekiranya tanaman masak dengan seragam atau tidak. Petani boleh menumpukan kepada kawasan tanaman padi yang tidak seragam berdasarkan peta NDVI bagi tujuan pemantauan. Bagi tujuan kajian yang lebih efektif, data lapangan dari *Greenseeker* perlu diambil bagi tujuan perbandingan dengan peta NDVI yang dihasilkan dari perisian komputer.

Pemberitahuan: Penyelidik berterima kasih di atas bantuan sokongan daripada En. Mohd ZalyNy Shah b. Noh, En Nasir Abd Rani dan juga sokongan kewangan daripada Kementerian Pendidikan Tinggi untuk projek “*Translational Research Grant Tr@M PadiU Putra: Accelerating Rice Food Security and Socio-Economics for Rice Farming Communities*” (Vote: 5526500 dan UPM GP-IPM (Vote: 9611400).

Konflik kepentingan: Penulis mengesahkan tiada konflik kepentingan di dalam terbitan ini.

References

- Abd Mutalib, Z. (2019, Ogos 6). MADA, KADA mula pelan tindakan dasar penyatuan tanah sawah. *Berita Harian*. <https://www.bharian.com.my/berita/nasional/2019/08/593306/mada-kada-mula-pelan-tindakan-dasar-penyatuan-tanah-sawah>.
- Bhumika, K., Vadher, B. M., & Agnihotri, P. G. (2019). Application of remote sensing and GIS in cropping pattern mapping: A case study of Olpad Taluka, Surat. *GRD Journal — Emerging Research and Innovations in Civil Engineering*, 4(9), 343–348.
- Faranak Ghobadifar. (2015). *Pest attack determination in paddy areas using multispectral remote sensing images* [Thesis]. Universiti Putra Malaysia.
- Farooq, M., Wahid, A. & Lee, D. (2009). Exogenously applied polyamines increased drought tolerance of rice by improving leaf water status, photosynthesis and membrane properties. *Acta Physiologiae Plantarum*, 31(5), 937–945.
- Guan, S., Fukami, K., Matsunaka, H. *et al.* (2019). Assessing correlation of high-resolution NDVI with fertilizer application level and yield of rice and wheat crops using small UAVs. *Remote Sensing*, 11(2), 112.
- Hashemi, S. A. & Chenani, S. K. (2011). Investigation of NDVI index in relation to chlorophyll content change and phenological event. *Recent Advances in Environment, Energy Systems and Naval Science*, 22–28.
- Jabatan Pertanian. (2019). *Booklet statistik tanaman 2019*. Dicapai dari http://www.doa.gov.my/index/resources/aktiviti_sumber/sumber_awam/maklumat_pertanian/perangkaan_tanaman/

booklet_statistik_tanaman_2019.pdf.

- Kazuki, M., Atsushi, I., Hiroyuki, H., *et al.* (2017). A study on growth condition analysis of rice using drone. *Pan Pacific Conference on Science, Computing and Telecommunications (PACT) 2017*.
- Kementerian Pertanian dan Industri Asas Tani. (2019). *Halatuju Kementerian Pertanian & Industri Asas Tani: Prioriti & Strategi 2019–2020*. Dicapai dari https://www.moa.gov.my/documents/20182/139717/Hala+Tuju+2019-2020_LowVer.pdf/1ca7c2b3-f4fb-460a-8e04-1fdd051360cb.
- Lee, L. S. (2019). *Rice monitoring using OBIA technique based on aerial imagery* [Thesis]. Universiti Putra Malaysia.
- Mahajan, U., & Bundel, B. R. (2017). Drone for normalized difference vegetation index (NDV) to estimate crop health for precision agriculture: a chapter alternative for spatial satellite sensors. *International Conference on Innovative Research in Agriculture, Food Science, Forestry, Horticulture, Aquaculture, Animal Sciences, Biodiversity, Ecological Sciences and Climate Change (AFHABEC-2016)*.
- Mohamad Halid, R, Berahim, Z., & Mohd Saud, H. (2019). Effects of inoculation of plant growth promoting rhizobacteria to minimize panicle grain shattering habit for increased yield of rice (*Oryza sativa* L.). *African Journal of Microbiology Research*, 13(13), 256–263.
- Mohd Zainudin, M. H., Mustapha, N. A., Hassan, M. A., *et al.* (2019). A highly thermostable crude endoglucanase produced by a newly isolated thermobifida fusca strain UPMC 901. *Scientific Reports*, 9, 13526.
- Mosleh, M. K., Hassan, Q. K., & Chowdhury, E. H. (2015). Application of remote sensors in mapping rice area and forecasting its production: A review. *Sensors*, 15(1): 769–791.
- Murugan, D., Ahmed, A., Greg, A. *et al.* (2016). Fusion of drone and satellite data for precision agriculture monitoring. *11th International Conference on Industrial and Information System (ICIIS)*.
- Norasma, C. Y. N., Abu Sari, M. Y., *et al.* (2018). Rice crop monitoring using multirotor UAV and RGB digital camera at early stage of growth. *IOP Conference Series: Earth and Environmental Science*, 169(2018), 012095.
- Parrot.com. (2019). Dicapai dari <https://www.parrot.com/global/parrot-professional/parrot-sequoia>
- Rosle, R., Che' Ya, N. N., Roslin, N. A., *et al.*, (2019). Monitoring early stage of rice crops growth using normalized difference vegetation index generated from UAV. *IOP Conference Series: Earth and Environmental Science*, 355(1), 012066.
- Sabarina, K., & Priya, N. (2015). Lowering data dimensionality in big data for the benefit of precision agriculture. *Procedia Computer Science*, 48(2015); 548–554.
- Srinivasan, A. (2006). *Handbook of Precision Agriculture: Principles and Applications*. CRC Press.
- Vergara-Diaz, O., Zaman-Allah, M. A., Masuka, B., *et al.* (2016). A novel remote sensing approach for prediction of maize yield under different conditions of nitrogen fertilization. *Frontiers in Plant Science*, 7, 666.
- Wakamori, K., Ichikawa, D., Oguri, N., *et al.* (2017). Estimation of rice growth status, protein content and yield prediction using multi-satellite data. *IEEE International Geoscience and Remote Sensing Symposium (IGARSS)*.





HH PUBLISHER

BUILDING SUCCESS & STRENGTHING PARTNERSHIP

HH ACADEMIC

(002672130-K)

PT. 321 Tingkat 1,

Jalan Bandar, 71000,

Port Dickson, Negeri Sembilan.

Tel: +60 12-359 0809

Email: inquiries@hh-publisher.com

Website: www.journals.hh-publisher.com/index.php/AAFRJ/index

eISSN 2735-1084



9 772735 108009